Dissertation zur Erlangung des Doktorgrades
der Fakultät für Chemie und Pharmazie
der Ludwig-Maximilians-Universität München

Development of Advanced Biomaterials for Bone Tissue Engineering

Winfried Schlögl
aus Ingolstadt, Deutschland

2012

Erklärung

Diese Dissertation wurde im Sinne von § 7 der Promotionsordnung vom 28. November 2011 von Herrn Prof. Dr. Wolfgang Frieß betreut.

Eidesstattliche Versicherung

Diese Dissertation wurde eigenständig und ohne unerlaubte Hilfe erarbeitet.

München, 26.04.2012

……

Winfried Schlögl

Dissertation eingereicht am 26.04.2012

1. Gutachter: Prof. Dr. Wolfgang Frieß

2. Gutachter: Prof. Dr. Gerhard Winter

Mündliche Prüfung am 06.06.2012

Acknowledgments

The presented doctoral thesis has been acquired at the Department of Pharmacy, Pharmaceutical Technology and Biopharmaceutics at the Ludwig-Maximilans-University in Munich.

Foremost, I would like to express my gratitude to my supervisor Prof. Dr. Wolfgang Frieß for offering me the possibility to join his working group, for his scientific guidance, for his ongoing interest in the progress of this work, for the creation of an outstanding, creative working atmosphere, and for his personal advice. I further very much appreciate the possibility of active participation in numerous local and global scientific meetings, discussions, and conferences.

I would like to thank Prof. Dr. Gerhard Winter for his modern and visionary leadership of the chair, providing excellent working conditions and for the co-referee of this work. Moreover, I want to express my thanks for the passionate scientific programme as well as for numerous social events creating a great and inspiring climate.

The AiF (Arbeitsgemeinschaft industrieller Forschungsvereinigungen) and the Bavarian Research Foundation are kindly acknowledged for the great financial support. The work of the presented doctoral thesis has been conducted among the ForZebRA-project (Bavarian Research Foundation) and the COMET-project (AiF).
I would like to thank all members of the ForZebRA team for the pleasant working atmosphere and their dedicative contribution. In particular, I would like to thank my direct cooperation partners from the clinical center of the LMU within our work package: Prof. Dr. Matthias Schieker, Dr. Elias Volkmer, and especially Uta Leicht and Verena Marschall for performing the cell culture experiments. Further, I would like to thank Dr. Michael Wiggenhorn, Dr. Frank Schaubhut, and Dr. Silke Reiffert from Coriolis Pharma (Martinsried) for their contribution to our part of the ForZebRA-project. Sebastian Basel and Andreas Tegel from PreSens GmbH (Regensburg) are acknowledged for providing the oxygen microsensors and their great technical support.

With regards to the COMET-project, I would like to express my thanks to the FILK-members (Research Institute for Leather and Plastic Sheeting, Freiberg) for supplying me with collagen material “ad libidum”. Especially, Dr. Ines Stachel and Dr. Michael Meyer are thanked for their scientific contribution. From the Technical University of Graz, Prof. Dr. Georg Gübitz and Dr. Suzana Jus are acknowledged for making the COMET-project become an enrichment.

I would like to thank Prof. Dr. Angelika Vollmar and her team at the Department of Pharmaceutical Biology. Prof. Dr. Stefan Zahler is kindly acknowledged for his help with confocal laser scanning microscopy. PD Dr. Robert Fürst is deeply acknowledged for his cooperation and scientific input regarding Western blot and ELISA analyses. I would like to thank Jana Peliskova and Bianca Hager for their practical help during Western blot analysis.

From the Department of Chemistry of the LMU Munich, I want to thank Christian Minke for his support with SEM analysis and Wolfgang Wünschheim for the access to the high temperature oven and the X-ray diffractometer.
Moreover, I would like to thank Dr. Gerhard Simon for the insights in the sterile facility and for his perfect assistance, whenever needed.

I am deeply thankful to my lab partner Imke Leitner for the professional assistance whenever I needed help and for the great time in our lab.

Furthermore, I would like to immensely thank all present and former colleagues and members at the chair for their warm welcome, their contribution to the working atmosphere, the inspiring scientific discussion, and their contribution to various leisure-time activities. I very much appreciate the scientific and personal support I have received from each of you individually and your friendship, in particular: Markus Hofer, Sarah Claus, Eva Ruberg, Julia Kasper, Kerstin Höger, Angelika Freitag, Tim Menzen, Philipp Matthias, Dr. Frank Schaubhut, Dr. Julia Myschik, Dr. Gerhard Sax, Dr. Miriam Printz, Dr. Lars Schiefelbein, Dr. Katja Schmid, Dr. Sarah Küchler, Madeleine Witting, Dr. Johannes Mathes, Raimund Geidobler, Sebastian Hertel, Elsa Etzl, Thomas Bosch, and Sebastian Hertel.

Dominik Dahlinger, Veronika Fischbacher, Marion Halimi, Angelina Klein, Andreas Kolb, Martin Schoder, Madeleine Witting, and Gabriele Zuchtriegel are acknowledged for the excellent work during their internships in my lab.

Dr. Stephan Kuklinski from PromoCell GmbH (Heidelberg) is acknowledged for his outstanding support regarding antibodies and cytokines.

Uwe Schwarick from Medtronic Sofamor Danek GmbH (Deggendorf, Germany) is acknowledged for the donation of biphasic calcium phosphate granules.

I want to express my special thanks to Dr. Cornelius Pompe for introducing me to the world of in-situ hardening systems and his start-up aid.

Finally, I want to thank my parents and my parents-in-law for the support they gave me over all the years and my wife Julia for her encouragement, for her appreciative patience, and for her incomparable love.

Table of Contents

1 Introduction and Objectives of the Thesis

1.1 Introduction

1.1.1 Bone Tissue Engineering

Bone is a living tissue, undergoing constant remodeling and self-renewal comprising the ability to repair itself [Hing, 2004; Phillips, 2005]. Due to this fact, restorative surgical intervention, e.g. after fractures, usually requires not more than alignment and stable fixation. However, if self-repair mechanisms are overstrained, in case of non-unions or critical size defects, bone grafting is necessary [Shepherd and Best, 2011]. In clinical use nowadays, the gold standard for bone regeneration still is the use of autologous bone grafting material [Dimitriou et al., 2011; Quarto et al., 2001]. However, harvesting surgery to obtain the graft material comprises the risk of infections or donor-site morbidity [Kurz et al., 1989; Seiler and Johnson, 2000]. The use of allograft material (e.g. demineralized bone matrix) can lead to immunologic reactions [Benichou, 1999; Stevenson, 1987], the transmission of diseases [Moucha et al., 2007], and increases the risk of infections [Lord et al., 1988].

A disease associated with increased fracture rates is osteoporosis [Johnell et al., 2004; Kanis, 1994]. A quarter of the Germans older than 50 years is currently suffering from osteoporosis [Häussler et al., 2006] and one out of three women and one out of five men over 50 years will suffer from a fracture caused by osteoporosis [Pollähne et al., 2007]. By the year 2030, about half of the German population will be 50 years or older [Statistisches Bundesamt, 2009].

With this in mind, there is an increasing demand for orthopedic implants (for replacement of diseased tissue and for non-union defects) integrating in recipient's body tissue and for fillers to treat critical size defects [Rose and Oreffo, 2002]. Tissue engineering is a considerable option as this interdisciplinary field aims on the development of adequate replacements for non-functional tissue to maintain, restore, or improve its function [Langer and Vacanti, 1993]. Currently bone tissue engineering is most frequently used in, but not limited to, dental applications, due to the relatively small defect sites needing reconstructive approaches [Ueda, 2011].

The generation of new tissue can be performed by in vitro expansion of harvested cells in a bioreactor and seeding on a 3-D scaffold (Figure 1-1). Alternatively the recipient body can be used as a bioreactor itself, when a freshly cell-seeded scaffold, or an unseeded scaffold is implanted into the defect site and cells are injected after a certain period or surrounding cells infiltrate the scaffold [Rose and Oreffo, 2002].

Figure 1-1: Typical strategy for tissue engineering, adapted from [Rose and Oreffo, 2002].

For successful bone regeneration, three key factors are required and will be further reviewed within the following sections: osteogenic cells, an osteoconductive scaffold, and osteoinductive growth factors [Giannoudis et al., 2005]. Cells generate the new tissue, facilitated by a scaffold providing the required atmosphere, while growth factors enhance tissue regeneration and ensure guidance towards the desired differentiation pathways [Ikada, 2006]. The following introduction will provide a brief overview over the three main factors, cells, scaffolds, and growth factors focusing on bone tissue engineering and on the types used within this thesis.

1.1.2 Cells as key factor in tissue regeneration

Osteogenic cells enable a bone grafting material to form new bone [Shepherd and Best, 2011]. Therefore, the potential to generate bone is a prerequisite for the use of a cell type in skeletal tissue engineering. This is given for osteoblasts, embryonic stem cells, and other postnatal mesenchymal cells [Levi and Longaker, 2011].

Embryonic stem cells (ESCs) are pluripotent and can therefore differentiate into any of the three germ layers (ectoderm, mesoderm, endoderm), but comprise the drawback of potential teratoma formation [Thomson et al., 1998]. Furthermore, their human blastocysts' origin is accompanied by ethical issues [McLaren, 2007]. In 2006, the reprogramming of somatic cells to induced pluripotent stem cells (iPSCs) was described in mice [Takahashi and Yamanaka, 2006] and was later transferred to human cells [Park et al., 2008; Takahashi et al., 2007; Yu et al., 2007]. The technique appears to be a promising alternative, generating pluripotent stem cells from autologous somatic cells. But it has to be considered that even syngeneic iPSCs were shown to cause immunogenic response [Zhao et al., 2011]. Besides ethical controversy, human embryonic stem cells (hESCs) and induced pluripotent stem cells (iPSCs) are currently under critical observation due to genomic alterations. A large number of duplications was reported for few of the tested hESCs, whereas iPSCs showed deletions in tumor-suppressor genes [Laurent et al., 2011].

Mesenchymal stem cells (MSCs) are an alternative cell type. They were named ”mesenchymal“ due to their ability to differentiate into bone, tendon, connective tissue, cartilage, smooth muscle, adipose tissue, and skeletal muscle [Caplan, 1991; Caplan, 2005].

Multipotent adipose-derived stromal cells (ASCs) represent another suitable cell type. They are present in the lipoaspirate, and can thereby be easily harvested during the one million liposuctions being performed annually [Yoshimura et al., 2006]. ASCs can be used as an alternative for skeletal regenerative medicine as they exhibit comparable morphology, differentiation capacity, and phenotype to MSCs [Levi and Longaker, 2011].

Osteoprogenitor cells are an alternative due to their ability to differentiate into bone tissue and can be harvested from the periost. The limited availability hinders a broader use, whereas they are used during periodontal surgery as they can easily be harvested during this setting [Agata et al., 2007].

All of the mentioned cell types need to be supplied with oxygen, being an intensively discussed factor regarding cellular behavior. Oxygen is known to be a metabolic substrate and a signaling molecule, but the role of oxygen on cellular behavior is not yet fully understood [Abdollahi et al., 2011]. While studies have shown that low oxygen concentrations help to maintain the multipotency of stem cells [Grayson et al., 2007], others identified low oxygen concentrations as a driving force for differentiation [Koay and Athanasiou, 2008]. In traditional cell cultures, the oxygen concentration is determined by the oxygen concentration of the ambient air being 21 %. This is far above the physiological tissue oxygen concentration being 3 % in mean [Csete, 2005]. The ideal oxygen concentration for bone tissue engineering remains to be found. Static 3D cell culture experiments have shown, that even in small cylindrical scaffolds (9 mm diameter, 5 mm height) oxygen levels in the center dropped to 0 % within 5 days of culture, leaving no vital cells left and cells only survived in the periphery [Volkmer et al., 2008]. In living organisms, oxygen is provided by diffusion from surrounding blood vessels, but at a distance exceeding 100 – 200 µm the oxygen supply is strongly reduced [Carmeliet and Jain, 2000]. In tissue engineering the use of oxygen generating biomaterials provides a possibility to overcome this limitation hindering the engineering of larger constructs [Oh et al., 2009]. Oxygen generating biomaterials were shown to extend cell viability under hypoxic conditions and prevented necrosis of unvascularized tissue in vivo for several days [Harrison et al., 2007]. In contrast, hypoxia is a powerful stimulus for angiogenesis by stimulating the expression of VEGF [Rehman et al., 2004; Thangarajah et al., 2009]. Also aging has an effect on bone regeneration. Lu et al. reported that VEGF-expression, vascularization and bone repair of tibial fractures were decelerated in elder mice [2008]. However, the timeframe between implantation of tissue engineering constructs and neovascularization is critical regarding cell survival and the use of oxygen generating scaffolds might reduce this threat [Oh et al., 2009].

Nonetheless, it was concluded that the application of cells alone is unlikely to be sufficient for bone regeneration. For large skeletal defects, a scaffold with adequate properties, such as size, shape, and mechanical strength is considered to be essential [Rose and Oreffo, 2002].

1.1.3 Scaffolds as key factor in tissue regeneration

In vivo, cells are embedded in extracellular matrix (ECM), guiding their development, arrangement, and regenerative abilities by specific signals, thus providing an appropriate environment for the cells. In tissue engineering, the role of the ECM needs to be executed by adequate scaffolds [Cunniffe and O'Brien, 2011]. A scaffold, used as a bone graft, needs to be osteoconductive, i.e. to "support the growth of bone over its surface" [Shepherd and Best, 2011]. Therefore, cellular adhesion to the scaffold is a prerequisite and can be modulated by the presence of adhesion domains in extracellular matrix proteins, containing the amino acid sequence Arg-Gly-Asp (RGD) [Pierschbacher and Ruoslahti, 1987]. Scaffolds for bony application sites, coated with the RGD-sequence, enabled superior cell ingrowth in vivo [Eid et al., 2001]. Scaffolds further need to exhibit a certain porosity and pore interconnectivity to allow cell spreading, nutrient exchange, and vascularization [Hutmacher, 2000]. The porosity of trabecular bone has been reported to vary between 30 – 90 % [Carter and Hayes, 1977] and the pore size considered to be ideal for tissue engineering applications is in the range of 100 – 1000 µm [Friess and Werner, 2008]. Scaffolds should further be biodegradable and the timeframe required for biodegradation should match the rate of how fast new bone is formed [Shepherd and Best, 2011]. For the fabrication of tissue engineering scaffolds, amongst others, a wide range of different biomaterials, such as polyglycolide (PGA), polylactide (PLA), poly(lactic-*co*-glycolic acid) (PLGA), polycaprolactone (PCL), calcium phosphates, or collagen can be used.

Collagen is the most abundant structural protein in the body and main component of the ECM, expressed in various tissues. Amongst the different (currently more than 20) collagens, collagen type I is the predominant type in the body, being expressed in bone, skin, tendon, ligaments, and cornea [Friess, 1998; Gelse et al., 2003]. It is the collagen type which is most frequently used in biomaterials research [Geiger et al., 2003; Lee et al., 2001]. The overall mechanical performance of collagen-based biomaterials is poor. In order to enhance the mechanical properties and to reduce the in vivo degradation rate, collagen is crosslinked by either chemical (e.g. aldehydes, cardbodiimides), physical (e.g. dehydrothermal treatment, UV radiation), or enzymatic methods (e.g. transglutaminase, laccases, tyrosinases) [Friess, 1998; Griffin et al., 2002; Jus et al., 2011]. Furthermore, collagen can be combined with

calcium phosphate ceramics, e.g. hydroxyapatite, or tricalcium phosphate to form composite materials with enhanced mechanical properties [Al-Munajjed and O'Brien, 2009; Bernhardt et al., 2008; Cunniffe et al., 2010; Geiger, 2001; Gelinsky et al., 2008; Lyons et al., 2010]. A combination of collagen and hydroxyapatite was found to promote osteogenic differentiation of bone marrow derived stromal cells in vivo [Dawson et al., 2008] and provided superior defect healing properties in a rat cranial defect model [Lyons et al., 2010].

Calcium phosphates themselves are frequently applied materials for bone repair as they exhibit a "chemical similarity to the mineral component of bone" [Shepherd and Best, 2011]. Hydroxyapatite (HA) and tricalcium phosphate (TCP) were used in numerous preclinical and clinical studies. They can be used in different morphologies, such as powders, cements, or granules [Geiger, 2001; Seeherman and Wozney, 2005; Sorensen et al., 2004]. TCP is resorbed faster compared to HA due to its higher solubility and osteoclastic remodeling [Allard and Swart, 1982; Bansal et al., 2009]. HA based scaffolds showed long term integration in cranical defects [Block and Thorn, 2000] and were successfully used in the reconstruction of the orbital roof [Allard and Swart, 1982]. Even long bone segmental defects (4-7 cm) were treated with the help of HA [Quarto et al., 2001]. TCP was successfully used as a bone filling material [Bansal et al., 2009; Erbe et al., 2001].

Moreover, PLGA (poly(lactic-*co*-glycolic acid)) is a compound frequently used for bone tissue engineering approaches. Constructs thereof can be adapted in shape and size to fit into the intended application site. 3D printed PLGA scaffolds seeded with osteoblasts formed a trabecular bone-like structure [Ge et al., 2009b] and in vivo studies successfully used PLGA scaffolds as bone graft materials [Ge et al., 2009a]. PLGA can further be used as a carrier material for growth factors like BMP-2 or parathyroid hormone in bone tissue engineering or other therapeutic proteins [Eliaz and Kost, 2000; Wei et al., 2004; Whang et al., 1998]. The degradation rates can be controlled by choosing the appropriate PLGA variant to obtain the desired release profile, but the degradation products can lead to pH decrease potentially influencing the stability of the incorporated drug [Göpferich, 1997; Lewis, 1990; Park, 1994]. All in all, collagen was named the „favoured carrier for BMPs" [Rose and Oreffo, 2002].

1.1.4 Growth factor delivery – bone morphogenetic proteins

Osteoinductive growth factors guide the differentiation of precursor cell types into bone forming osteoblasts [Shepherd and Best, 2011]. Bone morphogenetic proteins (BMPs) have been studied most extensively in bone tissue engineering, but also others such as vascular endothelial, insulin-like, platelet-derived, fibroblast, and transforming-growth factor are involved in the fracture healing cascade [Dimitriou et al., 2011; Phillips, 2005]. BMPs are produced by MSCs, osteoblasts and chondroblasts during fracture repair. They act on MSC proliferation, differentiation, angiogenesis, and synthesis of extracellular matrix [Al-Aql et al., 2008]. Widely used in clinical applications are BMP-2 and BMP-7 [Biase and Capanna, 2005]. BMPs were further shown to enhance vascularization during fracture repair by stimulating the expression of VEGF [Deckers et al., 2002]. Two approved products using bone morphogenetic proteins are currently on the market: Medtronic's INFUSE® bone graft, using rhBMP-2 for spinal fusion, non-union fractures, and oral maxillofacial applications [Medtronic Sofamor Danek, 2011], and Stryker's OP-1/Osigraft [Stryker GmbH & Co. KG, 2008] using rhBMP-7 for treating non-union defects. Both products are based on a collagen carrier material, but rhBMP-7 stability and the mechanisms underlying binding and release remain to be shown. BMP-7 was comparable or superior to autologous bone grafts in tibial fracture repair [Friedlaender et al., 2001; Zimmermann et al., 2007]. With the help of BMP-7, a complete mandible was successfully engineered and applied as a bone transplant [Warnke et al., 2004].

The strategies for delivery of BMPs comprise direct administration, scaffold-based delivery, and gene therapy, i.e. the delivery of genetically engineered cells expressing BMPs [Fischer et al., 2011]. Direct administration of BMPs results in fast clearance from the application site [Kirker-Head, 2000]. The scaffold-based approach is superior to application without scaffolds due to the increased retention at the application site [Geiger et al., 2003; Jeon et al., 2008]. For instance, combining BMP-2 with a collagen scaffold increased the retention period compared to the application of BMP-2 in pure buffer [Geiger et al., 2003; Seeherman et al., 2003] and the combination of BMP-2 with inorganic calcium phosphate material further increased the retention period [Seeherman et al., 2003]. For this thesis, the scaffold-based delivery approach for rhBMP-7 was chosen.

1.2 Objectives of the thesis

Aim of the thesis was to develop advanced biomaterials for bone regenerative purposes.

Chapter 2 deals with the development and characterization of an in-situ hardening PLGA based system, resulting in an open-porous scaffold with a certain mechanical stability after administration into body fluids. The in-situ hardening formulation overcomes the complex ex vivo preparation scheme for 3D scaffolds, circumventing the drawback of decreased mechanical stability ascribed to injectable formulations. For further optimization and to combine osteoconductive and osteogenic working principles, the in-situ hardening system was further evaluated as a cell delivery system to obtain an injectable formulation, generating a porous and mechanically stable scaffold preloaded with cells.

In Chapter 3 microbial transglutaminase was evaluated for enzymatic crosslinking of collagen with the aim to circumvent the toxicity of chemical crosslinkers typically used to enhance mechanical resistance and decrease the degredation rate of the collagen used for bioengineering [Speer et al., 1980]. Several methods to remove transglutaminase from collagen were evaluated and a method to demonstrate the absence of transglutaminase was established.

Chapter 4 reports about the development of a defined loading procedure for rhBMP-7 into collagen/ceramic composites. High binding efficiency needed to be ensured. Several quantification methods, including SEC, SDS-Page, and Western blot analysis had to be developed and a sterile filtration method, ensuring no loss of rhBMP-7, required for upcoming cell culture experiments, was established. The binding behavior of rhBMP-7 to the collagen/ceramic composites had to be assessed by extraction experiments.

In Chapter 5 a formulation providing sustained release of oxygen was developed and incorporated into collagen/ceramic composite scaffolds. The purpose of this scaffold architecture was to engineer scaffolds enabling to maintain cell viability in larger tissue engineering constructs, where oxygen diffusion is a limiting factor regarding cell survival [Volkmer et al., 2008]. A sustained effect was desired with at the same time limited hydrogen peroxide formation.

The objectives of this thesis were chosen to provide perspectives in order to meet future demands on bone tissue engineering, particularly in the context of an increasing elderly population, associated with degenerative skeletal diseases.

1.3 References

Abdollahi H., Harris L. J., Zhang P., McIlhenny S., Srinivas V., Tulenko T., DiMuzio P. J., The role of hypoxia in stem cell differentiation and therapeutics, Journal of Surgical Research, 165 (2011) 112-117.

Agata H., Asahina I., Yamazaki Y., Uchida M., Shinohara Y., Honda M. J., Kagami H., Ueda M., Effective bone engineering with periosteum-derived cells, Journal of Dental Research, 86 (2007) 79-83.

Al-Aql Z. S., Alagl A. S., Graves D. T., Gerstenfeld L. C., Einhorn T. A., Molecular mechanisms controlling bone formation during fracture healing and distraction osteogenesis, Journal of Dental Research, 87 (2008) 107-118.

Al-Munajjed A. A., O'Brien F. J., Influence of a novel calcium-phosphate coating on the mechanical properties of highly porous collagen scaffolds for bone repair, Journal of the Mechanical Behavior of Biomedical Materials, 2 (2009) 138-146.

Allard R. H., Swart J. G., Orbital roof reconstruction with a hydroxyapatite implant, Journal of Oral and Maxillofacial Surgery, 40 (1982) 237-239.

Bansal S., Chauhan V., Sharma S., Maheshwari R., Juyal A., Raghuvanshi S., Evaluation of hydroxyapatite and beta-tricalcium phosphate mixed with bone marrow aspirate as a bone graft substitute for posterolateral spinal fusion, Indian Journal of Orthopaedics, 43 (2009) 234-239.

Benichou G., Direct and indirect antigen recognition: The pathways to allograft immune rejection, Frontiers in Bioscience, 4 (1999) 476-480.

Bernhardt A., Lode A., Boxberger S., Pompe W., Gelinsky M., Mineralised collagen - an artificial, extracellular bone matrix - improves osteogenic differentiation of bone marrow stromal cells, Journal of Materials Science: Materials in Medicine, 19 (2008) 269-275.

Biase P. D., Capanna R., Clinical applications of BMPs, Injury, 36 (2005) S43-S46.

Block J. E., Thorn M. R., Clinical indications of calcium-phosphate biomaterials and related composites for orthopedic procedures, Calcified Tissue International, 66 (2000) 234-238.

Caplan A. I., Mesenchymal stem cells, Journal of Orthopaedic Research, 9 (1991) 641-650.

Caplan A. I., Review: Mesenchymal stem cells: Cell–based reconstructive therapy in orthopedics, Tissue Engineering, 11 (2005) 1198-1211.

Carmeliet P., Jain R. K., Angiogenesis in cancer and other diseases, Nature, 407 (2000) 249-257.

Carter D., Hayes W., The compressive behavior of bone as a two-phase porous structure, Journal of Bone & Joint Surgery, American Volume, 59 (1977) 954-962.

Csete M., Oxygen in the cultivation of stem cells, Annals of the New York Academy of Sciences, 1049 (2005) 1-8.

Cunniffe G., O'Brien F., Collagen scaffolds for orthopedic regenerative medicine, JOM Journal of the Minerals, Metals and Materials Society, 63 (2011) 66-73.

Cunniffe G. M., Dickson G. R., Partap S., Stanton K. T., O'Brien F. J., Development and characterisation of a collagen nano-hydroxyapatite composite scaffold for bone tissue engineering, Journal of Materials Science. Materials in Medicine, 21 (2010) 2293-2298.

Dawson J. I., Wahl D. A., Lanham S. A., Kanczler J. M., Czernuszka J. T., Oreffo R. O. C., Development of specific collagen scaffolds to support the osteogenic and chondrogenic differentiation of human bone marrow stromal cells, Biomaterials, 29 (2008) 3105-3116.

Deckers M. M. L., van Bezooijen R. L., van der Horst G., Hoogendam J., van der Bent C., Papapoulos S. E., Löwik C. W. G. M., Bone morphogenetic proteins stimulate angiogenesis through osteoblast-derived vascular endothelial growth factor A, Endocrinology, 143 (2002) 1545-1553.

Dimitriou R., Jones E., McGonagle D., Giannoudis P., Bone regeneration: current concepts and future directions, BMC Medicine, 9 (2011) 66.

Eid K., Chen E., Griffith L., Glowacki J., Effect of RGD coating on osteocompatibility of PLGA-polymer disks in a rat tibial wound, Journal of Biomedical Materials Research, 57 (2001) 224-231.

Eliaz R. E., Kost J., Characterization of a polymeric PLGA-injectable implant delivery system for the controlled release of proteins, Journal of Biomedical Materials Research, 50 (2000) 388-396.

Erbe E. M., Marx J. G., Clineff T. D., Bellincampi L. D., Potential of an ultraporous beta-tricalcium phosphate synthetic cancellous bone void filler and bone marrow aspirate composite graft, European Spine Journal, 10 (2001) S141-S146.

Fischer J., Kolk A., Wolfart S., Pautke C., Warnke P. H., Plank C., Smeets R., Future of local bone regeneration – Protein versus gene therapy, Journal of Cranio-Maxillofacial Surgery, 39 (2011) 54-64.

Friedlaender G. E., Perry C. R., Cole J. D., Cook S. D., Cierny G., Muschler G. F., Zych G. A., Calhoun J. H., Laforte A. J., Yin S., Osteogenic protein-1 (bone morphogenetic protein-7) in the treatment of tibial nonunions, Journal of Bone & Joint Surgery, American Volume, 83 (2001) S151-S158.

Friess W., Collagen - biomaterial for drug delivery, European Journal of Pharmaceutics and Biopharmaceutics, 45 (1998) 113-136.

Friess W., Werner J., Biomedical Applications, in: Handbook of Porous Solids 5, Schüth F., Sing K. S. W., Weitkamp J. (Eds.), Wiley-VCH Verlag GmbH, Weinheim, Germany, (2008), 2923-2970.

Ge Z., Tian X., Heng B. C., Fan V., Yeo J. F., Cao T., Histological evaluation of osteogenesis of 3D-printed poly-lactic-co-glycolic acid (PLGA) scaffolds in a rabbit model, Biomedical Materials, 4 (2009a) 21001.

Ge Z., Wang L., Heng B. C., Tian X., Lu K., Fan V. T. W., Yeo J. F., Cao T., Tan E., Proliferation and differentiation of human osteoblasts within 3D printed poly-lactic-co-glycolic acid scaffolds, Journal of Biomaterials Applications, 23 (2009b) 533-547.

Geiger M., Porous collagen/ceramic composite carriers for bone regeneration using recombinant human bone morphogenetic protein-2 (rhBMP-2), Dissertation, (2001), Friedrich-Alexander-University, Erlangen.

Geiger M., Li R. H., Friess W., Collagen sponges for bone regeneration with rhBMP-2, Advanced Drug Delivery Reviews, 55 (2003) 1613-1629.

Gelinsky M., Welzel P. B., Simon P., Bernhardt A., König U., Porous three-dimensional scaffolds made of mineralised collagen: Preparation and properties of a biomimetic nanocomposite material for tissue engineering of bone, Chemical Engineering Journal, 137 (2008) 84-96.

Gelse K., Poschl E., Aigner T., Collagens - structure, function, and biosynthesis, Advanced Drug Delivery Reviews, 55 (2003) 1531-1546.

Giannoudis P. V., Dinopoulos H., Tsiridis E., Bone substitutes: An update, Injury, 36 (2005) S20-S27.

Göpferich A., Polymer bulk erosion, Macromolecules, 30 (1997) 2598-2604.

Grayson W. L., Zhao F., Bunnell B., Ma T., Hypoxia enhances proliferation and tissue formation of human mesenchymal stem cells, Biochemical and Biophysical Research Communications, 358 (2007) 948-953.

Griffin M., Casadio R., Bergamini C. M., Transglutaminases: Nature's biological glues, Biochemical Journal, 368 (2002) 377-396.

Harrison B. S., Eberli D., Lee S. J., Atala A., Yoo J. J., Oxygen producing biomaterials for tissue regeneration, Biomaterials, 28 (2007) 4628-4634.

Häussler B., Gothe H., Mangiapane S., Glaeske G., Pientka L., Felsenberg D., Outpatient care for osteoporosis patients in Germany – results of the BoneEVA study, Deutsches Ärzteblatt International, 103 (2006) 2542-2548.

Hing K. A., Bone repair in the twenty–first century: biology, chemistry or engineering?, Philosophical Transactions of the Royal Society of London. Series A: Mathematical, Physical and Engineering Sciences, 362 (2004) 2821-2850.

Hutmacher D. W., Scaffolds in tissue engineering bone and cartilage, Biomaterials, 21 (2000) 2529-2543.

Ikada Y., Challenges in tissue engineering, Journal of The Royal Society Interface, 3 (2006) 589-601.

Jeon O., Song S. J., Yang H. S., Bhang S.-H., Kang S.-W., Sung M. A., Lee J. H., Kim B.-S., Long-term delivery enhances in vivo osteogenic efficacy of bone morphogenetic protein-2 compared to short-term delivery, Biochemical and Biophysical Research Communications, 369 (2008) 774-780.

Johnell O., Kanis J. A., Odén A., Sernbo I., Redlund-Johnell I., Petterson C., Laet C., Jönsson B., Fracture risk following an osteoporotic fracture, Osteoporosis International, 15 (2004) 175-179.

Jus S., Stachel I., Schloegl W., Pretzler M., Friess W., Meyer M., Birner-Gruenberger R., Guebitz G. M., Cross-linking of collagen with laccases and tyrosinases, Materials Science and Engineering: C, 31 (2011) 1068-1077.

Kanis J. A., Assessment of fracture risk and its application to screening for postmenopausal osteoporosis: Synopsis of a WHO report, Osteoporosis International, 4 (1994) 368-381.

Kirker-Head C. A., Potential applications and delivery strategies for bone morphogenetic proteins, Advanced Drug Delivery Reviews, 43 (2000) 65-92.

Koay E. J., Athanasiou K. A., Hypoxic chondrogenic differentiation of human embryonic stem cells enhances cartilage protein synthesis and biomechanical functionality, Osteoarthritis and Cartilage, 16 (2008) 1450-1456.

Kurz L. T., Garfin S. R., Booth R. E. J., Harvesting autogenous iliac bone grafts: a review of complications and techniques, Spine, 14 (1989) 1324-1331.

Langer R., Vacanti J., Tissue engineering, Science, 260 (1993) 920-926.

Laurent L. C., Ulitsky I., Slavin I., Tran H., Schork A., Morey R., Lynch C., Harness J. V., Lee S., Barrero M. J., Ku S., Martynova M., Semechkin R., Galat V., Gottesfeld J., Belmonte J. C. I., Murry C., Keirstead H. S., Park H.-S., Schmidt U., Laslett A. L., Muller F.-J., Nievergelt C. M.,

Shamir R., Loring J. F., Dynamic changes in the copy number of pluripotency and cell proliferation genes in human ESCs and iPSCs during reprogramming and time in culture, Cell Stem Cell, 8 (2011) 106-118.

Lee C. H., Singla A., Lee Y., Biomedical applications of collagen, International Journal of Pharmaceutics, 221 (2001) 1-22.

Levi B., Longaker M. T., Concise review: Adipose-derived stromal cells for skeletal regenerative medicine, Stem Cells, 29 (2011) 576-582.

Lewis D. H., Controlled Release of Bioactive Agents from Lactidel Glycolide Polymers, in: Biodegradable Polymers as Drug Delivery Systems, Chasin M., Langer R. S. (Eds.), Marcel Dekker, New York, (1990), 1-42.

Lord C. F., Gebhardt M. C., Tomford W. W., Mankin H. J., Infection in bone allografts. Incidence, nature, and treatment, Journal of Bone and Joint Surgery. American Volume, 70 (1988) 369-376.

Lu C., Hansen E., Sapozhnikova A., Hu D., Miclau T., Marcucio R. S., Effect of age on vascularization during fracture repair, Journal of Orthopaedic Research, 26 (2008) 1384-1389.

Lyons F. G., Al-Munajjed A. A., Kieran S. M., Toner M. E., Murphy C. M., Duffy G. P., O'Brien F. J., The healing of bony defects by cell-free collagen-based scaffolds compared to stem cell-seeded tissue engineered constructs, Biomaterials, 31 (2010) 9232-9243.

McLaren A., A scientist's view of the ethics of human embryonic stem cell research, Cell Stem Cell, 1 (2007) 23-26.

Medtronic Sofamor Danek, INFUSE® Bone Graft, Access: December 19, 2011, http://www.infusebonegraft.com/

Moucha C. S., Renard R. L., Gandhi A., Lin S. S., Tuan R. S., Bone Allograft Safety and Performance, in: Engineering of Functional Skeletal Tissues 3, Bronner F., Farach-Carson M. C., Mikos A. G. (Eds.), Springer London, (2007), 46-54.

Oh S. H., Ward C. L., Atala A., Yoo J. J., Harrison B. S., Oxygen generating scaffolds for enhancing engineered tissue survival, Biomaterials, 30 (2009) 757-762.

Park I. H., Zhao R., West J. A., Yabuuchi A., Huo H., Ince T. A., Lerou P. H., Lensch M. W., Daley G. Q., Reprogramming of human somatic cells to pluripotency with defined factors, Nature, 451 (2008) 141-146.

Park T. G., Degradation of poly(d,l-lactic acid) microspheres: effect of molecular weight, Journal of Controlled Release, 30 (1994) 161-173.

Phillips A. M., Overview of the fracture healing cascade, Injury, 36 (2005) S5-S7.

Pierschbacher M. D., Ruoslahti E., Influence of stereochemistry of the sequence Arg-Gly-Asp-Xaa on binding specificity in cell adhesion, Journal of Biological Chemistry, 262 (1987) 17294-17298.

Pollähne W., Pfeifer M., Minne H. W., Einsatz bildgebender Verfahren bei der Diagnostik der Osteoporose Interpretation der Röntgenbilder und Messprotokolle der Knochendichte, WMW Wiener Medizinische Wochenschrift, 157 (2007) 593-605.

Quarto R., Mastrogiacomo M., Cancedda R., Kutepov S. M., Mukhachev V., Lavroukov A., Kon E., Marcacci M., Repair of large bone defects with the use of autologous bone marrow stromal cells, New England Journal of Medicine, 344 (2001) 385-386.

Rehman J., Traktuev D., Li J., Merfeld-Clauss S., Temm-Grove C. J., Bovenkerk J. E., Pell C. L., Johnstone B. H., Considine R. V., March K. L., Secretion of angiogenic and antiapoptotic factors by human adipose stromal cells, Circulation, 109 (2004) 1292-1298.

Rose F. R. A. J., Oreffo R. O. C., Bone tissue engineering: hope vs hype, Biochemical and Biophysical Research Communications, 292 (2002) 1-7.

Seeherman H., Li R., Wozney J., A review of preclinical program development for evaluating injectable carriers for osteogenic factors, Journal of Bone & Joint Surgery, American Volume, 85 (2003) 96-108.

Seeherman H., Wozney J. M., Delivery of bone morphogenetic proteins for orthopedic tissue regeneration, Cytokine & Growth Factor Reviews, 16 (2005) 329-345.

Seiler J. G., 3rd, Johnson J., Iliac crest autogenous bone grafting: donor site complications, Journal of the Southern Orthopaedic Association, 9 (2000) 91-97.

Shepherd J., Best S., Calcium phosphate scaffolds for bone repair, JOM Journal of the Minerals, Metals and Materials Society, 63 (2011) 83-92.

Sorensen R. G., Wikesjö U. M. E., Kinoshita A., Wozney J. M., Periodontal repair in dogs: evaluation of a bioresorbable calcium phosphate cement (CeredexTM) as a carrier for rhBMP-2, Journal of Clinical Periodontology, 31 (2004) 796-804.

Speer D. P., Chvapil M., Eskelson C. D., Ulreich J., Biological effects of residual glutaraldehyde in glutaraldehyde-tanned collagen biomaterials, Journal of Biomedical Materials Research, 14 (1980) 753-764.

Statistisches Bundesamt, 12. koordinierte Bevölkerungsvorausberechnung, Wiesbaden, Germany, Access: December 15, 2011, Last updated: November 18, 2009, http://www.destatis.de/bevoelkerungspyramide/

Stevenson S., The immune response to osteochondral allografts in dogs, Journal of Bone and Joint Surgery. American Volume, 69 (1987) 573-582.

Stryker GmbH & Co. KG, Osigraft, Zusammenfassung der Merkmale des Arzneimittels, Duisburg, Germany, Access: December 9, 2011, Last updated: June 6, 2008, http://www.stryker.de/de_pdf_hinweise-osigraft.pdf

Takahashi K., Tanabe K., Ohnuki M., Narita M., Ichisaka T., Tomoda K., Yamanaka S., Induction of pluripotent stem cells from adult human fibroblasts by defined factors, Cell, 131 (2007) 861-872.

Takahashi K., Yamanaka S., Induction of pluripotent stem cells from mouse embryonic and adult fibroblast cultures by defined factors, Cell, 126 (2006) 663-676.

Thangarajah H., Vial I. N., Chang E., El-Ftesi S., Januszyk M., Chang E. I., Paterno J., Neofytou E., Longaker M. T., Gurtner G. C., IFATS collection: Adipose stromal cells adopt a proangiogenic phenotype under the influence of hypoxia, Stem Cells, 27 (2009) 266-274.

Thomson J. A., Itskovitz-Eldor J., Shapiro S. S., Waknitz M. A., Swiergiel J. J., Marshall V. S., Jones J. M., embryonic stem cell lines derived from human blastocysts, Science, 282 (1998) 1145-1147.

Ueda M., Tissue engineered bone; Application for implant surgery, Inflammation and Regeneration, 31 (2011) 202-218.

Volkmer E., Drosse I., Otto S., Stangelmayer A., Stengele M., Kallukalam B. C., Mutschler W., Schieker M., Hypoxia in static and dynamic 3D culture systems for tissue engineering of bone, Tissue Engineering. Part A, 14 (2008) 1331-1340.

Warnke P. H., Springer I. N. G., Wiltfang J., Acil Y., Eufinger H., Wehmöller M., Russo P. A. J., Bolte H., Sherry E., Behrens E., Terheyden H., Growth and transplantation of a custom vascularised bone graft in a man, The Lancet, 364 (2004) 766-770.

Wei G., Pettway G. J., McCauley L. K., Ma P. X., The release profiles and bioactivity of parathyroid hormone from poly(lactic-co-glycolic acid) microspheres, Biomaterials, 25 (2004) 345-352.

Whang K., Tsai D. C., Nam E. K., Aitken M., Sprague S. M., Patel P. K., Healy K. E., Ectopic bone formation via rhBMP-2 delivery from porous bioabsorbable polymer scaffolds, Journal of Biomedical Materials Research, 42 (1998) 491-499.

Yoshimura K., Shigeura T., Matsumoto D., Sato T., Takaki Y., Aiba-Kojima E., Sato K., Inoue K., Nagase T., Koshima I., Gonda K., Characterization of freshly isolated and cultured cells derived from the fatty and fluid portions of liposuction aspirates, Journal of Cellular Physiology, 208 (2006) 64-76.

Yu J., Vodyanik M. A., Smuga-Otto K., Antosiewicz-Bourget J., Frane J. L., Tian S., Nie J., Jonsdottir G. A., Ruotti V., Stewart R., Slukvin I. I., Thomson J. A., Induced pluripotent stem cell lines derived from human somatic cells, Science, 318 (2007) 1917-1920.

Zhao T., Zhang Z.-N., Rong Z., Xu Y., Immunogenicity of induced pluripotent stem cells, Nature, 474 (2011) 212-215.

Zimmermann G., Müller U., Löffler C., Wentzensen A., Moghaddam A., Therapieerfolg bei atrophen Tibiaschaftpseudarthrosen, Der Unfallchirurg, 110 (2007) 931-938.

2 Porosity and mechanically optimized PLGA based In-Situ Hardening Systems

This chapter has been submitted to the European Journal of Pharmaceutics and Biopharmaceutis:
Schloegl W., Marschall V., Witting M. Y., Volkmer E., Drosse I., Leicht U., Schieker M., Wiggenhorn M., Schaubhut F., Zahler S., Friess W., Porosity and mechanically optimized PLGA based in-situ hardening systems

Abstract

Goal of the present study was to develop and to characterize in-situ hardening, porous PLGA based systems for their future application as bone grafting materials. Therefore, we investigated the precipitation behavior of formulations containing PLGA and a water-miscible solvent, DMSO, PEG 400, and NMP. To increase porosity, a pore forming agent (NaCMC) was added and to enhance mechanical properties of the system an inorganic filler (α-TCP) was incorporated. The behavior upon contact with water and the influence of the prior addition of aqueous media on the morphology of the corresponding hardened implants were investigated. We proved cell compatibility by live/dead assays for the hardened porous polymer/ceramic-composite scaffolds. The IsHS formulations can therefore be used to manufacture hardened scaffolds ex vivo by using molds with the desired shape and size. Cells were further successfully incorporated into the IsHS by precultivating the cells on the α-TCP-powder prior to their admixing to the formulation. However, cell viability could not be maintained due to toxicity of the tested solvents. But the results demonstrate that in vivo cells should well penetrate, adhere, and profilerate in the hardened scaffolds. Consequently, we consider the in-situ hardening system being an excellent candidate as a filling material for non weight-bearing orthopedic indications, as the resulting properties of the hardened implant fulfill indication-specific needs like mechanical stability, elasticity, and porosity.

2.1 Introduction

For critical-size defects resulting from tumor resection or traumatic injuries adequate filling materials are needed, as clinical studies showed that the implantation of filling materials can facilitate bone regeneration [Groeneveld et al., 1999]. Autologous bone grafting comprises the drawback of additional harvesting surgery with the risk of infections or donor-site morbidity [Kurz et al., 1989; Seiler and Johnson, 2000]. Allograft material like demineralized bone matrix exhibits the risk of immunologic rejection [Benichou, 1999] or transmission of infectious diseases [Moucha et al., 2007]. Ceramic powders like tricalcium phosphate (TCP) or hydroxyapatite (HA) lack in cohesiveness, whereas preformed scaffolds need to be adapted to the desired shape and size of the application site prior to implantation. To overcome these limitations, implants based on PLGA (poly(lactic-co-glycolic acid)) have been developed. Tailor made properties and desired degradation profiles can be obtained by varying molecular mass [Park, 1994], lactic/glycolic acid ratio [Lewis, 1990], or esterification of carboxylic end-groups [Göpferich, 1997]. PLGA is FDA-approved for parenteral use, exhibits good biocompatibility and is used to design controlled drug release systems for therapeutic proteins [Eliaz and Kost, 2000] or antibiotics in bone regeneration [Price et al., 1996]. One drawback is the bulk erosion of PLGA leading to unfavorable acidic degradation products and pH decrease [Göpferich, 1997], which can be overcome by combining PLGA with basic calcium phosphates [Agrawal and Athanasiou, 1997]. According to the “diamond concept” as proposed by Giannoudis et al. an ideal bone substitute material should provide osteogenic cells, osteoconductive structures or scaffolds and growth factors besides mechanical stabilization and biological competence of the recipient [2007]. Thus, scaffolds for orthopedic indications require a certain porosity and pore interconnectivity to promote cell seeding, ingrowth, and proliferation [Hutmacher, 2000]. Porosity of trabecular bone is reported to be 30 – 90 % and a pore size of 100 – 1000 µm is considered to be ideal for the growth of bony tissue inside the implant [Carter and Hayes, 1977; Friess and Werner, 2008]. Human osteoblasts seeded on 3D printed PLGA formed a structure comparable to trabecular bone [Ge et al., 2009b] and 3D printed PLGA-scaffolds were successful in vivo as bone graft materials [Ge et al., 2009a]. CAD-

based 3D printed scaffolds are formed ex vivo to fill the designated void of any desired shape and size. An injectable in-situ hardening system could overcome this complex preparation scheme. Injectable formulations lack in mechanical stability required for bony applications. This lack of mechanical strength can be at least partially compensated by the addition of inorganic fillers [Pompe, 2008]. In the present study we developed a PLGA based, calcium phosphate enriched, in-situ hardening system (IsHS) with the purpose to allow bony regeneration right after administration by a self-setting mechanically stable osteoconductive scaffold with macro- and micro-porosity. Therefore, we examined compositions, based on the solvent-exchange-principle, where PLGA is dissolved in a water-miscible organic solvent [Hatefi and Amsden, 2002]. We furthermore studied the cell compatibility of the solvents used as well as of the IsHS and the hardened scaffolds.

2.2 Materials and Methods

Water used was highly purified from a USF ELGA PURELAB Plus UV/UF water purifier (Ransbach-Baumbach, Germany). All chemicals were purchased from Sigma-Aldrich (St. Louis, MO, USA) and analytical grade, unless otherwise stated.

2.2.1 Materials

Poly(D,L-lactic-co-glycolic acid) PLGA 50:50 Resomer® RG 503H (RG 503H) or RG 502H (RG 502H) (Boehringer Ingelheim, Ingelheim, Germany), Dimethyl sulfoxide (DMSO) and polyethylene glycol 400 (PEG) (Merck KGaA, Darmstadt, Germany), 1-methyl-2-pyrrolidone (NMP, Sigma-Aldrich) and sodium carboxymethyl-cellulose (NaCMC) Blanose® CMC 7HF PH (Hercules Int. GmbH, Zwijndrecht, Netherlands) with a particle size of 90 – 180 µm obtained by sieving were used. α-Tri-calcium-phosphate (TCP) was obtained by heating β-tri-calcium-phosphate (Sigma-Aldrich) at 1300 °C for 3 h followed by quench at room temperature. Phase-transition was monitored by X-ray diffraction and the desired particle size of 90 – 180 µm was obtained by sieving. Cell experiments were performed with human telomerase reverse transcriptase (hTERT) immortalized human mesenchymal stem cells (SCP-1) [Böker et al., 2008; Haasters et al., 2009; Polzer et al., 2011]. They were expanded in

DMEM GlutaMAX® (GIBCO 21885, 476174, Invitrogen, Carlsbad, USA) supplemented with 10 % fetal bovine serum (FBS; Sigma, Munich, Germany) and 40 IU/mL penicillin/streptomycin (PAA Laboratories GmbH, Pasching, Austria).

2.2.2 Methods

2.2.2.1 Precipitation studies

1:2 and 1:3 (w/w) mixtures of RG 503H or RG 502H and NMP, DMSO, and PEG were heated to 80 °C in a drying chamber (Memmert GmbH, Schwabach, Germany) for 2 h until the polymer was completely dissolved. Defined amounts of phosphate buffered saline (137 mM NaCl, 2.7 mM KCl, 12 mM phosphate, PBS), pH 7.4 were added dropwise to the PLGA solutions in 6R glass vials (Fiolax® clear, Schott AG, Mainz, Germany) and evaluated for visible precipitation. The precipitated samples inside the glass vials were further characterized concerning their moldability using a cylindrical piston (4 mm in diameter) with a Texture Analyser XTPlus (Stable Microsystems, UK) at 0.5 mm/s. The final endpoint of moldability was set, when more than 600 g were necessary for a 2.5 mm impression (~120 mN/mm²).

2.2.2.2 IsHS-Preparation

RG 503H or RG 502H solutions in organic plasticizer were mixed with various amounts of α-TCP and pore-forming agent (NaCMC) using a spatula. For detailed composition see Table 2-1.

Table 2-1: Formulations of the different IsHS samples.

Polymer: plasticizer = 1:2				Polymer: plasticizer = 1:3			
Polymer	22,0%	21,11%	20,00%	Polymer	16,5%	15,83%	15,00%
α-TCP	33,0%	31,67%	30,00%	α-TCP	33,0%	31,67%	30,00%
Solvent	44,0%	42,22%	40,00%	Solvent	49,5%	47,50%	45,00%
NaCMC	1,0%	5,00%	10,00%	NaCMC	1,0%	5,00%	10,00%

The preparations (0.3 g for each sample) were either directly injected into 12 mL of PBS by means of a 1 mL syringe without needle or admixed (“preincubated”) with the maximum amount of PBS-amounts ensuring persistent moldability (see 2.2.2.1) prior to their application into PBS. The samples were incubated in a shaking water bath (Julabo SW 21; Julabo Inc., USA) at 37 °C for 24 h at 30 rpm and subsequently vacuum dried in a desiccator at 50 mbar (KNF Neuberger GmbH, Freiburg, Germany) for 48 h and analyzed with a Keyence VHX-500F digital microscope (Keyence Corporation, Osaka, Japan).

2.2.2.3 Investigation of porosity

Porosity was determined by the water evaporation method. Therefore vacuum dried, hardened IsHS based on RG 503H 1:3 (w/w) formulations (n=3) were weighed and soaked with water for 12 h at RT. Pore volume was calculated as (weight of saturated sample – weight of dried sample)/density of water. The theoretical volume of the dried sample without pores was calculated based on the densities of the ingredients of the respective formulation. Porosity was calculated as pore volume/(pore volume + volume of the dried sample). Furthermore, dry specimens were analyzed with a Keyence VHX-500F digital microscope (Keyence Corporation, Osaka, Japan) regarding pore size distribution.

2.2.2.4 Mechanical behavior

Vacuum dried, hardened IsHS based on RG 503H 1:3 (w/w) formulations (n=3) were cut to cuboids. Their heights (4.1 ± 0.9 mm) were determined with a caliper and samples were incubated for 2 h at 37 °C in PBS-buffer (pH 7.4). The samples were uniaxially compressed 3 mm with a cylindrical piston (4 mm in diameter) with a Texture Analyser XTPlus (Stable Microsystems, UK) at 0.25 mm/s. After vacuum drying in a desiccator at 50 mbar (KNF Neuberger GmbH, Freiburg, Germany) for 48 h the height was measured with a caliper. The required force for compression to 50 % of the initial height was investigated and relaxation as percentage of regained height after compression was calculated. For statistical analysis Student’s t–test was used.

2.2.2.5 Cell survival in plasticizers

10^6 SCP-1 cells were cultivated in 6-well cell culture plates (BD Falcon, Bedford, MA, USA) for 24 hours. The medium was replaced by mixtures of plasticizer and cell culture medium. The experiment was run either at room temperature or after precooling the cells for 30 min at 4 °C and adding precooled plasticizer/cell culture medium mixtures at 4 °C. After incubation for 5 min live/dead assays were carried out. After double staining with fluoresceindiacetate (FDA) and propidium iodide-solution (PI, 1 mg/mL Sigma-Aldrich) viable cells appear green and nonviable red, when analyzed with a laser scanning fluorescence microscope (LSM 510, Axiovert 200M, Zeiss, Jena, Germany). Therefore, 10 mg of FDA were dissolved in 2 mL of acetone and diluted 1:500 in phosphate buffered saline (PBS). 0.5 mL of the final mixture of FDA/PI (1:1) were administered to each well after removal of the incubation medium and incubated for 1 minute. After washing with 0.5 mL of PBS the samples were analyzed with the fluorescence microscope.

2.2.2.6 IsHS-Preparation for cell loading

1:2 and 1:3 (w/w) mixtures of RG 503H or RG 502H and organic plasticizer NMP or DMSO representing 60 % of the final composition, were prepared in 6R glass vials (Fiolax® clear, Schott AG, Mainz, Germany). They were heated up to 80 °C in a drying chamber (Memmert GmbH, Schwabach, Germany) until the polymer was completely dissolved and subsequently quenched to room temperature. 30 % inorganic filler (TCP) and 10 % pore forming agent (NaCMC) were homogenously dispersed in the polymer solutions with a spatula. The following steps were carried out in a 4° C cold room with IsHS and SCP-1 cells precooled at 4° C. The scaffold matrix (n=3) was weighed on a glass petri dish (m = 0.3 g) and mixed with 10^6 SCP-1 cells which were dispersed in the maximum DMEM cell culture medium content, determined according to 2.2.2.1. The putty system was subsequently transferred into a 6-well cell culture plate (BD Falcon, Bedford, MA, USA) containing 12 mL DMEM cell culture medium heated to 37 °C in a water bath (Julabo SW 21; Julabo USA Inc.). After 20 minutes of incubation the hardened, cell-enriched IsHS was removed, cut in halves with a scalpel and cell viability was investigated via live/dead assays (see 2.2.2.5).

2.2.2.7 IsHS-Preparation for cell loading via TCP-settlement

6-well cell culture plates (BD Falcon, Bedford, MA, USA) were homogeneously covered with the amount of TCP that would make 30 % of the final IsHS-composition. 10^6 SCP-1 cells, dispersed in the maximum DMEM cell culture medium content, determined according to 2.2.2.1 were seeded into each well and incubated for 24 hours. 1:3 (w/w) mixtures of RG 503H and organic plasticizer NMP or DMSO representing 60 %, or PEG, representing 63.3 % of the final composition, were prepared in 6R glass vials. They were heated up to 80 °C in a drying chamber until the polymer was completely dissolved, subsequently quenched to room temperature and enriched by 10 % (5 % for PEG) pore forming agent (NaCMC) with a spatula. This composition was homogenously dispersed in the pre-seeded TCP/cell/DMEM-mixture with a spatula. The putty system was subsequently transferred into a 6-well cell culture plate (BD Falcon, Bedford, MA, USA) containing 12 mL DMEM cell culture medium heated to 37 °C by means of a water bath. After 5 minutes of incubation for solvent exchange and further precipitation the hardened, cell-enriched IsHS was removed, cut in halves with a scalpel and cell viability was investigated with live/dead assay.

2.2.2.8 Cell settlement on hardened IsHS

For the preparation of IsHS-formulations 1:2 (w/w) mixtures of RG 503H and organic plasticizers NMP, DMSO, or PEG in 6R glass vials were heated up to 80 °C in a drying chamber until the polymer was completely dissolved and subsequently quenched to room temperature. 33 % α-TCP and 1 % NaCMC were admixed with a spatula. The preparations (0.3 g for each sample) were injected into 12 mL of PBS by means of a syringe and incubated in a shaking water bath at 37 °C for 24 h at 30 rpm and subsequently vacuum dried in a desiccator at 50 mbar (KNF Neuberger GmbH, Freiburg, Germany) for 48 h. The hardened scaffolds were completely soaked with ethanol (96 %) for disinfection. After ethanol evaporation, 300.000 SCP-1 cells were seeded onto each scaffold and cell culture was performed for 72 h before live/dead-staining and microscopic analysis.

2.3 Results and Discussion

2.3.1 Precipitation studies

To evaluate the maximum loading capacity of aqueous medium in the later IsHS-mixture as well as the overall in-situ hardening behavior precipitation studies were performed. The used organic plasticizers DMSO, NMP, and PEG are water miscible in any ratio. Water miscibility is a prerequisite for the fundamental working principle of the IsHS, which is the water exchange of the plasticizer leading to precipitation of the PLGA due to its insolubility in aqueous atmospheres [Hatefi and Amsden, 2002]. This principle is utilized in Atrigel® and has been established by Dunn et al. [1998; 1990] amongst others as a drug delivery system [Patel, 2010]. The solvent-exchange process has even been investigated in vivo [Kempe et al., 2008]. The focus of the present study was to find an optimized formulation for the in-situ hardening system exhibiting high porosity while maintaining mechanical strength and high cell compatibility. As cells require aqueous medium, a certain water miscibility of the system is a benefit for successful cell penetration in vivo into an applied cell-free carrier or when pursuing a cell carrying system The addition of small volumes of PBS reflecting only a few percent of the IsHS mass always led to a visible initial phase separation at the admixing focus but the system cleared after gentle shaking for several minutes. With further admixing of PBS the precipitation manifested itself, but the system remained moldable with a spatula. The point when the force required for a 2.5 mm impression with a cylindrical piston (4 mm in diameter) exceeded 600 g was set as the endpoint of potential pre-admixing of PBS. This was considered acceptable for a surgeon during a surgical setting for adapting the shape to the desired dimensions. As can be seen in Figure 2-1 PLGA dissolved in PEG exhibits only low miscibility with PBS without visible precipitation of maximally 2 %. The NMP (~ 6 – 12 %) and DMSO (~ 5 – 12 %) based systems showed higher miscibility without precipitation with only marginal differences among the different formulations. The PBS amount which can be added until moldability is no longer given strongly depended on the chosen polymer and the plasticizer:polymer ratio. The values obtained for RG 502H based systems were higher due to the lower molecular weight

of the polymer and the resulting lower inherent viscosity. A higher plasticizer:polymer ratio kept the system moldable at higher PBS contents due to the plasticizing effect of PEG, NMP, and DMSO. The highest values were obtained for RG 502H dissolved 1:3 in NMP. Up to 12.6 % (ref. to total solvent content) were tolerated without irreversible precipitation and up to 46 % PBS could be admixed to the system while formability was maintained. It is described that the application of PLGA injectables based on the solvent exchange principle into an aqueous surrounding is followed by the subsequent formation of a semi-solid implant [Matschke et al., 2002]. A semi-solid state ensures an adequate formability of the PBS-admixed IsHS and can therefore be used during the timeframe of a surgical setting.

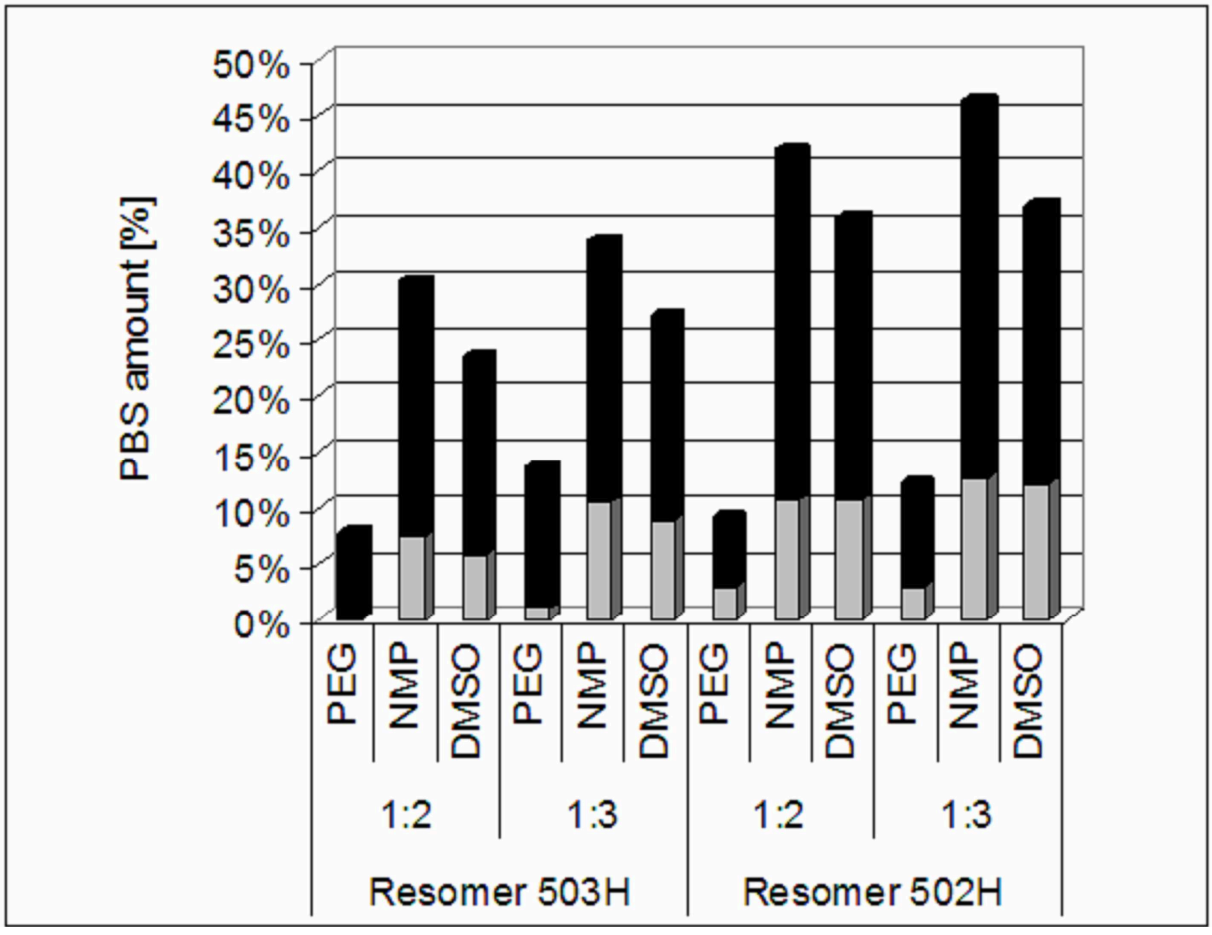

Figure 2-1: PBS-amount added to Resomer® RG 503H and RG 502H in different solvents without visible precipitation (grey bars) and with ongoing moldability (black bars).

2.3.2 IsHS-Preparation

One basic requirement for the IsHS was high porosity inside the hardened IsHS and at the surface to allow nutrient exchange with the surrounding tissue at the site of in vivo application [Karande et al., 2004]. In addition, high water miscibility is desired to keep the concentration of the organic solvent low to maintain viability of incorporated and migrating cells. The system is furthermore expected to show sufficient mechanical stability to resist pressure from surrounding tissue. Compositions with RG 502H and a polymer:plasticizer ratio of 1:3 yielded dense, waxy clots and were discarded. Figure 2-2 shows images of cross-sections of DMSO-based formulations. Porosity increased with an increasing amount of NaCMC as pore-forming agent.

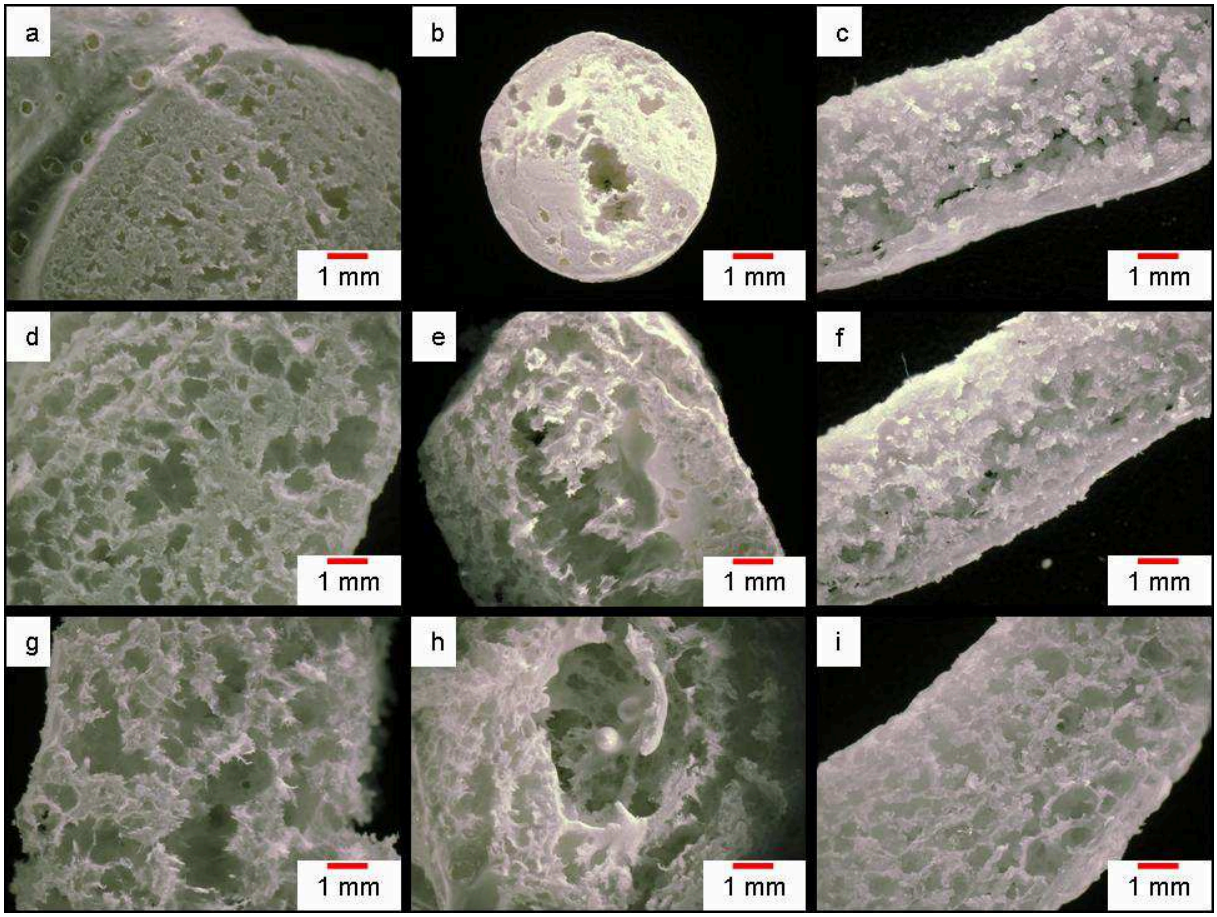

Figure 2-2: Cross sections of incubated IsHS with DMSO as plasticizer; formulations with 1 % NaCMC: a RG 503H 1:2, b RG 503H 1:3, c RG 502H 1:2; formulations with 5 % NaCMC: d RG 503H 1:2, e RG 503H 1:3, f RG 502H 1:2; formulations with 10 % NaCMC: g RG 503H 1:2, h RG 503H 1:3, i RG 502H 1:2.

The sample surfaces are shown in Figure 2-3, revealing that a higher NaCMC content provides a suitable way to avoid the formation of a dense layer at the surface which could hinder liquid exchange and cell migration. NMP-based formulations showed similar appearance (not shown).

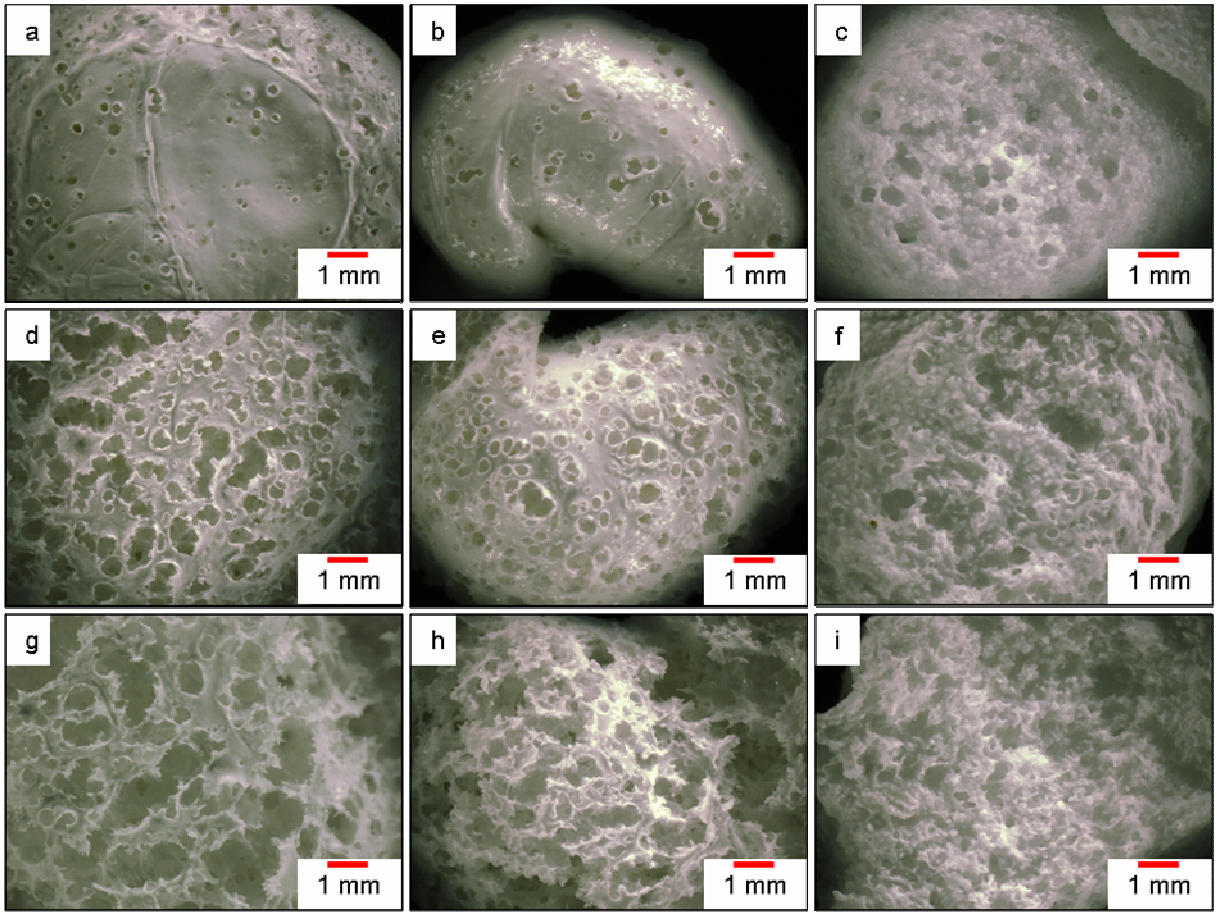

Figure 2-3: Surface of incubated IsHS with DMSO as plasticizer; formulations with 1 % NaCMC: a RG 503H 1:2, b RG 503H 1:3, c RG 502H 1:2; formulations with 5 % NaCMC: d RG 503H 1:2, e RG 503H 1:3, f RG 502H 1:2; formulations with 10 % NaCMC: g RG 503H 1:2, h RG 503H 1:3, i RG 502H 1:2.

In contrast, PEG-based formulations collapsed with 10 % NaCMC, whereas formulations with a 1:2 ratio (polymer:plasticizer) formed dense structures lacking in porosity. The best results for PEG-based systems were obtained for RG 503H based formulations with a polymer:plasticizer ratio of 1:3 (Figure 2-4). The standard incubation protocol consisted of direct injection into PBS. As an alternative, admixing the IsHS with the previously determined maximum PBS-amounts ensuring persistent moldability (see 2.2.2.1) prior to their application into PBS (“preincubated”) generated comparable morphology of the resulting specimens (Figure 2-4).

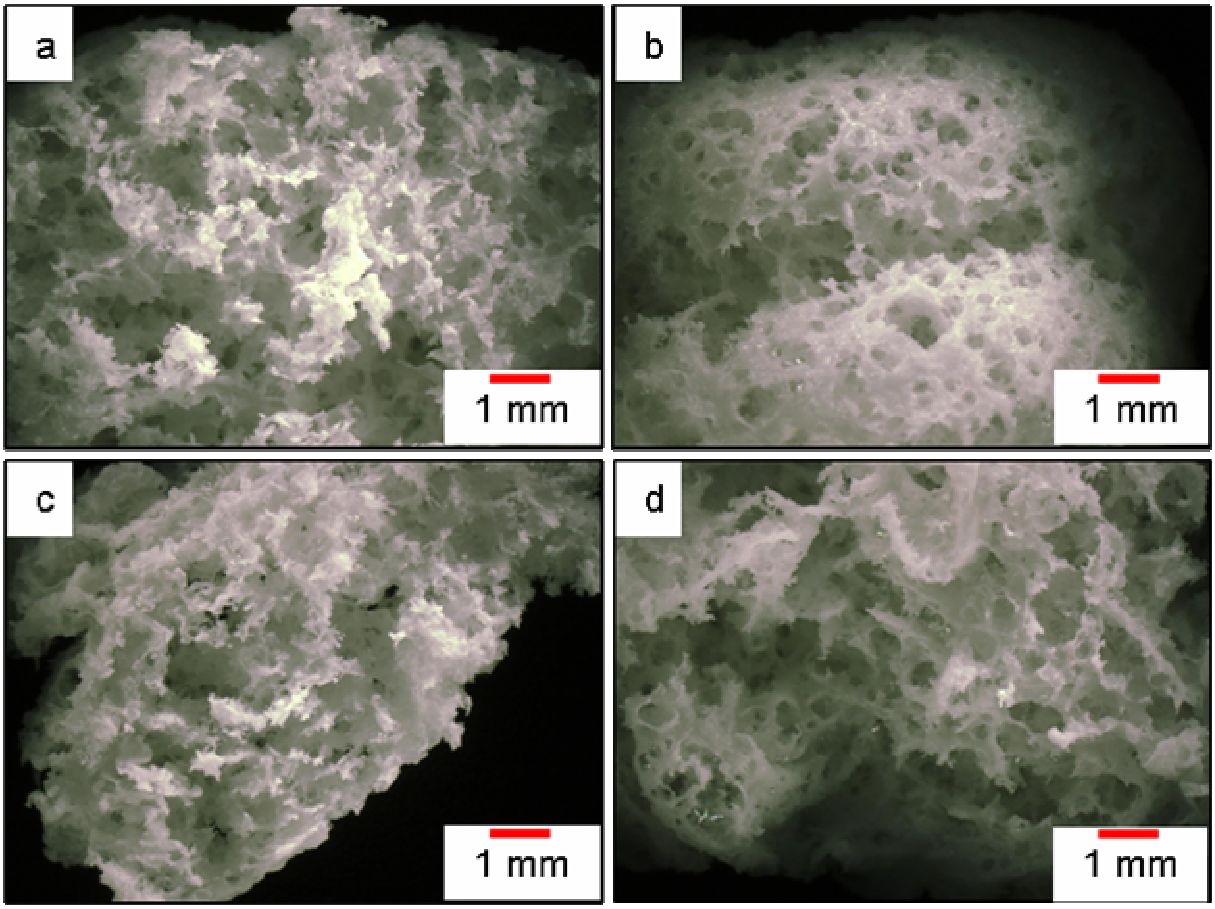

Figure 2-4: RG 503H-based IsHS with PEG 400 as solvent and 5 % NaCMC; standard incubation: a cross section, b surface; preincubated formulations: c cross section, d surface.

This is in accordance with Brodbeck et al., who reported that water addition to PLGA dissolved in NMP leads to faster solvent exchange upon contact with water without influencing the morphology of the hardened product [1999]. RG 502H 1:2 and RG 503H 1:3 with 10 % NaCMC for DMSO and NMP-based formulations and RG 503H 1:3 with 5 % NaCMC with PEG as plasticizer appeared to be the most promising candidates. These formulations showed the desired porosity and high PBS amounts could be admixed while moldability was maintained. Consequently, they were selected further cell compatibility testing (see 2.2.2.7).

2.3.3 Investigation of porosity

The used pore-forming agent NaCMC is conventionally used as tablet disintegrant [Khan and Rhodes, 1975]. By expansion of NaCMC upon contact with water, an increasing NaCMC content led to increased volumes of the specimens with high

porosity. Figure 2-5 shows the gravimetrically determined water-uptake-factor (as multiple of the dry mass) as a measure of porosity, known as water evaporation method.

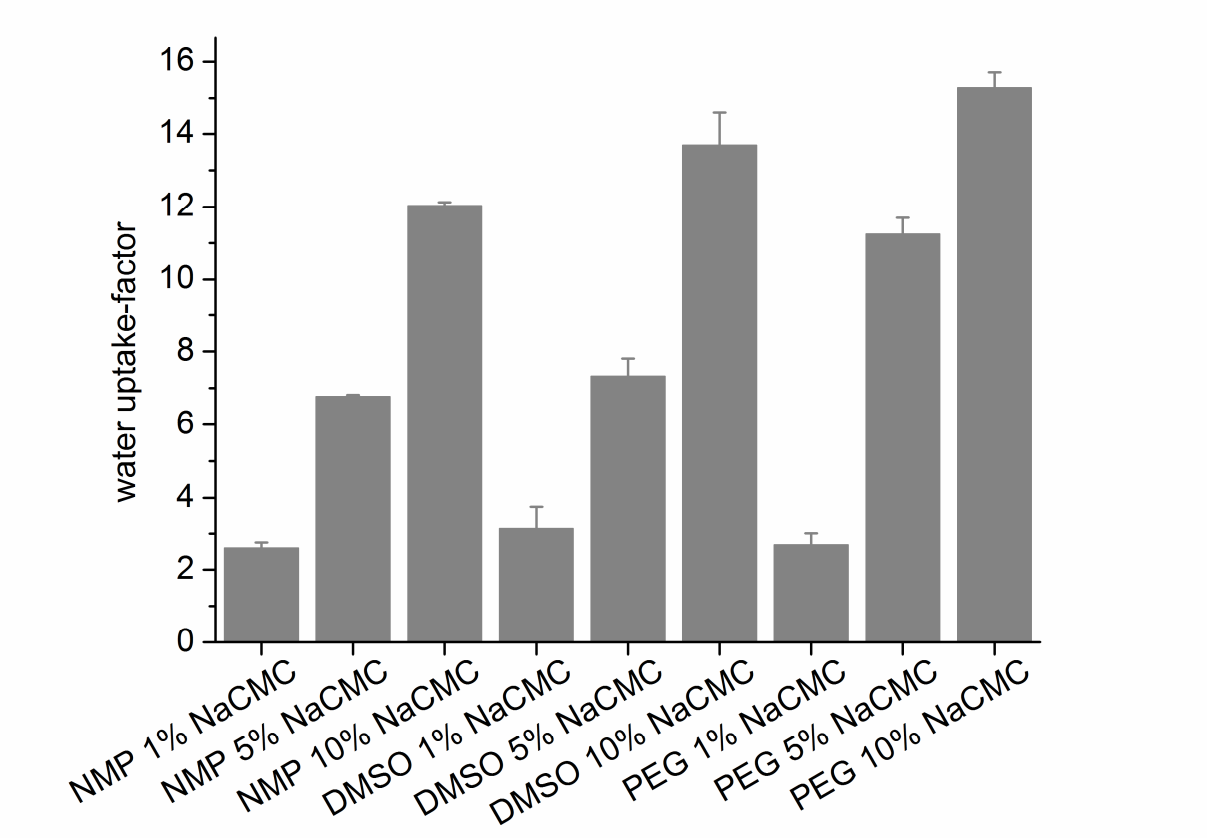

Figure 2-5: Water-uptake of hardened IsHS as multiple of the dry mass of fully soaked hardened specimens based on RG 503H 1:3 (w/w) formulations.

The total porosity of the resulting hardened specimens was calculated being 81.2 ± 2.1 % for 1 % NaCMC, 94.3 ± 1.6 % for 5 % NaCMC, and 96.5 ± 0.4 % for 10 % NaCMC. Khan and Rhodes reported that NaCMC adsorbed 50 % (w/w) water during 25 h of storage at 100 % relative humidity at 37 °C [1975]. With regards to that fact, porosity was calculated being 81.1 ± 2.1 % for 1 % NaCMC, 94.3 ± 1.6 % for 5 % NaCMC, and 96.5 ± 0.4 % for 10 % NaCMC. In comparison, the porosity of trabecular bone is reported to vary between 30 and more than 90 % [Carter and Hayes, 1977]. A pore size between 100 and 1000 µm is considered as ideal for growth of bony tissue within the implant and minimization of fibrous tissue at the interface between implant and tissue [Friess and Werner, 2008]. As determined by microscopy (see 2.2.2.3) this was given for 88.4 ± 2.8 % of the pores with no

statistically significant difference among the formulations. No difference between the surface and the cross-section of the specimens was observed, what can be ascribed to the defined particle size of the NaCMC.

2.3.4 Mechanical behavior

The wet and therewith moldable specimens were uniaxially compressed and the required force for compaction to 50 % of the initial height was measured and divided through the contact area of the compacting punch. As shown in Figure 2-6, the mechanical strength strongly decreased with increasing porosity (see 2.3.3), achieved by higher NaCMC concentrations ($p < 0.05$).

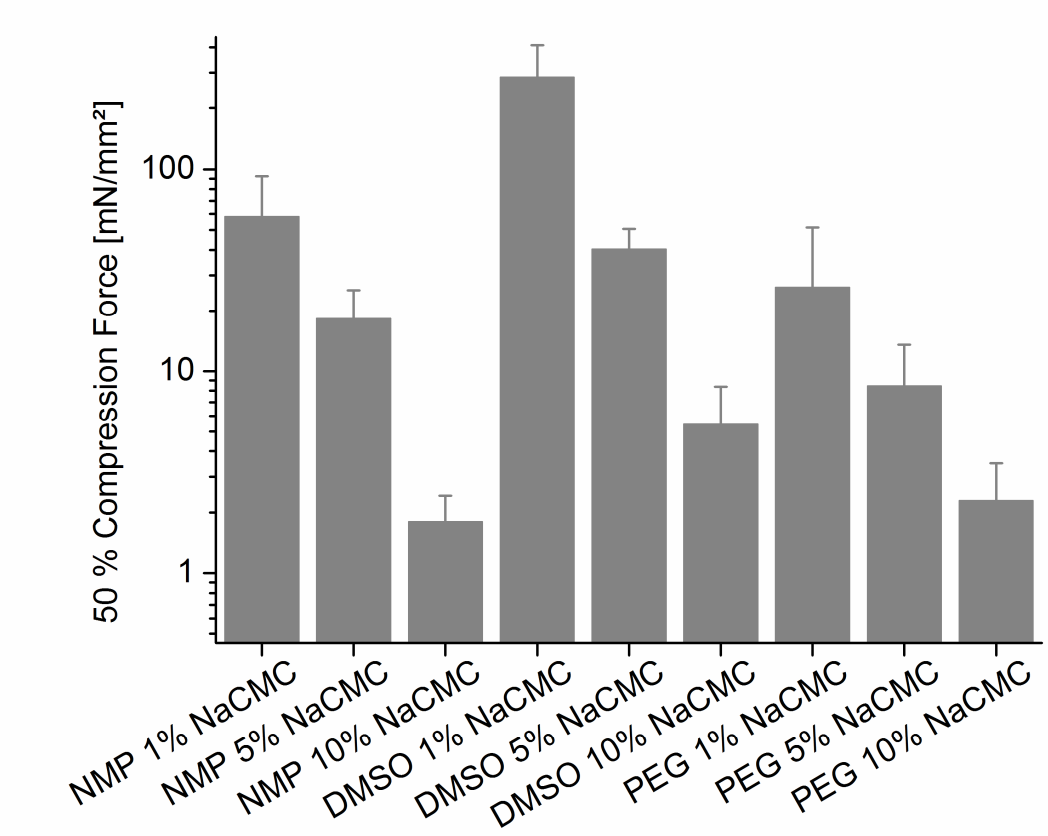

Figure 2-6: Compressive strength of fully soaked hardened specimens based on RG 503H 1:3 (w/w) formulations.

No statistically significant differences among the use of different plasticizers were observed. The highest value was obtained for the DMSO-based formulation containing 1 % NaCMC being 285 ± 125 mN/mm², which is around 10 times higher

than for mineralized collagen [Gelinsky et al., 2008] and around 6 times higher compared to a collagen/hydroxyapatite (50:50) composite material [Ciardelli et al., 2010]. The lowest force of 1.8 ± 0.6 mN/mm² for compression to 50 % original height was required for the NMP-based formulation containing 10 % NaCMC. For completely soaked pure collagen-scaffolds values lower than 1 mN/mm² were reported [Geiger, 2001]. Tissue pressure is normally near 0 and pressures above 1.3 – 4 mN/mm² can lead to inadequate perfusion [Whitesides et al., 1975]. A pressure of 4 mN/mm² would result in a compression of the developed scaffolds with NMP or DMSO and 5 % NaCMC or less to 74.4 % of their original height at most. Figure 2-7 illustrates that all samples were highly elastic as they relaxed to their dimensions prior to compression to 66 – 90 % depending on the formulation.

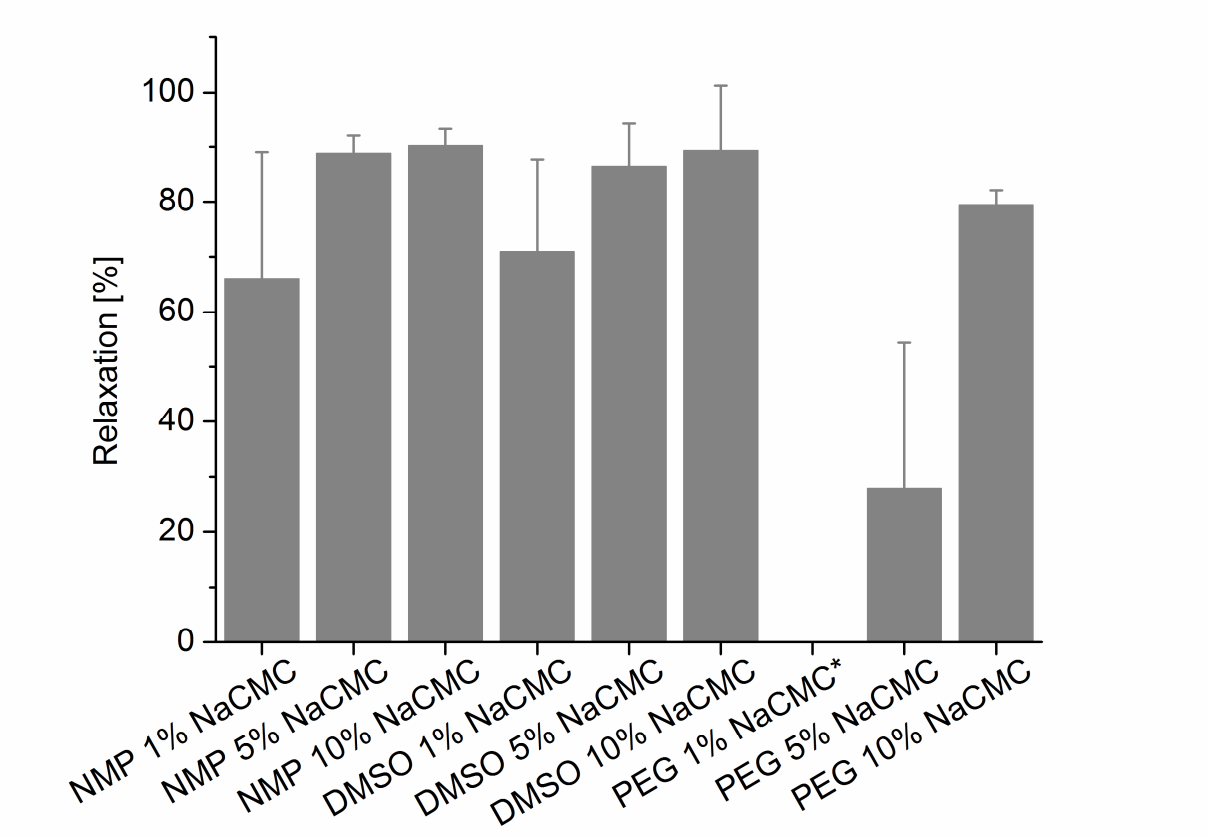

*Figure 2-7: Relaxation of previously compressed, fully soaked hardened specimens based on RG 503H 1:3 (w/w) formulations as % of regained former height; * scaffolds collapsed during vacuum drying.*

Higher NaCMC contents led to higher relaxations, statistically significant ($p < 0.05$) for the DMSO and NMP-based formulations with 1 % NaCMC compared to 5 or 10 %. The most pronounced relaxation as percentage of regained height after

compression was obtained for the DMSO and NMP-based specimens containing 10 % NaCMC with 89,4 ± 11.9 % and 90.2 ± 3.1 % respectively. The lowest value was observed for the 5 % NaCMC containing PEG-based specimens with 27.9 ± 26.5 %. After compression and subsequent vacuum drying, the PEG-based specimens with 1 % NaCMC in the formulation were too brittle for further investigation. Regarding their compressive strength, elasticity, and high porosity we consider the NMP and DMSO-based formulations with 5 % NaCMC as ideal candidates as bone graft substitutes for non weight-bearing application sites.

2.3.5 Cell survival in plasticizers

Cell compatibility of the used organic solvents was consequently evaluated. Figure 2-8 shows pictures obtained by fluorescence microscopy after live-dead staining of cells incubated for 5 min in mixtures of cell culture medium with 30 % and 60 % of PEG, NMP, and DMSO at 37 °C.

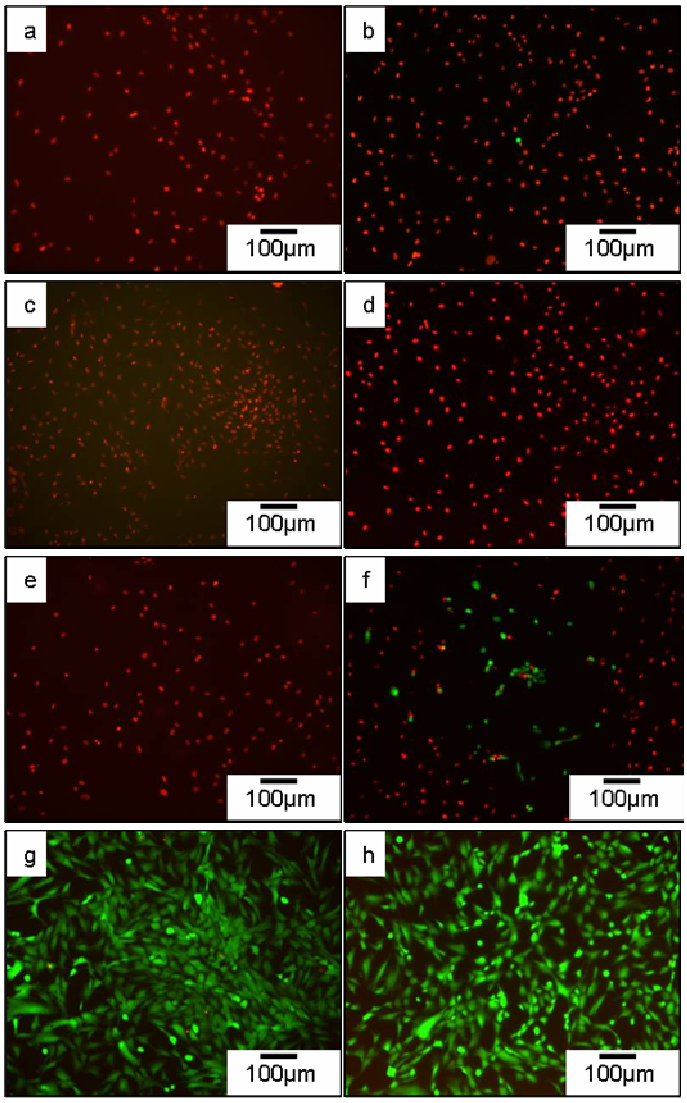

Figure 2-8: Live/dead assay of plasticizer-incubated SCP-1 cells after 5 min. incubation; a&b DMSO 60 % & 30 %, c&d NMP 60 % & 30 %, e&f PEG 60 % & 30 %, g&h controls.

Picture f shows several viable SCP-1 cells after 5 minutes incubation in cell culture medium containing 30 % PEG. All other incubation protocols at RT resulted in non-viable cells. Consequently, cell survival in presence of plasticizer concentrations necessary to maintain a moldable IsHS (see 2.3.1) is not given. Higher temperatures are supposed to increase membrane permeability [Bischof et al., 1995] and cooling is an appropriate way to reduce metabolism [Ducommun et al., 2002]. Therefore, in an attempt to enhance viability the experiments were performed at 4 °C to induce a metabolic arrest of the cells and thereby extend their vitality. Figure 2-9 shows the results of live/dead-assay of the cell incubation with 30 and 60 % organic solvent performed at 4 °C.

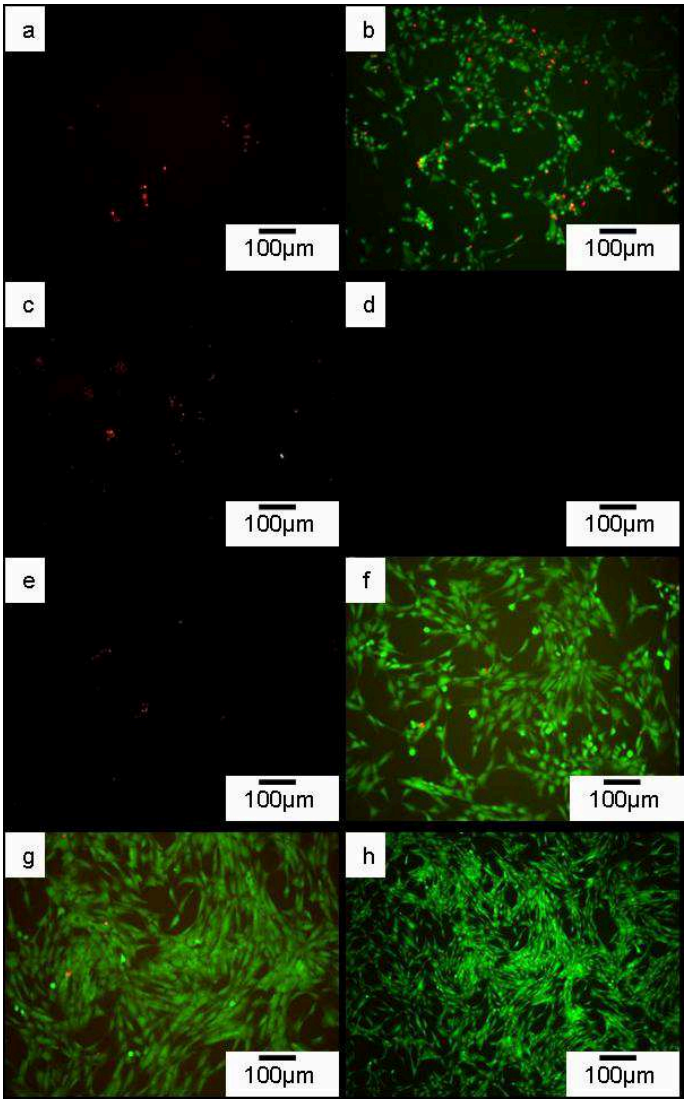

Figure 2-9: Live/dead assay of plasticizer-incubated SCP-1 cells after 5 min. incubation at 4 °C; a&b DMSO 60 % & 30 %, c&d NMP 60 % & 30 %, e&f PEG 60 % & 30 %, g&h controls.

SCP-1 cells were able to maintain their viability after incubation with 30 % DMSO or PEG after 5 minutes incubation at 4 °C (Figure 2-9 b & f), whereas cells were not able to resist 60 % solvent. Incubation with NMP did not leave adherent cells in the well behind. The LD_{50} for PEG 300 in rats is reported to be 17 g/kg and the solvent is known to cause necrotic reactions at the administration site [Smyth et al., 1950]. But tissue response was considered to be a mild chemical inflammation and damage was nonpermanent [Carpenter and Shaffer, 1952]. PEG 400 is FDA-approved for i.v. and i.m.-administration in concentrations of up to 20.3 % [FDA, 2011]. The LD_{50} for NMP is reported with 4 g/kg in rats [Lee et al., 1987]. For DMSO an LD_{50} of 12 g/kg in rats is reported [David, 1972]. DMSO is also used to reduce the damage resulting from

cryopreservation in concentrations of up to 10 % [Stylianou et al., 2006]. DMSO is FDA-approved for subcutaneous implants in a dosage of up to 104 mg. Assuming the body weight of a rat to be 300 g, the LD_{50} values would be exceeded by the administration of the following dosages of formulations with a ratio of 1:3 (polymer:plasticizer) containing 5 % NaCMC: 9.8 g for PEG, 2.3 g for NMP, and 6.9 g for the DMSO based formulation. Taking those facts into account, we expected a certain, but less pronounced cell death in presence of the tested solvents. We expect the formulation to harm cells lethally in the first instance after administration. In vivo studies are required to evaluate the clinical relevance of this assumption. But after solvent exchange and thereby hardening a mechanically stable, open porous structure will result and allow a cellular ingrowth and nutrient exchange. Nevertheless, we performed cell incorporation tests to elucidate the vitality of the cells in the complete formulation.

2.3.6 Cell incorporation

We further evaluated the incorporation of cells into the previously optimized in-situ hardening system. Key challenge was to maintain cell viability in the presence of the organic solvents by keeping their concentrations at the lowest possible levels. On the one hand precipitation studies of the different polymer solutions revealed a maximum PBS-content in the solvent-phase of 35.9 % for RG 502H dissolved 1:2 in DMSO. On the other hand, biocompatibility testing of the solvents showed that only 30 % organic solvent can be tolerated. This leaves a gap where viability was uncertain. Consequently, IsHS were mixed with SCP-1 cells containing cell culture medium that represented the maximum that could be admixed retaining the formability of the systems. The cell viability results are depicted in Figure 2-10.

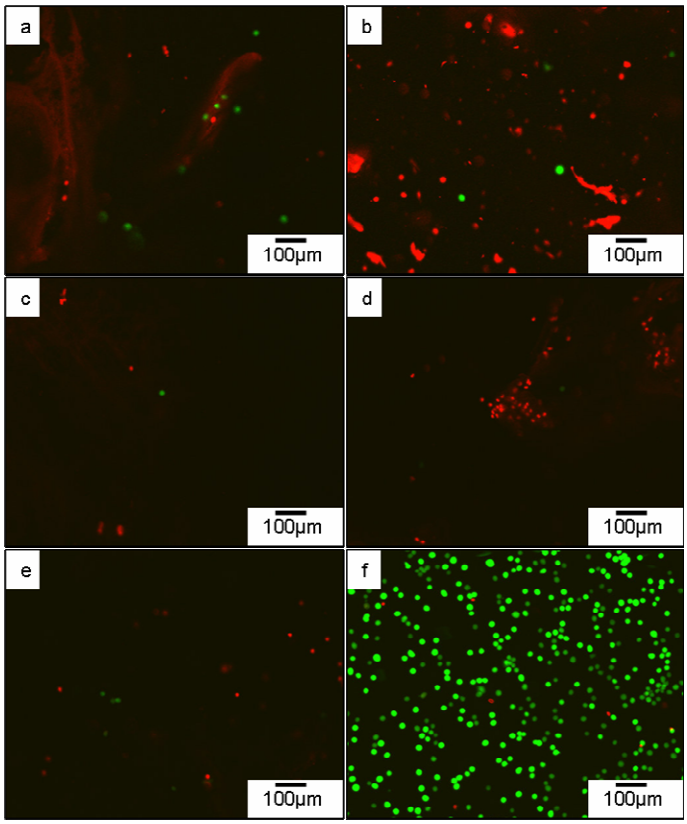

Figure 2-10: Live/dead assay of SCP-1 cells after direct addition to IsHS at 4 °C, a RG 502H, 1:2, 10 % NaCMC, DMSO, b RG 502H, 1:2, 10 % NaCMC, NMP, c RG 503H, 1:3, 10 % NaCMC, DMSO, d RG 503H, 1:3, 10 % NaCMC, e RG 503H, 1:3, 5 % NaCMC, PEG, f control.

A very low number of cells maintained their viability. Moreover, the phenomenon can likely be ascribed to cells being dispersed in the medium and attaching to the specimen instantaneously prior to microscopic analysis. The overall incorporation efficacy is low, suggesting that the cells did not adhere to the material, whereas the contact time with the organic plasticizers is considered to be too long to maintain cell viability. To overcome this adherence problem and to shorten the contact time with the organic plasticizers, cells were precultivated for 24 h directly on the TCP-powder. Figure 2-11 shows that the adherence-problem was successfully overcome by the preseeding procedure, while the cells were not able to maintain their vitality. Therefore, we conclude that the high amounts of organic solvents hinder a direct incorporation of cells into the IsHS. The hardening system remains a promising biomaterial for non weight-bearing application sites due to its porosity, mechanical behavior, and convenient application mode.

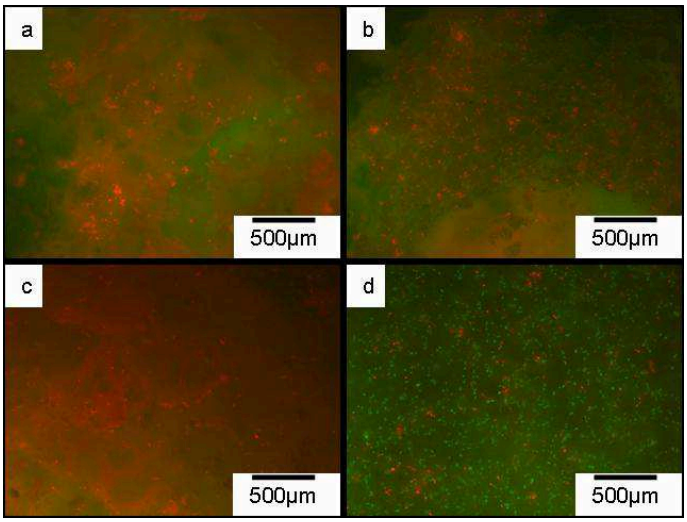

Figure 2-11: Live/dead assay of IsHS with SCP-1 cells preseeded on the TCP-powder at 4 °C, a RG 503H, 1:3, 10 % NaCMC, DMSO, b RG 503H, 1:3, 10 % NaCMC, NMP, c RG 503H, 1:3, 5 % NaCMC, PEG, d control.

2.3.7 Cell settlement on hardened IsHS

For the applicability of the system as a bone grafting material cellular adhesion and cell survival are prerequisites. This was investigated by cell seeding on hardened scaffolds prepared of the IsHS by solvent exchange and subsequent drying. Figure 2-12 demonstrates excellent cell compatibility after 24 h solvent exchange and hardening of the IsHS.

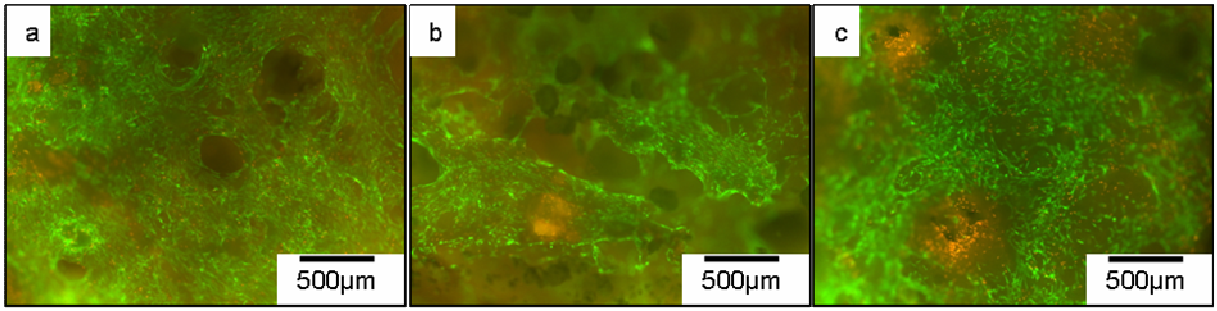

Figure 2-12: Live/dead assay of SCP-1 cells seeded on IsHS hardened in PBS for 24 h at 37°C; a RG 503H, 1:2, 1 % NaCMC, DMSO, b RG 503H, 1:2, 1 % NaCMC, NMP, c RG 503H, 1:2, 1 % NaCMC, PEG.

Thus, in vivo the materials will provide good scaffolds for tissue regeneration. The formulations could also be used to generate scaffolds ex vivo of the desired shape and size by using specific molds for solvent exchange.

2.4 Conclusion

The aim of the present study was to develop an injectable, putty-like in-situ hardening system based on PLGA. The materials can be adapted to the desired size and shape for bony applications, what is especially beneficial for the augmentation of voids resulting e.g. from resections. It was of special interest to optimize porosity and mechanical strength of the hardened structure. In addition, a special focus was placed on the understanding of the interaction of the material with cells. On the one hand cell survival in the solvent based system was studied and on the other hand cell compatibility of the hardened structure with SCP-1 cells was tested. We investigated several polymers, solvents, and polymer:plasticizer-ratios. Mechanical properties were adapted by the incorporation of an inorganic filler and porosity was adjusted by admixing NaCMC as a pore forming agent. Semi-solid formulations were found, which, after solvent exchange hardened and provided highly porous 3D constructs while maintaining mechanical resistance to uniaxial compression, beneficial for cellular ingrowth. The addition of aqueous medium to the polymer-solution did not alter the morphology of the corresponding implants nor change the system from being a formable putty besides precipitation and increased viscosity. Cells were successfully incorporated into the formulation via cultivation on α-TCP prior to the final mixing with the remnant IsHS-formulation. However, the viability of the SCP-1 cells could not be maintained during this procedure. We conclude that a cell-enriched in-situ hardening system based on PLGA cannot be realized with the organic solvents used in this study. Upon administration of the cell-free IsHS-formulation the contained solvent is expected to locally damage cells in the very beginning, but should soon provide a highly cell compatible environment. However, the clinical relevance of this phenomenon needs to be addressed in further in vivo studies. The developed formulations can furthermore be used to generate scaffolds ex vivo of the desired shape and size by using specific molds for solvent exchange. Cell compatibility of the hardened system is fully given and cells can penetrate the system and maintain their viability. Overall, an optimized formulation for a putty-like system, which generates a highly porous, mechanically stable scaffold at the site of application was successfully developed.

2.5 Acknowledgments

The above work has been supported by the Bavarian Research Foundation and is embedded in the “ForZebRA”-project.

2.6 References

Agrawal C. M., Athanasiou K. A., Technique to control pH in vicinity of biodegrading PLA-PGA implants, Journal of Biomedical Materials Research, 38 (1997) 105-114.

Benichou G., Direct and indirect antigen recognition: The pathways to allograft immune rejection, Frontiers in Bioscience, 4 (1999) 476-480.

Bischof J. C., Padanilam J., Holmes W. H., Ezzell R. M., Lee R. C., Tompkins R. G., Yarmush M. L., Toner M., Dynamics of cell membrane permeability changes at supraphysiological temperatures, Biophysical Journal, 68 (1995) 2608-2614.

Böker W., Yin Z., Drosse I., Haasters F., Rossmann O., Wierer M., Popov C., Locher M., Mutschler W., Docheva D., Schieker M., Introducing a single-cell-derived human mesenchymal stem cell line expressing hTERT after lentiviral gene transfer, Journal of Cellular and Molecular Medicine, 12 (2008) 1347-1359.

Brodbeck K. J., DesNoyer J. R., McHugh A. J., Phase inversion dynamics of PLGA solutions related to drug delivery: Part II. The role of solution thermodynamics and bath-side mass transfer, Journal of Controlled Release, 62 (1999) 333-344.

Carpenter C. P., Shaffer C. B., A study of the polyethylene glycols as vehicles for intramuscular and subcutaneous Injection, Journal of the American Pharmaceutical Association, 41 (1952) 27-29.

Carter D., Hayes W., The compressive behavior of bone as a two-phase porous structure, Journal of Bone & Joint Surgery, American Volume, 59 (1977) 954-962.

Ciardelli G., Gentile P., Chiono V., Mattioli-Belmonte M., Vozzi G., Barbani N., Giusti P., Enzymatically crosslinked porous composite matrices for bone tissue regeneration, Journal of Biomedical Materials Research. Part A, 92A (2010) 137-151.

David N. A., The pharmacology of dimethyl sulfoxide, Annual Review of Pharmacology, 12 (1972) 353-374.

Ducommun P., Ruffieux P. A., Kadouri A., von Stockar U., Marison I. W., Monitoring of temperature effects on animal cell metabolism in a packed bed process, Biotechnology and Bioengineering, 77 (2002) 838-842.

Dunn R. L., English J. P., Cowsar D. R., Vanderbilt D. D., Biodegradable in-situ forming implants and methods of producing the same, US Patent 5739176, (1998).

Dunn R. L., English J. P., Cowsar D. R., Vanderbilt D. P., Biodegradable in-situ forming implants and methods of producing the same, US Patent 4938763, (1990).

Eliaz R. E., Kost J., Characterization of a polymeric PLGA-injectable implant delivery system for the controlled release of proteins, Journal of Biomedical Materials Research, 50 (2000) 388-396.

Food and Drug Administration, Inactive ingredient search for approved drug products, Silver Spring, USA, 2011, Access: February 21, 2011, Last updated: January 12, 2011, http://www.accessdata.fda.gov/scripts/cder/iig/getiigWEB.cfm

Friess W., Werner J., Biomedical Applications, in: Handbook of Porous Solids 5, Schüth F., Sing K. S. W., Weitkamp J. (Eds.), Wiley-VCH Verlag GmbH, Weinheim, Germany, (2008), 2923-2970.

Ge Z., Tian X., Heng B. C., Fan V., Yeo J. F., Cao T., Histological evaluation of osteogenesis of 3D-printed poly-lactic-co-glycolic acid (PLGA) scaffolds in a rabbit model, Biomedical Materials, 4 (2009a) 21001.

Ge Z., Wang L., Heng B. C., Tian X., Lu K., Fan V. T. W., Yeo J. F., Cao T., Tan E., Proliferation and differentiation of human osteoblasts within 3D printed poly-lactic-co-glycolic acid scaffolds, Journal of Biomaterials Applications, 23 (2009b) 533-547.

Geiger M., Porous collagen/ceramic composite carriers for bone regeneration using recombinant human bone morphogenetic protein-2 (rhBMP-2), Dissertation, (2001), Friedrich-Alexander-University, Erlangen.

Gelinsky M., Welzel P. B., Simon P., Bernhardt A., König U., Porous three-dimensional scaffolds made of mineralised collagen: Preparation and properties of a biomimetic nanocomposite material for tissue engineering of bone, Chemical Engineering Journal, 137 (2008) 84-96.

Giannoudis P. V., Einhorn T. A., Marsh D., Fracture healing: The diamond concept, Injury, 38 (2007) S3-S6.

Göpferich A., Polymer bulk erosion, Macromolecules, 30 (1997) 2598-2604.

Groeneveld E. H. J., van den Bergh J. P. A., Holzmann P., ten Bruggenkate C. M., Tuinzing D. B., Burger E. H., Mineralization processes in demineralized bone matrix grafts in human maxillary sinus floor elevations, Journal of Biomedical Materials Research, 48 (1999) 393-402.

Haasters F., Prall W. C., Anz D., Bourquin C., Pautke C., Endres S., Mutschler W., Docheva D., Schieker M., Morphological and immunocytochemical characteristics indicate the yield of early progenitors and represent a quality control for human mesenchymal stem cell culturing, Journal of Anatomy, 214 (2009) 759-767.

Hatefi A., Amsden B., Biodegradable injectable in situ forming drug delivery systems, Journal of Controlled Release, 80 (2002) 9-28.

Hutmacher D. W., Scaffolds in tissue engineering bone and cartilage, Biomaterials, 21 (2000) 2529-2543.

Karande T. S., Ong J. L., Agrawal C. M., Diffusion in musculoskeletal tissue engineering scaffolds: design issues related to porosity, permeability, architecture, and nutrient mixing, Annals of Biomedical Engineering, 32 (2004) 1728-1743.

Kempe S., Metz H., Mäder K., Do in situ forming PLG/NMP implants behave similar in vitro and in vivo? A non-invasive and quantitative EPR investigation on the mechanisms of the implant formation process, Journal of Controlled Release, 130 (2008) 220-225.

Khan K. A., Rhodes C. T., Water-sorption properties of tablet disintegrants, Journal of Pharmaceutical Sciences, 64 (1975) 447-451.

Kurz L. T., Garfin S. R., Booth R. E. J., Harvesting autogenous iliac bone grafts: a review of complications and techniques, Spine, 14 (1989) 1324-1331.

Lee K. P., Chromey N. C., Culik R., Barnes J. R., Schneider P. W., Toxicity of N-methyl-2-pyrrolidone (NMP): teratogenic, subchronic, and two-year inhalation studies, Fundamental and Applied Toxicology, 9 (1987) 222-235.

Lewis D. H., Controlled Release of Bioactive Agents from Lactidel Glycolide Polymers, in: Biodegradable Polymers as Drug Delivery Systems, Chasin M., Langer R. S. (Eds.), Marcel Dekker, New York, (1990), 1-42.

Matschke C., Isele U., van Hoogevest P., Fahr A., Sustained-release injectables formed in situ and their potential use for veterinary products, Journal of Controlled Release, 85 (2002) 1-15.

Moucha C. S., Renard R. L., Gandhi A., Lin S. S., Tuan R. S., Bone Allograft Safety and Performance, in: Engineering of Functional Skeletal Tissues 3, Bronner F., Farach-Carson M. C., Mikos A. G. (Eds.), Springer London, (2007), 46-54.

Park T. G., Degradation of poly(d,l-lactic acid) microspheres: effect of molecular weight, Journal of Controlled Release, 30 (1994) 161-173.

Patel D. B., A review on atrigel drug delivery system, Journal of Global Pharma Technology, 2 (2010) 85-90.

Polzer H., Volkmer E., Saller M. M., Prall W. C., Haasters F., Drosse I., Anz D., Mutschler W., Schieker M., Long-term detection of fluorescently labeled hMSC in vitro and in vivo by semi-automated microscopy, Tissue Engineering Part C: Methods, 18 (2011) 156-165.

Pompe C., Development of new in-situ hardening and bioactivated composite materials for orthopedic indications, Dissertation, (2008), Ludwig-Maximilians-University, Munich.

Price J. S., Tencer A. F., Arm D. M., Bohach G. A., Controlled release of antibiotics from coated orthopedic implants, Journal of Biomedical Materials Research, 30 (1996) 281-286.

Seiler J. G., 3rd, Johnson J., Iliac crest autogenous bone grafting: donor site complications, Journal of the Southern Orthopaedic Association, 9 (2000) 91-97.

Smyth H. F., Jr., Carpenter C. P., Weil C. S., The toxicology of the polyethylene glycols, Journal of the American Pharmaceutical Association, 39 (1950) 349-354.

Stylianou J., Vowels M., Hadfield K., Novel cryoprotectant significantly improves the post-thaw recovery and quality of HSC from CB, Cytotherapy, 8 (2006) 57 - 61.

Whitesides T. E., Haney T. C., Morimoto K., Harada H., Tissue pressure measurements as a determinant for the need of fasciotomy, Clinical Orthopaedics and Related Research, 113 (1975) 43-51.

3 Residual Transglutaminase in Collagen – Effects, Detection, Quantification and Removal

This chapter has been published in the European Journal of Pharmaceutics and Biopharmaceutis:
Schloegl W., Klein A., Fürst R., Leicht U., Volkmer E., Schieker M., Jus S., Guebitz G. M., Stachel I., Meyer M., Wiggenhorn M., Friess W., Residual transglutaminase in collagen – Effects, detection, quantification, and removal, European Journal of Pharmaceutics and Biopharmaceutics, 80 (2012) 282-288.

Abstract

In the present study, we developed an enzyme-linked immunosorbent assay (ELISA) for microbial transglutaminase (mTG) from *Streptomyces mobaraensis* to overcome the lack of a quantification method for mTG. We further performed a detailed follow-on-analysis of insoluble porcine collagen type I enzymatically modified with mTG primarily focusing on residuals of mTG. Repeated washing (4x) reduced mTG-levels in the washing fluids but did not quantitatively remove mTG from the material ($p < 0.000001$). Substantial amounts of up to 40 % of the enzyme utilized in the crosslinking mixture remained associated with the modified collagen. Binding was non-covalent as could be demonstrated by Western blot analysis. Acidic and alkaline dialysis of mTG treated collagen material enabled complete removal the enzyme. Treatment with guanidinium chloride, urea, or sodium chloride was less effective in reducing the mTG content.

3.1 Introduction

Collagen is a widely used biomaterial for biomedical applications like wound healing sutures, spongy implants, injectable dispersions, or controlled release systems. However, a major drawback of sheets or porous systems made from collagen is the lack of mechanical stability. This deficiency may be overcome by applying external crosslinking to regain stability or to even provide mechanical strength beyond the natural capacity lost during the isolation processes [Friess, 1998; Friess and Schlapp, 2001]. Widely used chemical crosslinking methods comprise residue problems with potential or well-known toxicity [Speer et al., 1980]. Enzymatic crosslinking might help to circumvent this situation. Microbial transglutaminase (mTG) derived from *Streptomyces mobaraensis* is a commonly used enzyme in pharmaceutical research and food industry as well as in tissue engineering and biomaterials research [Besheer et al., 2009; Fontana et al., 2008; Garcia et al., 2008; O Halloran et al., 2006; Zhu et al., 1995]. It catalyzes the formation of a covalent amide bond between an ε-amino-group of a lysine residue and the γ-carboxamid group of a glutamine residue [Folk, 1980]. It is a 38 kDa non-glycosylated 331 amino-acid protein with one single cysteine residue, which is essential for its catalytic activity [Ando et al., 1989; Kanaji et al., 1993]. Crystal structure and the catalytic scheme have been discovered [Kashiwagi et al., 2002] and an activity-assay for tissue type II transglutaminase has been developed [Raghunath et al., 1998]. The effects of transglutaminases in tissue engineering have been intensively studied [Zeugolis et al., 2010]. Cells seeded on mTG-treated collagen show better adhesion, proliferation, and osteogenic differentiation [Chau David et al., 2005]. It has been reported that treatment with mTG increases the storage modulus of chicken sternal collagen type II [O Halloran et al., 2006], enhances neovascularisation of wound healing constructs made of bovine calf skin type I collagen [Garcia et al., 2008] and increases tensile strength and melting temperature of porcine skin collagen type I [Chen et al., 2005]. However, in these studies, the obtained materials were analyzed without any purification and, thus, not considering potential residuals of mTG. Ciardelli et al. attempted to remove mTG by washing the specimens twice with water but did not elucidate, whether residuals were left [2010]. The question arises

whether the obtained results were due to mTG-mediated crosslinking of the collagen or due to other effects that can be ascribed to mTG-residuals. This has become even more important since Stachel et al. reported that mTG does not establish ε-(γ-glutamyl)-lysine bonds in native collagen type I derived from both calf skin and bovine hide [2010]. Even though mTG seems to exhibit no cytotoxicity [Chen et al., 2005; O Halloran et al., 2006], it might provoke severe immune responses as any foreign protein can. From the analytical point of view, the determination of the enzymatic activity of mTG has been established in the 1960s [Folk and Cole, 1965] but this procedure, however, cannot be utilized to detect residuals in mTG-treated materials due to the potential activity loss resulting from material processing. The present publication closes the described analytical gap in mTG-quantification developing a specific ELISA, which can detect mTG in presence of collagen. Furthermore, it helps to give more insight into the fate of mTG after its addition to the substrate, its interactions, removal, and potential residuals.

3.2 Materials and Methods

All water used was highly purified and deionized with the help of a USF ELGA PURELAB Plus UV/UF water purifier (Ransbach-Baumbach, Germany). All chemicals were purchased from Sigma-Aldrich (St. Louis, MO, USA), unless otherwise stated. For Elisa, Maxisorp® 96-well flat-bottom plates were purchased from Nunc Inc. (Roskilde, Denmark), rabbit anti-bacterial-transglutaminase antibody (A019) was from ZEDIRA GmbH (Darmstadt, Germany), mouse anti-bacterial-transglutaminase antibody (Cov3C7) and biotinylated rabbit anti-mouse IgG were from Covalab (Villeurbanne, France), and streptavidin poly-HRP Calbiochem® was obtained from Merck KGaA (Darmstadt, Germany).

3.2.1 mTG modification of collagen

Porcine-skin derived collagen-suspension was prepared according to Meyer et al. [2010] and freeze-dried (Christ Epsilon 2-6D®, Osterode am Harz, Germany) to obtain insoluble porcine collagen type I raw material. The dried collagen (nonxl) was dispersed in 800 mL Soerensen-buffer (pH 6.0) at a concentration of 0.5 % (w/w) as

transglutaminase is more active around neutral pH. AktivaWM® transglutaminase (activity: 51.8 U/g) from Ajinomoto (Hamburg, Germany) was added at 2 g/L for “tgxl” samples and 5 g/L for “tgxl high” samples. The enzymatic activity therefore was 20.7 U/g collagen for tgxl and 51.8 U/g collagen for tgxl high, respectively. The mTG-preparation was used without further purification and therefore contained 99 % maltodextrin. The initial content of pure mTG in tgxl and tgxl high collagen was then calculated to be 0.4 % and 1 %, respectively. The dispersion was incubated at 30 °C for 2 h and centrifuged at 2739 g (Sigma 4K15®, Osterode am Harz, Germany) after incubation. The supernatants (770 mL of the initial 800 mL) were removed, and pH values were measured before freezing the material at -40 °C for further ELISA-analysis. The pellets were washed four times by resuspending each with 150 mL water (pH adjusted to 3.7 with concentrated acetic acid). This pH condition (pH 3.7) was chosen to ensure that both, collagen with an isoelectric point of 7.8 and mTG, for which an isoelectric point of 9 has been reported by Ando et al. [1989], show a highly positive net charge resulting in substantial repulsive interaction. After centrifugation, the washing solutions were collected, pH-values were measured, and the solutions were subsequently deep-frozen at -40 °C for further analysis. The mTG-modified collagen pellets were freeze dried. Collagen treated with either Kristallpur RC 0811 maltodextrin “malto” (Hafen-Muehlen-Werke GmbH, Bremen, Germany) or heat inactivated mTG (95 °C, 45 min.) “inactivated” were processed in the same manner as tgxl-material to obtain references.

3.2.2 Collagen sample preparation

Samples were prepared by dispersing the different collagen materials (nonxl, tgxl, tgxl high, malto, inactivated) in water (pH adjusted to 3.7 with concentrated acetic acid) at a concentration of 2 % (w/w). After swelling for 4 h, the dispersions were homogenized with an ESGE® immersion blender (Unold AG, Germany). Dispersion-aliquots of 1.5 mL per well were distributed in Costar® polystyrene 24-well plates (Corning Inc., Corning, USA) and freeze dried.

3.2.3 Melting temperature

Melting temperatures were determined using a Mettler Toledo DSC821^{e} differential scanning calorimeter. Therefore, 3 mg samples (n=3) were incubated with 10 µL PBS-buffer in 40 µL aluminum crucibles (Mettler, ME-26763) for at least 2 h at room temperature and then heated from 20 to 90 °C with a heating rate of 10 K/min.

3.2.4 Enzymatic degradation

Collagen samples of 6 mg (n=3) were incubated in 1 ml TES-buffer (N-tris(hydroxymethyl)methyl-2-aminoethanesulfonic acid, adjusted to pH 7.4 with 1 M sodium hydroxide) at 37 °C for one hour to allow wetting and swelling of the collagen. 20 µg collagenase (*Clostridium histolyticum* type H, Sigma) was added to each sample and incubated for 2, 5, or 24 h. Samples were centrifuged with 186,000 g (Optima TLX-CA, Beckman Coulter, Brea, CA, USA) for 45 min at 4 °C and the supernatants were removed. Supernatants of the 24 h incubation were analyzed by ELISA and Western blot. To evaluate whether mTG was degraded by collagenase under these conditions, mTG alone was treated in the same way. After vacuum drying, the weight loss was determined gravimetrically.

3.2.5 Tensile strength measurement

For tensile strength measurements, strips of 10 x 50 mm displaying a height of 3 - 5 mm (determined with a caliper) were manufactured by dispersing the collagen materials of interest in water (pH adjusted to 3.7 with concentrated acetic acid) at a concentration of 2 %, followed by swelling for 4 h, homogenization with an ESGE® immersion blender (Unold AG, Germany) and freeze drying in polyethylene molds. Cutting with a scalpel rendered the desired dimensions. The obtained strips were incubated in PBS for at least 2 h at room temperature (RT). The wet specimens (n=6) were elongated with a Texture Analyser XTPlus (Stable Microsystems, UK) at a speed of 0.5 mm/s at RT until rupture and the highest force measured was divided through the cross-section areas of the corresponding collagen strips.

3.2.6 ELISA-procedure

For the development of an ELISA for mTG, all incubation steps were performed at RT on an orbital shaker (Titramax 101, Heidolph Instruments GmbH, Schwabach, Germany) at 150 RPM unless otherwise stated. Microplate wells were coated for 4 h with 100 µL of 2 µg/mL rabbit anti-mTG antibody (ZEDIRA) in 50 mM carbonate buffer (pH 9.6). Plates were rinsed five times with wash/dilution buffer (10 mM phosphate buffer (pH 7.4) containing 0.1 % polysorbate 20 and 0.5 M sodium chloride) and blocked with 200 µL of 0.5 % BSA in wash/dilution buffer for one hour followed by five washing steps with wash/dilution buffer. For preparation of the calibration curves, mTG-preparation was diluted to concentrations between 100 ng/mL and 5 µg/mL (i.e. mTG concentration: 1-50 ng/mL) in TES-buffer (N-tris(hydroxymethyl)methyl-2-aminoethanesulfonic acid) adjusted to pH 7.4 with 1 M sodium hydroxide and incubated for 24 h at 37 °C in the presence or absence of collagenase (19.6 µg/mL). Calibration standards and protein samples were added to the wells (100 µL) and incubated overnight at 4 °C without agitation. After rinsing five times with wash/dilution buffer, 100 µL of mouse anti-mTG antibody (Covalab; 1 µg/mL in wash/dilution buffer) were added to each well and incubated for 1 h and subsequently washed five times. 100 µL of biotinylated IgG H + L (Covalab; 1 µg/mL in wash/dilution buffer) was added to each well and incubated for 1 h, followed by five washing steps and the subsequent addition of 100 µL streptavidin poly-HRP (Merck; 0.1 µg/mL in wash/dilution buffer). After one hour of incubation, the plate was rinsed five times with wash/dilution buffer before the addition of 100 µL citric acid buffer solution (pH 5) containing 0.005 % H_2O_2 and 0.5 mg/mL o-phenylenediamin. The reaction was stopped by adding 100 µL of 1 N H_2SO_4 after 6 min, and the absorbance was measured at 490 nm with a FLUOstar Omega® microplate reader (BMG LABTECH GmbH, Offenburg, Germany).

3.2.7 Western blot analysis

Samples were prepared according to 3.2.4 or without the addition of collagenase. Standard Laemmli sample buffer was added, and samples were boiled for 5 min at 95 °C. Sodium dodecylsulfate polyacrylamide gel electrophoresis (SDS-Page, Bio-Rad, Munich, Germany) was performed and separated proteins were transferred

onto Hybond-ECL nitrocellulose membranes (Amersham Biosciences, Freiburg, Germany) by tank electroblotting. Membranes were blocked with bovine serum albumin (Sigma Aldrich). A rabbit polyclonal anti-mTG antibody (1:1,000, overnight incubation) from ZEDIRA (Darmstadt, Germany) was used as primary antibody. For detection, horseradish peroxidase-labeled goat anti-rabbit antibody (1:10,000, 2 h incubation) from DIANOVA (Hamburg, Germany) and ECL Plus Western Blotting Detection Reagent from GE Healthcare (Munich, Germany) were used. The appearing luminescence was detected by exposure (1 min.) of the membrane to an X-ray film (Super RX, Fuji, Düsseldorf, Germany), which was subsequently developed with a Curix 60 developing system (AGFA-Gaevert, Cologne, Germany).

3.2.8 Dialysis

Dialysis was performed to reduce mTG concentration in tgxl samples. Collagen material (tgxl) and mTG as reference were dispersed at concentrations of 10 % in HCl (pH 2) or NaOH (pH 12). After swelling for 2 h, the materials were placed in Spectra/Por® PVDF membranes with a 500 kDa cut-off (Spectrum® Laboratories Inc., Rancho Dominguez, CA, USA) and dialyzed in three consecutive steps (3 h, 18 h, and 3 h) against 1.5 L HCl (10mM, pH 2) or NaOH (10 mM, pH 12) per g collagen or mTG, respectively. The dialyzed samples were freeze dried to obtain material for Western blot and ELISA determination after enzymatic degradation. As reference, the materials (tgxl and mTG) were treated accordingly at pH 2 or pH 12 without dialysis.

3.2.9 Washing with additives

Nonxl and tgxl collagens were dispersed at a concentration of 1 % (m/m) in 100 mL water containing either 1 M sodium chloride, guanidinium chloride, or urea with an ESGE® immersion blender (Unold AG, Germany) and incubated for 18 h at RT. The dispersions were sonified for 5 min after 1, 16, and 17 h using a USC1200TH ultrasonic device (VWR, Darmstadt, Germany). After centrifugation at 2739 g (Sigma 4K15®, Osterode am Harz, Germany), the supernatants were removed and the

collagens were washed twice with 100 mL water. Finally, the collagen materials were lyophilized and analyzed by Western blot (see 3.2.7).

3.3 Results and Discussion

3.3.1 Melting temperature

The melting temperature (T_m) or denaturation temperature is a parameter obtained during DSC-analysis of collagen samples. T_m strongly depends on the hydration of the collagen molecules. This hydration obviously depends on the water content of the samples [Miles and Ghelashvili, 1999; Zeugolis and Raghunath, 2010] and T_m increases with decreasing water content. But T_m also increases with increasing crosslinking degree [Miles et al., 2005]. To compare different crosslinking degrees of the collagen samples, the measurements were performed in the presence of an excess of water. Thus, a fully hydrated state is achieved, and differences caused by a different water content on T_m can be ruled out [Zeugolis and Raghunath, 2010]. The starting material used in our studies displayed a T_m of 60.1 ± 0.6 °C. This T_m is in agreement with native fibrillar collagen. The T_m for mTG-treated collagen (tgxl) was 58.6 ± 0.5 °C. The melting temperature for "tgxl high" material was 58.4 ± 0.9 °C. This finding is in accordance with Collighan et al. who previously reported no effect on T_m for mTG and guinea pig liver transglutaminase (gTG) treatment of bovine hide or soluble rat collagen [2004]. Furthermore, the results correspond to the findings of Stachel et al. who reported that acid soluble collagen type I does not act as a substrate for mTG in the native state [2010]. However, Ciardelli et al. presented contradictory results revealing an increase of T_m by ~18 K for acid soluble calf skin collagen type I incubated with mTG (0.025 U/mg of protein) for 30 min at 37 °C [2010]. Since these latter authors used an incubation temperature of 37 °C, their results are again in good agreement with the findings of Stachel et al. who reported that mTG-derived crosslinks are formed at 37 °C, whereas they are not established at 30 °C incubation temperature [2010]. Taking these findings into account, the effect of mTG-treatment of collagen on T_m depends on the raw material being soluble or insoluble, on the incubation temperature as well as on alkaline or acidic pretreatments. Furthermore, in the case of the insoluble, acid derived porcine

material presented here, the crosslinking degree of the raw material is already at a high level and incubation temperature was low to maintain its native state. Therefore, mTG-treatment did not lead to a further increase in T_m.

3.3.2 Enzymatic degradation

For collagen material characterization, the resistance to enzymatic degradation by collagenase is a commonly used in vitro model. The gravimetrical determination is an established method since the work of Olde Damink et al. [1995; 1996]. Rault et al. showed that crosslinking of calf skin collagen with hexamethylene-diisocyanate (HMDC) and 1-ethyl-3-(3-dimethyl-aminopropyl)carbodiimide (EDC) reduces enzymatic degradation [1996]. In Figure 3-1, the degradation rate of collagen is presented as a function of time.

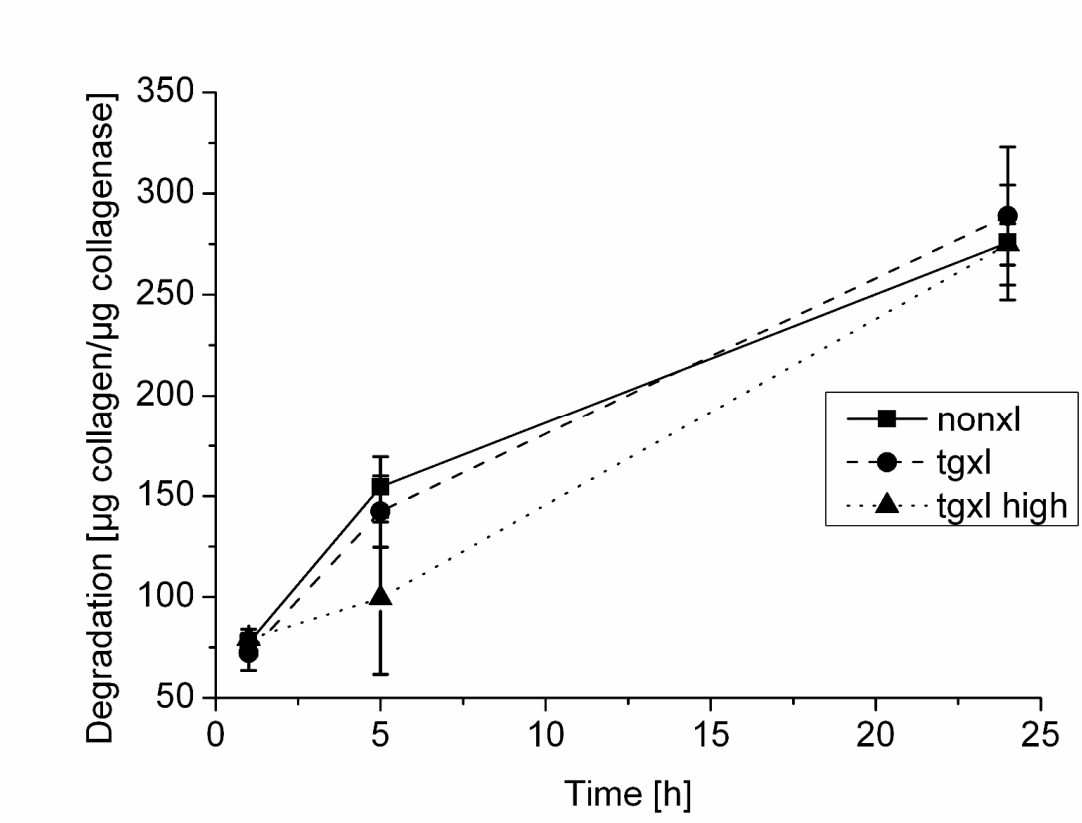

Figure 3-1: Degradation rates as a function of time of collagen raw material (nonxl) and mTG-treated collagen material (tgxl (0.004 g mTG/g collagen) & tgxl high (0.01 g mTG/g collagen)) subjected to 20 µg Clostridium histolyticum collagenase per 6 mg collagen.

After 2 and 24 h, the degraded amount is not influenced by mTG-treatment, contradicting Ciardelli et al. who reported reduced enzymatic degradation by ~50 % for calf skin collagen type I incubated with mTG (0.025 U/mg of protein) for 30 min at 37 °C [2010]. However, after 5 h of incubation, the values of the samples that had been modified with the higher mTG-concentration indicate a slightly, but not significantly, higher resistance to collagenase. It is important to note that ultracentrifugation was mandatory to obtain meaningful data, whereas centrifugation at only 2739 g did render irreproducible and varying results.

3.3.3 Tensile strength

Figure 3-2 shows the displacement data of the nonxl and tgxl collagen strips during their elongation until rupture. The highest force obtained for each sample was taken to calculate the force upon rupture of the wet strips, which is presented in Figure 3-3.

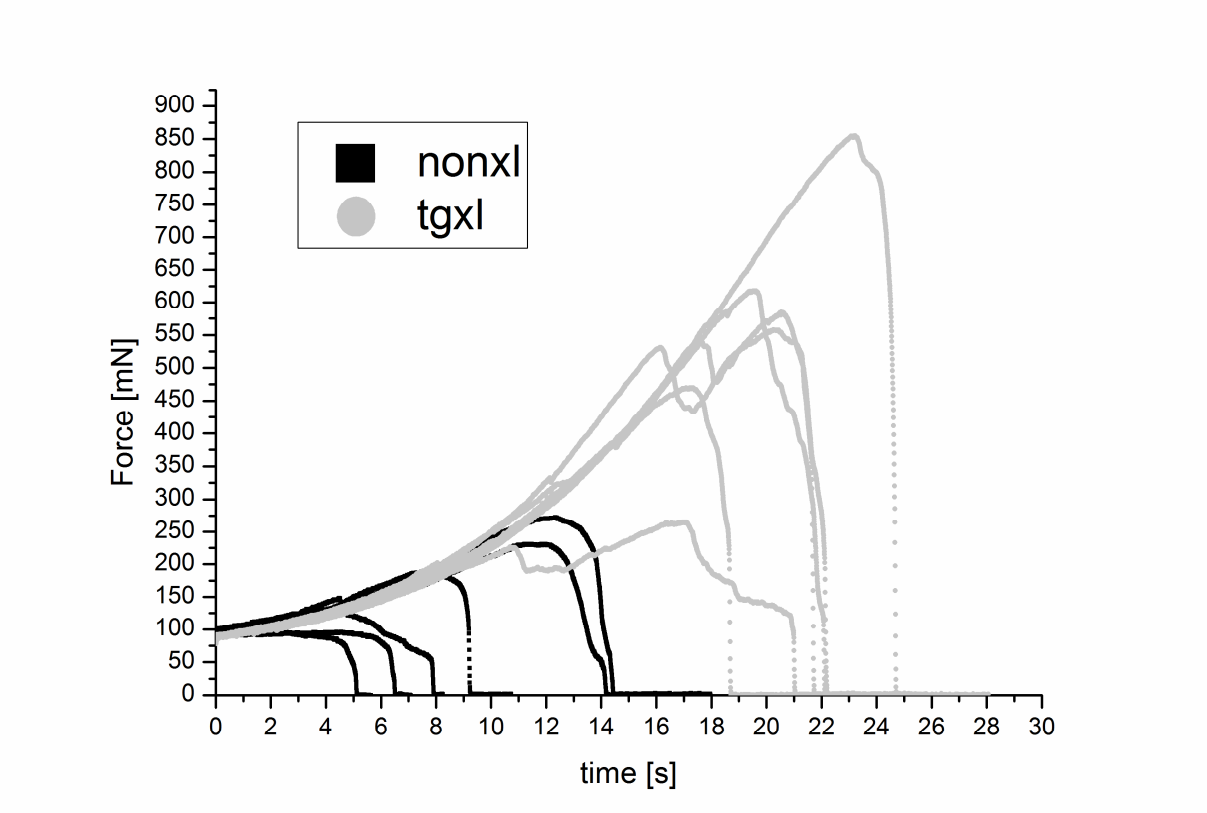

Figure 3-2: Displacement-data (0.5 mm/s) of elongated wet collagen strips (2 % collagen content), raw material (nonxl) and mTG-treated collagen (tgxl (0.004 g mTG/g collagen)) recorded with a Texture Analyser XTPlus.

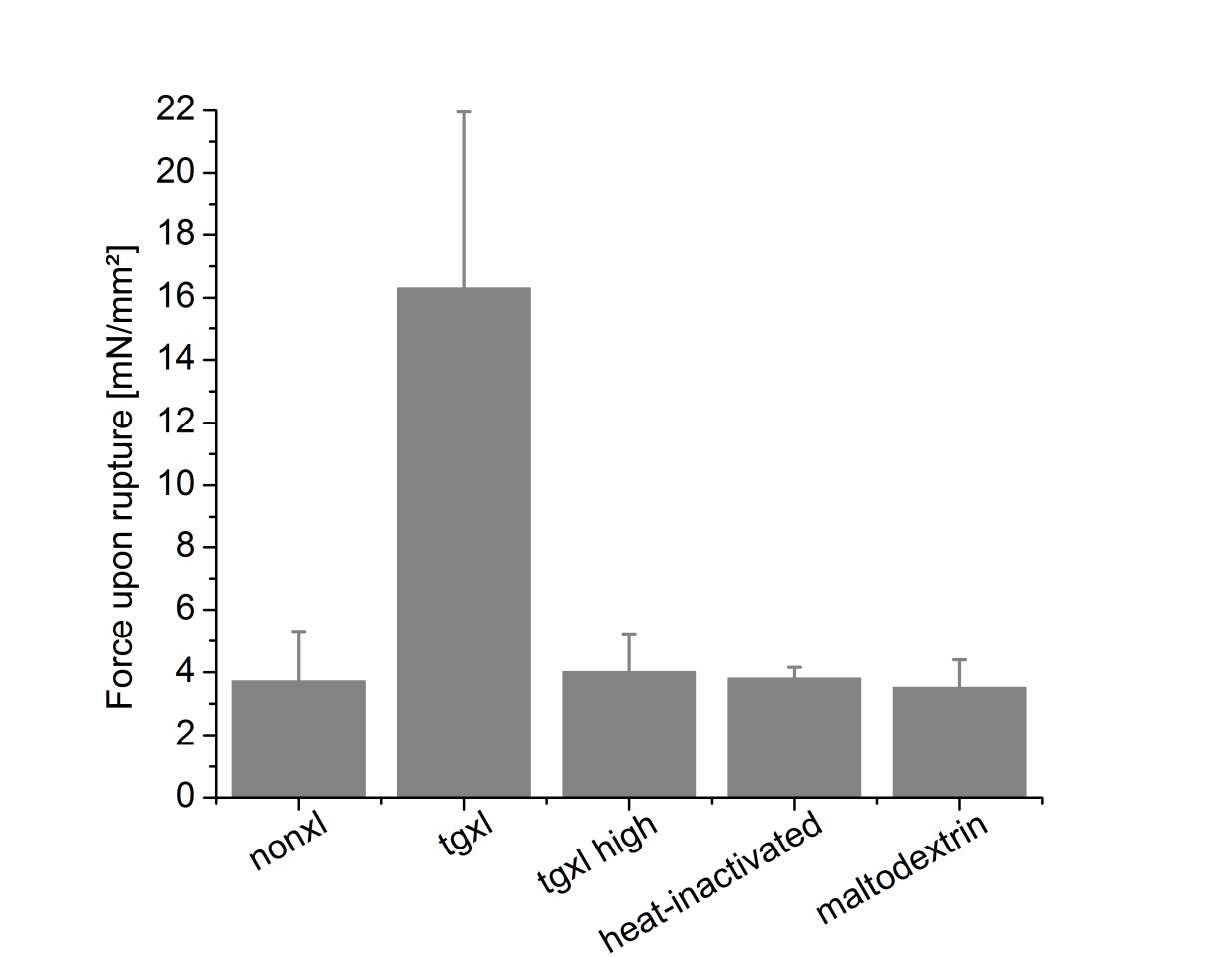

Figure 3-3: Force upon rupture of wet collagen samples: untreated material (nonxl), mTG-treated collagen (tgxl (0.004 g mTG/g collagen), tgxl high (0.01 g mTG/g collagen), heat inactivated) and maltodextrin-treated collagen.

The maximum force increased from 3.7 mN/mm² for the unmodified insoluble collagen to 16.3 mN/mm² for the mTG-treated tgxl material. The difference was proven to be statistically significant ($p < 0.01$) using a t-test. The general finding of increasing tensile strength by mTG-treatment is in accordance with literature, even though some of the reported data in literature lack control values for untreated raw material [Chen et al., 2005]. The increase in tensile strength being 440 % for the mTG-treated material is remarkable considering that it cannot be ascribed to the formation of ε-(γ-glutamyl)-lysine bonds, which is the typical reaction product of mTG-catalysis [Folk, 1980], since Stachel et al. showed that these bonds are not established in native acid soluble bovine calf skin collagen type I under the tested conditions [2010] and insoluble collagen material should be a less suitable substrate. Freeze-drying might induce crosslinking by dehydrating conditions, but the nonxl material as well as the controls (maltodextrin only and heat inactivated

transglutaminase) was freeze dried according to the same protocol. The tensile strength values obtained for collagen treated with inactivated mTG or maltodextrin were similar to the nonxl material. Therefore, we can exclude a contribution of the freeze-drying steps to the increased tensile strength. What in fact increases tensile strength of the mTG treated collagen samples can only be hypothesized. We assume that mTG itself interacts with the collagen leading to better coherence. The tgxl high collagen exhibited a tensile strength comparable to the untreated material. After incubation with mTG, the dispersion appeared grainy and homogeneity could not be achieved during treatment with the immersion blender. Therefore, finding the ideal incubation conditions for modification with mTG is of crucial interest for material modification. After dialysis at pH 2 or pH 12, a tensile strength-determination is not feasible due to amide-bond hydrolysis occurring under these conditions that led to a strong decrease in tensile strength (data not shown).

3.3.4 Western blot analysis

Western blot analysis was performed to evaluate, whether the washing steps enable the removal of mTG from the treated collagen material, and to gain insight into the type of interactions between collagen and mTG.

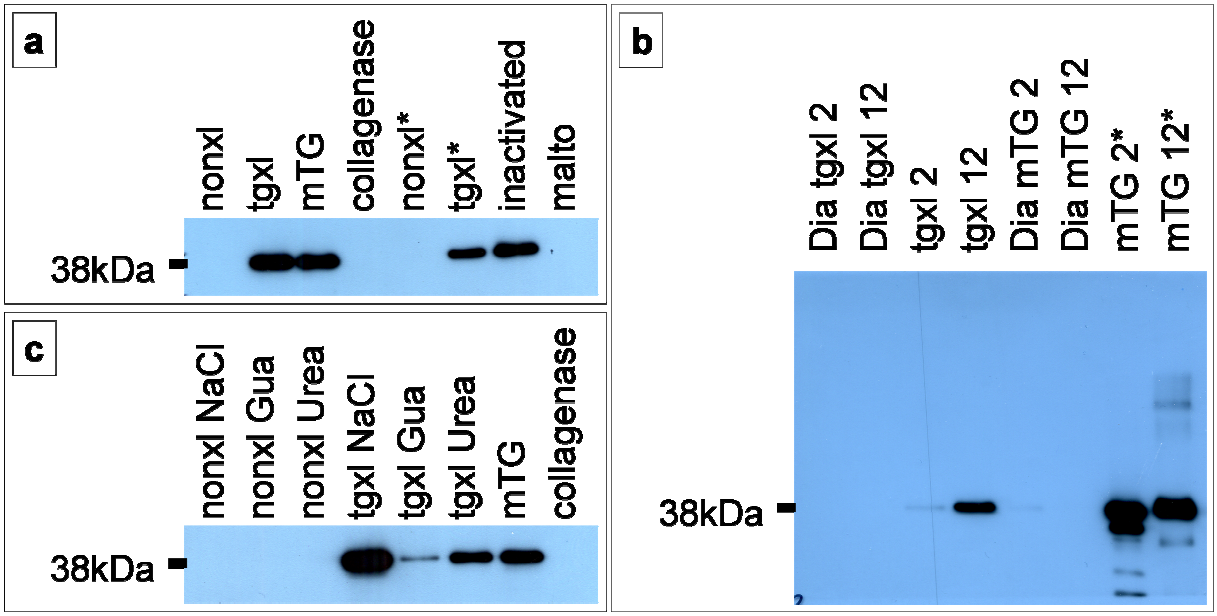

Figure 3-4: Western blot, samples marked with (*) were not subjected to collagenase; a collagen raw material (nonxl), mTG-treated collagen (tgxl (0.004 g mTG/g collagen)), mTG-only, collagenase-only, collagen treated with heat inactivated mTG (inactivated) and maltodextrin-only control; b dialyzed mTG (Dia mTG) and dialyzed mTG-treated collagen (Dia tgxl) at pH 2 & 12 and undialyzed controls; c mTG-treated collagen (tgxl (0.004 g mTG/g collagen)) after washing with NaCl, urea or guanidiniumchloride and controls.

Figure 3-4a shows a band for mTG at around 38 kDa, which is in accordance with previously reported results [Ando et al., 1989]. The mTG band is equally present in the enzymatically degraded tgxl collagen (lane 2 from the left) as well as in the tgxl sample not treated with collagenase (lane 6 from the left). As expected, mTG was not detected in the nonxl materials or controls. Obviously, mTG was not degraded by collagenase under the tested conditions and was therefore still accessible for analytical methods. Furthermore, the results show that the enzyme could not be quantitatively removed during washing steps. The distinct mTG band in the non-degraded tgxl material revealed that mTG was not completely removed from mTG-

treated collagen materials by four washing steps with water (pH adjusted to 3.7 with concentrated acetic acid). A clear quantification was not feasible, but the band intensity indicated the presence of substantial amounts of mTG. Microbial transglutaminase was not covalently bound to collagen as it could still be separated during electrophoresis.

3.3.5 ELISA of washing solutions

Despite numerous washing steps with water (pH adjusted to 3.7 with concentrated acetic acid), Western blot analysis rendered considerable amounts of mTG that remained in the tgxl-material. Quantification of mTG in the incubation medium after mTG-modification as well as in the washing fluids (see 3.2.1) should allow the calculation of the total amount of mTG that had been removed from the reaction mixture and consequently the mTG-amount remaining in the tgxl material. Figure 3-5 demonstrates the decrease of mTG-concentration in the washing fluids with each washing step.

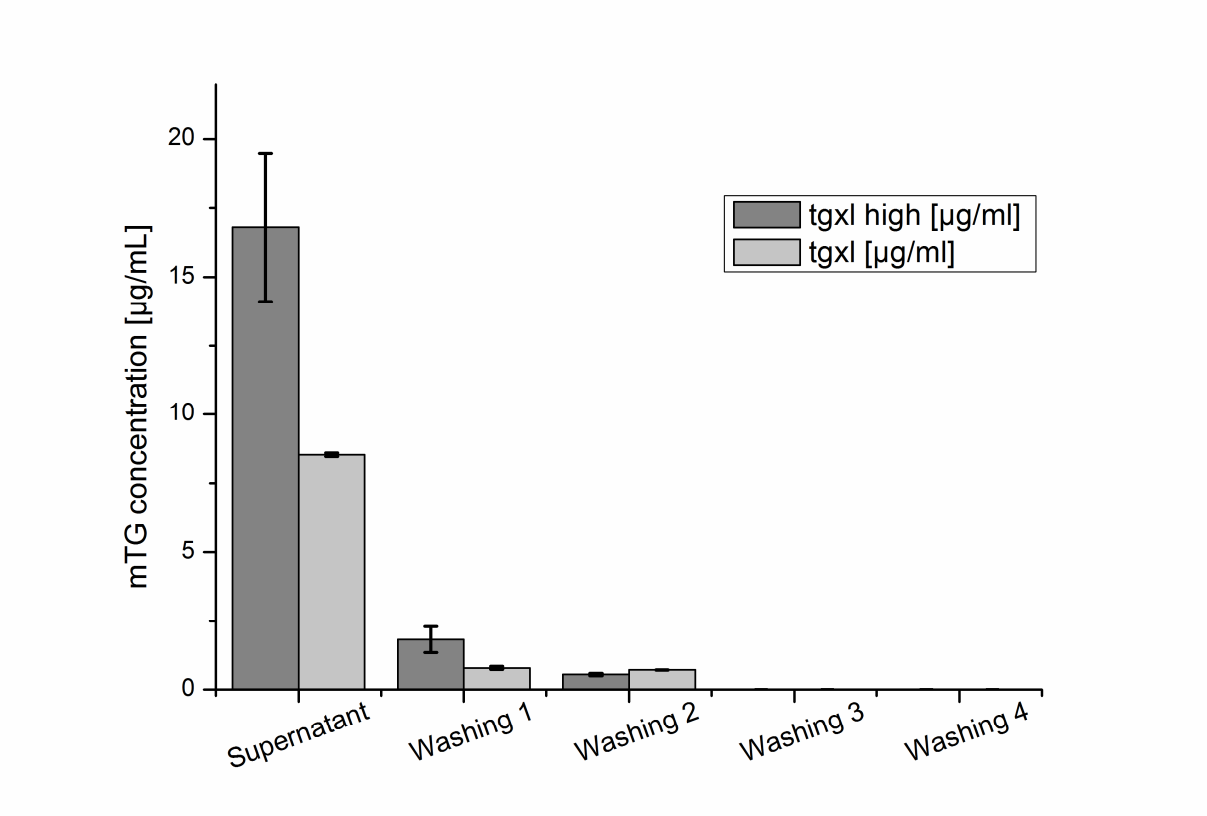

Figure 3-5: Concentration of mTG in incubation-solution and in the washing fluids (washing 1-4) of mTG-treated collagen (tgxl (0.004 g mTG/g collagen) & tgxl high (0.01 g mTG/g collagen)) determined by ELISA.

The concentration determined in the supernatant after incubation and centrifugation was 8.54 µg/mL ± 0.68 µg/mL for tgxl and 16.80 µg/mL ± 2.68 µg/mL for tgxl high, respectively, whereas the initial concentration of mTG added for modification was either 20 µg/mL or 50 µg/mL. The third and the fourth washing step could only remove marginal amounts of the enzyme. The total amount of mTG that had been removed by all of the performed centrifugation and washing steps was 42.5 ± 7.8 % for the treatment leading to tgxl and 33.2 ± 16.1 % for the treatment leading to tgxl high. From these values, the residual amount of mTG in the collagen materials, based on the initial mTG amount during incubation, 0.4 % for tgxl and 1 % for tgxl high, can be calculated to be 0.23 ± 0.04 % mTG in the tgxl-collagen material and 0.66 ± 0.16 % mTG in the tgxl high collagen material, assuming that collagen itself was not removed during washing. This finding confirms the Western blot observation that mTG cannot be quantitatively removed by washing steps. The pH-value decreased with each washing step from 5.9 to 4.1 to 3.7 and finally to 3.7. This ensures that both, collagen with an isoelectric point of 7.8 and mTG, for which an isoelectric point of 9 has been reported by Ando et al. [1989], show a highly positive net charge resulting in substantial repulsive interaction. Additionally, Western blot analysis proved that the interaction is non-covalent (see 3.3.4). Furthermore, hydrophobic interactions are expected to be less pronounced between the two rather hydrophilic molecules. Consequently, we conclude that mTG is mechanically entrapped in a network created by its own catalytic activity in the mTG-treated collagen materials.

3.3.6 ELISA of collagen samples

To confirm the amount of mTG calculated to be still present in the collagen after reduction of the enzyme by washing steps, a direct quantification method for mTG in the collagen was evaluated. Therefore, the collagen material needed to be hydrolyzed by collagenase. Additionally, it had to be clarified whether or not collagenase interfered with the ELISA. Two calibration curves of mTG were prepared, one in the presence and one in the absence of collagenase. These curves are presented in Figure 3-6.

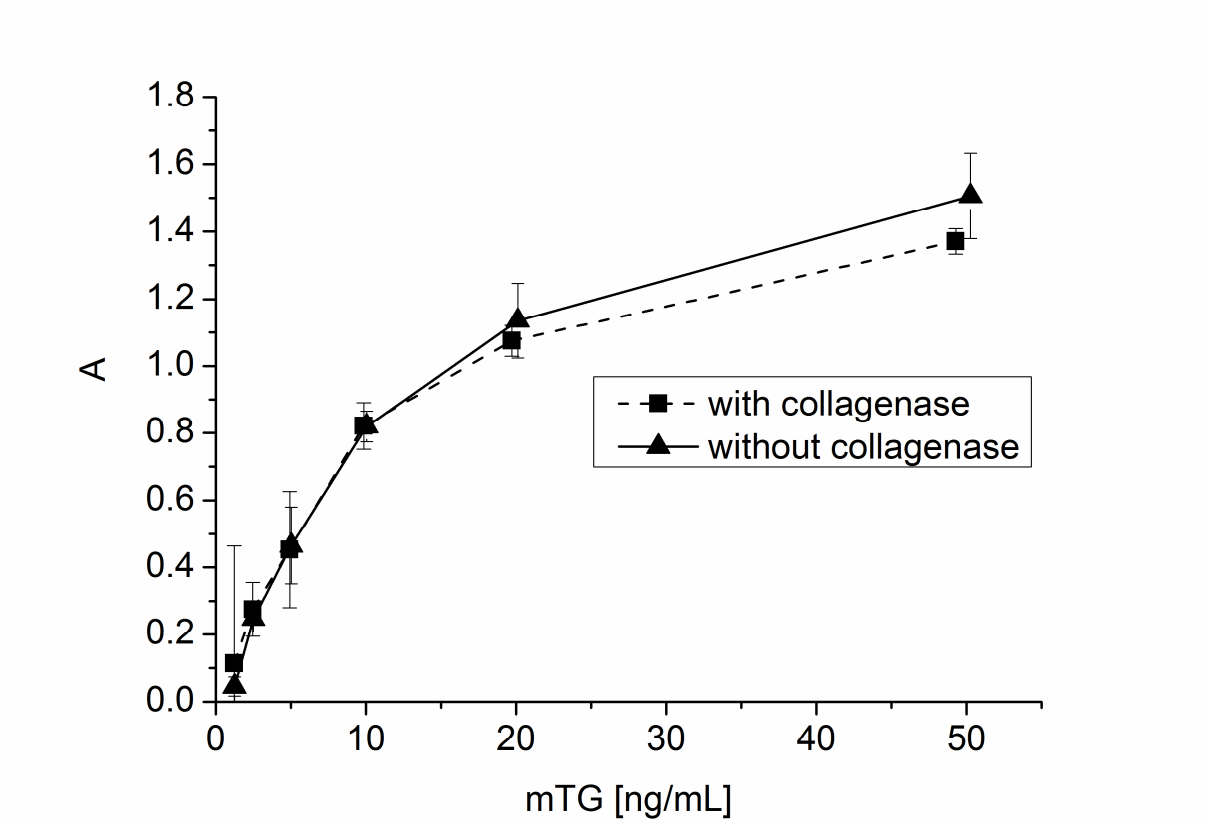

Figure 3-6: ELISA calibration curves (mTG-quantification) in the absence and in the presence of Clostridium histolyticum collagenase type H (20 µg collagenase, 24 h incubation, 37 °C).

As can be seen, no significant difference was observed, confirming that mTG is not degraded by collagenase under the tested conditions (mTG degraded according to 3.2.4) and that the enzyme is still accessible for Western blot and ELISA analysis. Therefore, the desired samples were enzymatically degraded (see 3.2.4) and mTG concentrations in the supernatants of the 24 h samples were determined with the newly developed ELISA after 1:1000 dilution. Nonxl collagen samples treated with the same conditions served as blanks. Table 3-1 shows the residual mTG amounts determined being 0.157 ± 0.008 % in the tgxl collagen and 0.406 ± 0.004 % in the tgxl high samples. These amounts are lower than the calculated values based on washing fluid concentrations (see 3.3.5). This indicates a removal of collagen during washing procedure creating a systematic error of the calculation. The direct quantification of mTG in the collagen samples is therefore regarded as superior and much more reproducible considering the standard deviations.

Table 3-1: mTG content in mTG-treated collagen before and after washing (tgxl (0.004 g mTG/g collagen) & tgxl high (0.01 g mTG/g collagen)).

	tgxl	tgxl high
Before washing	0.398 %	0.990 %
After washing	0.157 ± 0.008 %	0.406 ± 0.004 %

3.3.7 Dialysis

Our findings obtained so far clearly show that mTG could not be quantitatively removed at pH 3.7 although numerous washing steps were performed but instead remained in the mTG-treated collagen material to a high extent. As an alternative approach, a dialysis procedure was carried out to remove unbound mTG by means of a concentration gradient, enforced by application of either more acidic (pH 2) or strong alkaline conditions (pH 12). ELISA quantification of mTG in dialyzed collagen samples after degradation by collagenase revealed that mTG could not be detected in mTG-modified collagen material at both pH conditions during dialysis. This finding indicates that mTG is removed by these dialysis procedures. Furthermore, Western blot analysis after enzymatic degradation by collagenase (see 3.2.4) showed, that mTG was no longer present in the mTG treated materials and therefore had been quantitatively removed by the dialysis procedures (Figure 3-4b, lanes 1&2 from the left). Although treatment at pH 2 led to partial fragmentation of mTG (Figure 3-4b, lane 7 from the left) and treatment at pH 12 caused partial aggregation (Figure 3-4b, lane 8 from the left), mTG remained detectable for Western blot analysis. Treatment of tgxl collagen at pH 2 or 12 without dialysis was not able to quantitatively remove mTG (Figure 3-4b, lanes 3&4 from the left). However, these harsh pH conditions led to a decrease in tensile strength due to amide bond hydrolysis (data not shown) and thereby interfered with the beneficial use of mTG.

3.3.8 Washing with additives

The understanding of the effects of specific ions on proteins is currently changing. There is increasing evidence that salting-in and salting-out effects of ions on proteins need to be ascribed to ion-protein and ion-shell-water-molecule interaction rather

than on ions changing the water structure and thereby affecting protein behavior [Zhang and Cremer, 2006]. To test whether the reduction of ionic interactions may enable mTG removal from the collagen samples, the collagen materials were subjected to washing with sodium chloride, guanidinium chloride, or urea. Western blot analysis showed that the mTG content in tgxl collagen increased in the following order: guanidinium chloride < urea < sodium chloride (Figure 3-4c). Although the used additives are known to have a lyotropic effect on collagen [Ranganayaki et al., 1982; Russell and Cooper, 1972] only treatment with guanidinium chloride seems to be an effective tool to decrease mTG content but is less effective than dialysis (see 3.3.7).

3.4 Conclusion

In the present study, we investigated the effects of *Streptomyces mobaraensis* derived transglutaminase (mTG) treatment on insoluble porcine skin collagen type I. The results showed neither increased melting temperatures nor reduced enzymatic degradation assuming that the tested material is an improper substrate for mTG. The use of soluble collagen would have been beneficial for that purpose. Nevertheless, an increase in tensile strength was detected demonstrating a significant effect on material characteristics, even though native collagen type I is not a good substrate for mTG regarding the installation of ε-(γ-glutamyl)-lysine bonds under the tested conditions [Stachel et al., 2010]. To address the question whether mTG could be removed by numerous washing steps, a Western blot analysis of the collagen materials was performed, revealing that mTG was still present in mTG-treated collagen material. The Western blot analysis further showed that mTG was not covalently bound to the collagen material and that it was not degraded by *Clostridium histolyticum* collagenase type H being still accessible for further analysis. To determine the amount of mTG that can be removed via centrifugation and washing, an enzyme-linked immunosorbent assay (ELISA) was developed to quantify mTG in the washing solutions. ELISA-analysis showed that mTG could only be partially removed by centrifugation and washing. It was shown by the direct quantification after degradation by collagenase that around 40 % of the initially applied enzyme remained in the mTG-treated collagen materials. To further reduce mTG-residuals,

dialysis procedures at acidic or alkaline pH and incubation with different additives were performed. Western blot analysis showed that especially guanidinium chloride treatment reduced the mTG content. The dialysis procedure was superior to all other treatments and enabled to quantitatively remove mTG. However, this method comprises the drawback of amide bond hydrolysis leading to decreased tensile strength. These findings strongly suggest that future studies using transglutaminase for the “crosslinking” treatment of collagen should address potential residuals of mTG and investigate, whether observed effects are due to mTG-induced changes of the collagen structure or due to remaining transglutaminase itself. If mTG cannot be quantitatively removed, the question of potential immunogenicity of mTG needs to be addressed in future studies.

3.5 Acknowledgments

We thank the the German AiF-project “Collagen modification by enzymatic technologies” (COMET) for financial support. The above work is embedded in the “ForZebRA”-project and therefore supported by the Bavarian Research Foundation.

3.6 References

Ando H., Adachi M., Umeda K., Matsuura A., Nonaka M., Uchio R., Tanaka H., Motoki M., Purification and characteristics of a novel transglutaminase derived from microorganisms (food & nutrition), Agricultural and biological chemistry, 53 (1989) 2613-2617.

Besheer A., Hertel T. C., Kressler J., Mäder K., Pietzsch M., Enzymatically catalyzed HES conjugation using microbial transglutaminase: Proof of feasibility, Journal of Pharmaceutical Sciences, 98 (2009) 4420-4428.

Chau David Y. S., Collighan Russell J., Verderio Elisabetta A. M., Addy Victoria L., Griffin M., The cellular response to transglutaminase-cross-linked collagen, Biomaterials, 26 (2005) 6518-29.

Chen R.-N., Ho H.-O., Sheu M.-T., Characterization of collagen matrices crosslinked using microbial transglutaminase, Biomaterials, 26 (2005) 4229-4235.

Ciardelli G., Gentile P., Chiono V., Mattioli-Belmonte M., Vozzi G., Barbani N., Giusti P., Enzymatically crosslinked porous composite matrices for bone tissue regeneration, Journal of Biomedical Materials Research. Part A, 92A (2010) 137-151.

Collighan, J. R., Li, X., Parry, J., Griffin, M., Clara, S., Transglutaminases as tanning agents for the leather industry, Journal of the American Leather Chemists Association, 99 (2004) 293-302.

Folk J. E., Transglutaminases, Annual Review of Biochemistry, 49 (1980) 517-531.

Folk J. E., Cole P. W., Structural requirements of specific substrates for guinea pig liver transglutaminase, Journal of Biological Chemistry, 240 (1965) 2951-2960.

Fontana A., Spolaore B., Mero A., Veronese F. M., Site-specific modification and PEGylation of pharmaceutical proteins mediated by transglutaminase, Advanced Drug Delivery Reviews, 60 (2008) 13-28.

Friess W., Collagen - biomaterial for drug delivery, European Journal of Pharmaceutics and Biopharmaceutics, 45 (1998) 113-136.

Friess W., Schlapp M., Effects of processing conditions on the rheological behavior of collagen dispersions, European Journal of Pharmaceutics and Biopharmaceutics, 51 (2001) 259-265.

Garcia Y., Wilkins B., Collighan R. J., Griffin M., Pandit A., Towards development of a dermal rudiment for enhanced wound healing response, Biomaterials, 29 (2008) 857-868.

Kanaji T., Ozaki H., Takao T., Kawajiri H., Ide H., Motoki M., Shimonishi Y., Primary structure of microbial transglutaminase from Streptoverticillium sp. strain s-8112, Journal of Biological Chemistry, 268 (1993) 11565-11572.

Kashiwagi T., Yokoyama K.-i., Ishikawa K., Ono K., Ejima D., Matsui H., Suzuki E.-i., Crystal structure of microbial transglutaminase from Streptoverticillium mobaraense, Journal of Biological Chemistry, 277 (2002) 44252-44260.

Meyer, M., Baltzer, H., Schwikal, K., Collagen fibres by thermoplastic and wet spinning, Materials Science and Engineering: C, 30 (2010) 1266-1271.

Miles C. A., Avery N. C., Rodin V. V., Bailey A. J., The increase in denaturation temperature following cross-linking of collagen is caused by dehydration of the fibres, Journal of Molecular Biology, 346 (2005) 551-556.

Miles C. A., Ghelashvili M., Polymer-in-a-box mechanism for the thermal stabilization of collagen molecules in fibers, Biophysical Journal, 76 (1999) 3243-3252.

O Halloran D. M., Collighan R. J., Griffin M., Pandit A. S., Characterization of a microbial transglutaminase cross-linked type II collagen scaffold, Tissue Engineering, 12 (2006) 1467-1474.

Olde Damink L. H. H., Dijkstra P. J., Van Luyn M. J. A., Van Wachem P. B., Nieuwenhuis P., Feijen J., Changes in the mechanical properties of dermal sheep collagen during in vitro degradation, Journal of Biomedical Materials Research, 29 (1995) 139-147.

Olde Damink L. H. H., Dijkstra P. J., van Luyn M. J. A., van Wachem P. B., Nieuwenhuis P., Feijen J., In vitro degradation of dermal sheep collagen cross-linked using a water-soluble carbodiimide, Biomaterials, 17 (1996) 679-684.

Raghunath M., Hennies H. C., Velten F., Wiebe V., Steinert P. M., Reis A., Traupe H., A novel in situ method for the detection of deficient transglutaminase activity in the skin, Archives of Dermatological Research, 290 (1998) 621-627.

Ranganayaki M. D., Asghar A., Henrickson R. L., Influence of anion and cation on the water-holding capacity of bovine hide collagen at different pH values. Effect of sodium chloride and polyphosphates on hydration, Journal of Food Science, 47 (1982) 705-710.

Rault I., Frei V., Herbage D., Abdul-Malak N., Huc A., Evaluation of different chemical methods for cross-linking collagen gel, films and sponges, Journal of Materials Science: Materials in Medicine, 7 (1996) 215-221.

Russell A. E., Cooper D. R., Effect of compounds of the urea-guanidinium class on renaturation and thermal stability of acid-soluble collagen, Biochemical Journal, 127 (1972) 855-863.

Speer D. P., Chvapil M., Eskelson C. D., Ulreich J., Biological effects of residual glutaraldehyde in glutaraldehyde-tanned collagen biomaterials, Journal of Biomedical Materials Research, 14 (1980) 753-764.

Stachel I., Schwarzenbolz U., Henle T., Meyer M., Cross-linking of type I collagen with microbial transglutaminase: Identification of cross-linking sites, Biomacromolecules, 11 (2010) 698-705.

Zeugolis D. I., Panengad P. P., Yew E. S. Y., Sheppard C., Phan T. T., Raghunath M., An in situ and in vitro investigation for the transglutaminase potential in tissue engineering, Journal of Biomedical Materials Research Part A, 92A (2010) 1310-1320.

Zeugolis D. I., Raghunath M., The physiological relevance of wet versus dry differential scanning calorimetry for biomaterial evaluation: a technical note, Polymer International, 59 (2010) 1403-1407.

Zhang Y., Cremer P. S., Interactions between macromolecules and ions: the Hofmeister series, Current Opinion in Chemical Biology, 10 (2006) 658-663.

Zhu Y., Rinzema A., Tramper J., Bol J., Microbial transglutaminase—a review of its production and application in food processing, Applied Microbiology and Biotechnology, 44 (1995) 277-282.

4 rhBMP-7 in Collagen/Ceramic Composites – Incorporation, Quantification, and Recovery

Abstract

In the present study, a defined loading procedure for rhBMP-7 into collagen/ceramic composites ensuring high binding efficiency was established. An SEC quantification method for rhBMP-7 was developed, but failed detecting the very low rhBMP-7 concentrations in presence of an excessive of collagen fragments. In the silver-stained SDS-Page, rhBMP-7 signals were also covered by collagen. A Western blot analysis enabled to quantify rhBMP-7 in the presence of collagen and to determine the loss upon sterile filtration. For upcoming cell culture experiments, a defined and aseptic loading procedure of rhBMP-7 into collagen/ceramic composites was established. For the analysis of the binding behavior, methods to extract high amounts of rhBMP-7 from the carrier materials were developed. Arginin/histidine buffer pH 6.5 was the most effective rinse liquid to remove rhBMP-7 and enabled to recover 32.7 ± 12.7 % from the collagen/ceramic composites. Detailed Western blot analysis showed a synergistic binding capacity of collagen/ceramic composites for rhBMP-7 compared to the individual components, collagen and biphasic calcium phosphate. Extracted rhBMP-7 showed no signs of degradation. The rhBMP-7 loaded collagen/ceramic composites are therefore considered to be promising functionalized biomaterials for further cell culture experiments.

4.1 Introduction

For successful bone healing, besides a regenerative capacity of the recipient organism, the following prerequisites are demanded according to the diamond concept proposed by Giannoudis et al.: an osteoconductive structure, sufficient mechanical stability, osteogenic cells and growth factors [2007]. Marshall Urist discovered bone induction after implanting demineralized bone segments into rabbits [1965]. Bone inducing factors, which were later named bone morphogenetic proteins (BMPs), were held responsible for this observation. BMPs belong to the transforming growth factor-ß (TGF-ß) superfamily, except BMP-1 belonging to the group of metalloproteinases [Hofbauer and Heufelder, 1996]. During fracture repair BMPs recruite pluripotent stem cells and conduct the ossification by stimulating osteogenic and chondrogenic differentiation [Bostrom et al., 1995; Shen et al., 2010]. Of crucial interest for the clinical success of BMPs is an adequate retention at the site of application by carrier materials [Geiger et al., 2003; Jeon et al., 2008]. The combination of BMP-2 with a collagen scaffold significantly increases the retention period compared to the application of BMP-2 in pure buffer [Geiger et al., 2003; Seeherman et al., 2003]. The combination of BMP-2 with inorganic calcium phosphate material further prolongs the retention period [Seeherman et al., 2003] and reduces BMP-2 losses during implantation due to squeezing of the flexible collagen systems [Geiger, 2001]. The second clinically used BMP, BMP-7, has shown its comparability or superiority to autologous bone grafts in various studies without incidences of local or systemic toxicity or ectopic bone formation [Friedlaender et al., 2001; Vaccaro et al., 2008; Warnke et al., 2004; Zimmermann et al., 2007]. Osigraft® is a commercially available BMP-7 preparation, consisting of 3.5 mg rhBMP-7 and 1 g bovine collagen which is reconstituted with 0.9 % (w/v) sodium chloride solution prior to application [Stryker GmbH & Co. KG, 2008]. The question of BMP-7 binding to collagen and therewith retention at the site of application has not been clearly addressed. Goal of the present study was to load collagen/ceramic composites (CCCs) with defined amounts of BMP-7 under aseptic conditions. Therefore, quantification methods for BMP-7 and extraction strategies needed to be established to investigate whether protein integrity was affected by the

loading procedure. The BMP-7 enriched CCCs were to be transferred to the Clinical Center of the University of Munich for further in vitro studies with BMP-2 overexpressing human mesenchymal stem cells (hMSCs), as synergistic osteogenic effects were described for the combination of BMP-2 and BMP-7 [Buket Basmanav et al., 2008; Laflamme and Rouabhia, 2008].

4.2 Materials and Methods

All water used was highly purified and deionized using a USF ELGA PURELAB Plus UV/UF water purifier (Ransbach-Baumbach, Germany). To obtain insoluble porcine collagen type I raw material, porcine-skin derived collagen-suspension was prepared according to Meyer et al. [2010] and freeze-dried (Christ Epsilon 2-6D®, Osterode am Harz, Germany). Biphasic calcium phosphate granules (BCP, 60 % Hydroxyapatite, 40 % ß-Tricalcium-Phosphate, 0.8 – 1.6 mm) were provided from Medtronic Sofamor Danek Deggendorf GmbH (Deggendorf, Germany). Recombinant human bone morphogenetic protein 7 (BMP-7) was purchased from PromoKine GmbH (Heidelberg, Germany). Histidine, arginine, TRIS, polysorbate 20, bromophenol blue sodium salt, disodiumhydrogenphosphate-dihydrate, and potassiumdihydrogen-phosphate were from Merck KGaA (Darmstadt, Germany), methanol and acetic acid from VWR International (Darmstadt, Germany), glutamic acid from Fluka Chemie AG (Buchs, Switzerland) and sodium azide from ACROS ORGANICS (Thermo Fisher Scientific, Morris Plains, NJ, USA). All other chemicals were purchased from Sigma-Aldrich (St. Louis, MO, USA) and analytical grade. Buffer compositions are listed in Table 4-1. All buffers contained 0.02 % sodium azide for preservation and pH was adjusted with 1 N hydrochloric acid or 1 N sodium hydroxide (VWR International, Darmstadt, Germany). Unless stated otherwise, all buffers contained 0.005 % polysorbate 20.

Table 4-1: Buffer compositions.

Substance	Concentration	Composition [g]
Glycine buffer pH 4.0		
glycine	20 mM	0.1501
purified water		ad 100 mL
Histidine buffer pH 6.0		
L-histidine	20 mM	0.3104
purified water		ad 100 mL
TRIS buffer pH 8.0		
TRIS	20 mM	0.2423
purified water		ad 100 mL
Arg-Glu buffer pH 4.5 (SEC-buffer)		
L-arginine·HCl	0.4 M	8.43
glutamic acid	5 mM	0.074
purified water		ad 100 mL
Arg-His buffer pH 6.5		
L-arginine·HCl	0.5 M	10.5330
L-histidine	10 mM	0.1552
purified water		ad 100 mL
PBS buffer pH 7.4		
sodium chloride	137 mM	0.8
potassium chloride	2.7 mM	0.02
disodiumhydrogenphosphate	10 mM	0.144
potassiumdihydrogenphosphate	1.76 mM	0.024
purified water		ad 100 mL
PBST buffer pH 7.4		
sodium chloride	137 mM	0.8
potassium chloride	2.7 mM	0.02
disodiumhydrogenphosphate	10 mM	0.144
potassiumdihydrogenphosphate	1.76 mM	0.024
polysorbate 20		0.1
purified water		ad 100 mL

4.2.1 Manufacturing of collagen/ceramic composites

CCCs were prepared by dispersing the collagen raw material in water (pH adjusted to 3.7 with concentrated acetic acid) at a concentration of 4 % (w/w). After swelling for 4 h, the dispersions were homogenized with an ESGE® immersion blender (Unold AG, Germany). Biphasic calcium phosphate granules (BCP, 60 % Hydroxyapatite & 40 % ß-Tricalciumphosphate, 0.8 – 1.6 mm, 50 % (m/m) related to collagen dispersion) were homogeneously admixed to the collagen dispersion. Dispersion-aliquots were distributed into custom-made poly(methyl methacrylate) wells (diameter 9 mm, height 5 mm) and freeze dried according to the protocol described in Table 4-2. Based on dry mass each CCC consisted of 11.1 mg of collagen and 138.9 mg of BCP.

Table 4-2: Freeze-drying protocol of collagen/ceramic composites.

Process phase	Time [hh:mm]	Temperature [°C]	Vacuum [mbar]
Loading	00:00	20	---
Freezing	00:30	-5	---
Freezing	00:30	-5	---
Freezing	01:40	-15	---
Freezing	00:20	-35	---
Freezing	00:30	-35	---
Primary drying	00:01	-15	1.03
Primary drying	00:29	-15	1.03
Primary drying	23:00	-15	1.03
Secondary drying	00:01	20	0.1
Secondary drying	00:29	20	0.1
Secondary drying	14:00	20	0.1

4.2.2 Size exclusion chromatography (SEC)

An Agilent Technologies 1100 series instrument (Agilent Technologies, Böblingen, Germany), comprising degasser (1100 series), isocratic pump (IsoPump, 1100 series), autosampler, variable wavelength detector (VWD, 1100 series) and fluorescence detector (FLD, 1200 series) was used. For sample separation a TSK-Gel®G2000SWxl (7.8 mm x 30 cm, 5 µm particle size, TOSOH Bioscience GmbH, Stuttgart, Germany) with a guard column (TSK-Gel®SWxl Guard Column, 6 mm x 4 cm, particle size 7 µm, TOSOH Bioscience GmbH, Stuttgart, Germany) was used. Isocratic elution with 0.4 M L-arginine·HCl/5 mM glutamic acid buffer pH 4.5 containing 0.4 % SDS at a flow rate of 0.6 mL/min was applied. Samples were pipetted into polypropylene inserts (Agilent Technologies), which were stuck into HPLC vials. Injection volume was 100 µL. Wavelengths used were λ = 230 nm (VWD) and λ_{ex} = 230 nm and λ_{em} = 330 nm (FLD), previously determined by performing multi-emission and multi-excitation scans. Data analysis was performed with Agilent ChemStation® software (Agilent Technologies).

4.2.3 SDS-Page

NuPAGE® 10 % Bis-Tris gels and the protein standard Mark12® (Invitrogen, Carlsbad, USA) were used for electrophoresis. All samples were diluted 1:1 with sample buffer (25 ml Tris 1 M, 0.4 g SDS, 0.23 ml glycerin (87 %) and 1 ml bromophenol blue (0.1 %) made up to 100 mL with water, adjusted to pH 6.8 with 1 N HCl) and heated to 95 °C for 20 min. 20 µL of the samples were then applied to the gels and electrophoresis was run at 30 mA for 1.5 h. For protein visualization, the gels were stained with the silver staining kit SilverXpress® (Invitrogen, Carlsbad, USA).

4.2.4 Western blot analysis

Proteins were separated by SDS-Page (see 4.2.3). A prestained RTU protein ladder from PromoKine GmbH (Heidelberg, Germany) was used as standard. Samples were

transferred onto nitrocellulose membranes (Invitrogen) using an XCell II™ Blot Module (Invitrogen). All incubation steps were carried out at RT on an orbital shaker (Titramax 101, Heidolph Instruments GmbH, Schwabach, Germany) at 150 RPM unless otherwise stated. After washing with PBS-buffer, the membranes were blocked with 0.2 % Super-block (PromoKine GmbH) in PBST-buffer for 60 min. After washing with PBS-buffer, a rabbit polyclonal anti-BMP-7 antibody (0.2 µg/mL, overnight incubation at 2 - 8 °C) from PromoKine GmbH was used as primary antibody. After washing four times with PBST-buffer, PF-670 antibody conjugate goat anti-rabbit (PromoKine GmbH) was used for detection (1:2,000, 2 h incubation). After washing four times with PBST and three times with PBS-buffer, fluorescence intensity signals (k counts) were analyzed. Therefore, identical choice boxes were manually distributed to the respective signals and signal intensity was automatically determined using the Odyssey® imaging system (LI-COR Biosciences, Lincoln, USA).

4.2.5 RhBMP-7 loading of collagen/ceramic composites

For incorporation of rhBMP-7 into CCCs 10 µg of the lyophilized protein were reconstituted in different volumes (350 µL for SDS-Page analysis, 1050 µL for Western blot analysis) of glycine buffer pH 4.0 containing 0.005 % polysorbate 20. 105 µL of rhBMP-7 were pipetted directly onto the scaffolds. After 5 min incubation at RT, 105 µL of a second buffer (histidine pH 6, TRIS pH 8, or TRIS pH 10) were added and the system incubated for 30 min. The liquids were loaded dropwise onto the center of the scaffold surface to ensure complete soaking into the composite material and to avoid protein loss due to adsorption to the surface of the eppendorf cups. To evaluate the incorporation efficiency a hole was pierced into the bottom of the eppendorf cups by means of a cannula (Terumo Neolus, 20G x 1 1/2, 0.9 x 40 mm, Terumo Europe N.V., Leuven, Belgium). The caps were stuck into intact eppendorf cups and centrifuged for 10 min at 14000 rpm (Sigma 1-15, Christ GmbH, Osterode am Harz, Germany). Aliquots of the centrifugate in the lower eppendorf cups were analyzed by SDS-PAGE. The procedure is visualized in Figure 4-1. Negative controls (n=4) without rhBMP-7 were prepared accordingly and pH values were measured using a MP220 pH Meter (Mettler Toledo GmbH, Giessen, Germany).

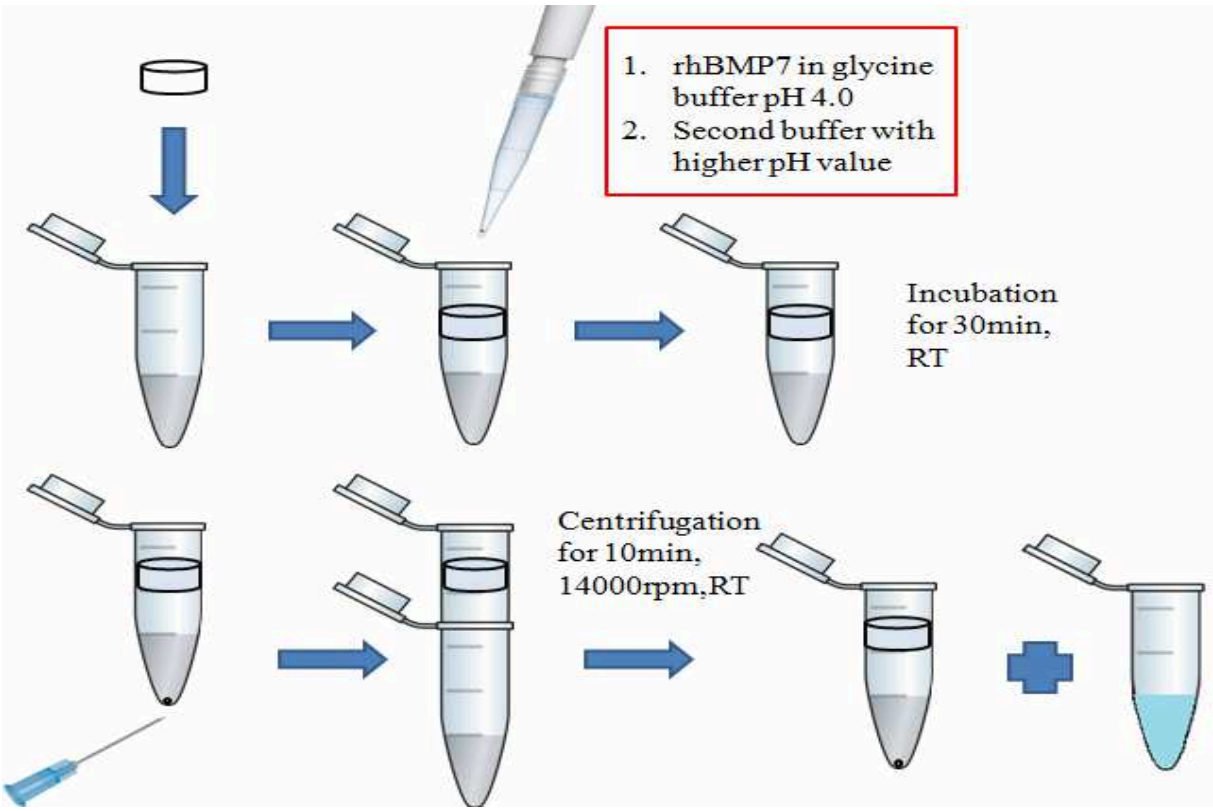

Figure 4-1: Scheme for rhBMP-7 loading of collagen/ceramic composites.

4.2.6 Aseptic manufacturing of rhBMP-7 loaded collagen/ceramic composites for cell culture testing

All manufacturing steps were carried out under a HERAsafe® HS laminar flow box (Thermo Scientific, Massachusetts, USA). RhBMP-7 was diluted in glycine buffer pH 4.0 at 0.2 mg/mL and sterile-filtered by means of a Millex®-GV PVDF filter (Millipore, Billerica, USA) with a pore size of 0.22 µm. Loss upon filtration was determined by Western blot analysis (see 4.2.4) and aliquots were deep frozen at -80 °C until further use. CCCs, manufactured according to 4.2.1 were fully soaked with 96 % ethanol. After evaporation of the ethanol, the CCCs were loaded each with 1 µg of rhBMP-7 according to protocol 4.2.5 with TRIS buffer pH 8.0 as second buffer and directly transferred to Ph.D. cand. Ms. Uta Leicht for cell culture testing at the Clinical Center of the University of Munich.

4.2.7 Extraction of rhBMP-7 from collagen/ceramic composites and evaluation of binding behavior

Either CCCs (see 4.2.1) or the respective components (11.1 mg of collagen or 138.9 mg of BCP) or eppendorf cups without scaffolds were loaded with rhBMP-7 (n=5) according to protocol 4.2.5 with TRIS buffer pH 8.0 as second buffer. In order to extract rhBMP-7, 1 mL of either HCl (pH 1) or Arg/His buffer (pH 6.5) were added and incubated on an orbital shaker (30 min, 400 rpm, Heidolph Titramax 101). A hole was pierced into the bottom of the eppendorf cups by means of a cannula (Terumo Neolus, 20G x 1 1/2, 0.9 x 40 mm). The caps were stuck into intact eppendorf cups and centrifuged for 10 min at 14,000 rpm (Sigma 1-15). Aliquots of the centrifugates were analyzed by Western blot (see 4.2.4). For statistical analysis Student's t-test was used.

4.3 Results and Discussion

4.3.1 Incorporation of rhBMP-7 into collagen/ceramic composites

In previous studies, besides successful outcome regarding osteogenic effects, little attention has been paid to the question, whether BMPs are in fact incorporated into the carrier materials. This concerns both combinations of rhBMP-7 with collagen and calcium phosphate [Cook et al., 1995; Gao et al., 1996]. Aim of our studies was to develop a defined loading procedure, enabling to quantitatively incorporate rhBMP-7 into CCCs, while minimizing protein alteration. RhBMP-7 is used in a formulation buffer pH 4.0. Previous studies demonstrated that a pH shift from 5 to 7 leads to increased incorporation efficiency of rhBMP-2 into absorbable collagen sponges [Friess et al., 1999; Geiger et al., 2003]. The isoelectric point of the collagen used in our studies was 7.8 and the isoelectric point of rhBMP-7 was calculated to be 8.2. Consequently, increasing the pH in the course of the incorporation procedure was considered to be a promising way to decrease electrostatic repulsion between the two proteins and thereby to obtain higher incorporation efficiency. But it has also been shown that increasing the pH above 6.5 results in a decreased solubility of rhBMP-2 [Friess et al., 1999; Geiger, 2001] and a shift towards the isoelectric point

induced aggregation of rhBMP-2 [Luca et al., 2010]. Therefore, the desired pH, to combine efficient protein loading with a low protein alteration and precipitation was expected to be in the range between 4.0 and 8.2. The pH values resulting after loading procedures with different buffer combinations without rhBMP-7 are shown in Table 4-3.

Table 4-3: Buffer combinations and resulting pH values measured after placebo loading CCCs (n=4).

Buffer combinations	pH
glycine buffer pH 4 + histidine buffer pH 6	6.04 ± 0.05
glycine buffer pH 4 + TRIS buffer pH 8	6.64 ± 0.21
glycine buffer pH 4 + TRIS buffer pH 10	7.60 ± 0.18

All tested loading buffer combinations rendered pH values within the desired range and were therefore further evaluated. Figure 4-2 exemplarily shows the silver stained SDS-Page analysis of the centrifuge effluent after loading rhBMP-7 onto collagen/ceramic scaffolds by using glycine buffer pH 4 and histidine buffer pH 6 and after extraction with Arg/His buffer pH 6.5.

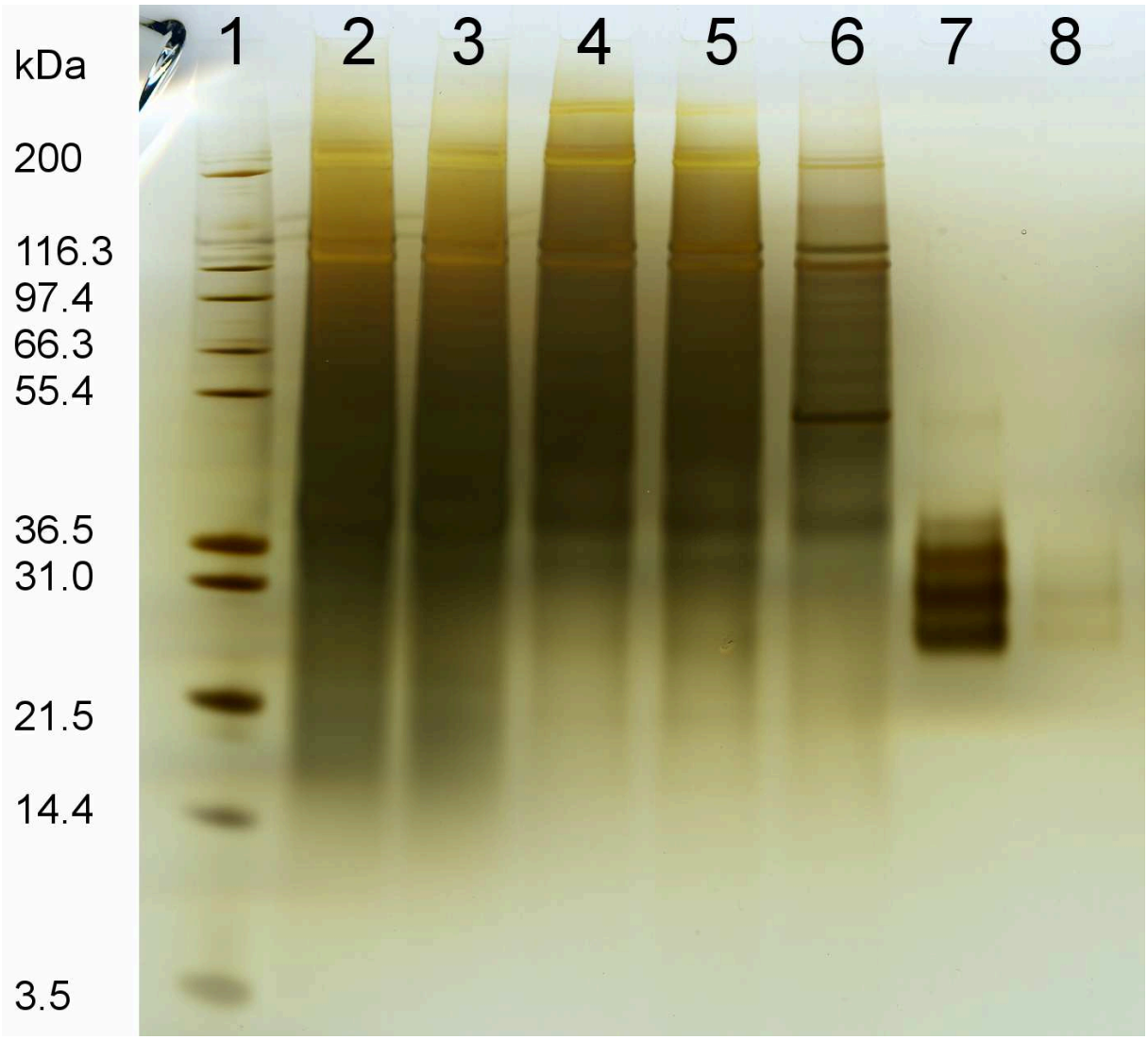

Figure 4-2: SDS-Page of centrifugates and extracts after incorporating 143 ng rhBMP-7 into CCCs (glycin buffer pH 4 & histidine buffer pH 6; extraction with Arg/His buffer pH 6.5): Lanes (from the left): 1: Marker; 2: centrifugate blank; 3: centrifugate verum; 4: extract blank; 5: extract verum; 6: Diluted centrifugate verum (1:4.8); 7: 83.6 ng rhBMP-7; 8: 8.36 ng rhBMP-7.

Due to the low quantity of 3 µg of rhBMP-7 loaded onto the scaffolds, compared to the 11.1 mg of collagen present in the composites, the rhBMP-7 bands are covered by collagen fragments in the silver stained SDS-Page analysis. Nevertheless, a semi-quantitative assumption can be postulated: no signal with a comparable intensity to lane 7 representing 83.6 ng of rhBMP-7 is detectable, neither in the incorporation sample (lane 3) nor in the extraction sample (lane 5), indicating that a high amount of rhBMP-7 is bound to the CCC which could not be quantitatively removed. Incorporation at pH 6.6 and 7.6 led to comparable results, whereas incorporation without raising the pH led to incomplete binding efficiency (data not shown). Shifting

the pH towards higher values is therefore an effective method to increase the binding efficiency of rhBMP-7 to CCCs. However, a rhBMP-7 quantification method was still required and therefore SEC and Western blot analysis were further evaluated.

4.3.2 Quantification of rhBMP-7 via SEC

Literature is available describing the quantification of rhBMP-2 via SEC [Geiger, 2001]. BMP-2 is a 32 kDa protein with an isoelectric point (IEP) of 8.2 [Geiger, 2001; Luca et al., 2010]. The molecular weight of BMP-7 is reported to be 25 - 40 kDa, depending on the grade of glycosylation, and its IEP can be calculated based on its amino acid sequence to be 8.2 [Griffith et al., 1996; PromoCell, 2011]. Due to the similarities beween BMP-2 and BMP-7, SEC column type, injection volume, elution buffer, and flow rate were adapted from Geiger [2001]. To obtain ideal wavelength settings, multi-emission and multi-excitation scans were performed, revealing a minimized signal to noise ratio at λ = 230 nm (for UV-detection) and an excitation wavelength of λ_{ex} = 230 nm and detection at λ_{em} = 330 nm (for fluorescence detection). RhBMP-7 concentrations of 0.05 - 10 µg/mL in glycine buffer pH 4.0 were analyzed. To prevent protein adsorption to surfaces, 0.4 % sodium dodecyl sulfate (SDS) was added, which is above the critical micelle concentration for SDS in water, reported to be 0.23 % [Fuguet et al., 2005]. BMP-7 was eluted at a retention time of 11.3 min and peak heights were used for calibration (see Figure 4-3). Linearity was fully given between 0.1 and 10 µg/mL and the limit of quantification was 0.25 µg/mL. However, the excessive presence of collagen interfered with the detection method despite the low aromatic amino acid content of collagen, responsible for the fluorescence signal. Consequently the method could not be used for the quantification of rhBMP-7 in combination with the CCCs (data not shown). Furthermore, the method was not feasible for a release testing, as a release of 100 % would typically result in a maximum concentration of 0.83 µg/mL when using 1 mL release medium (see 4.2.7).

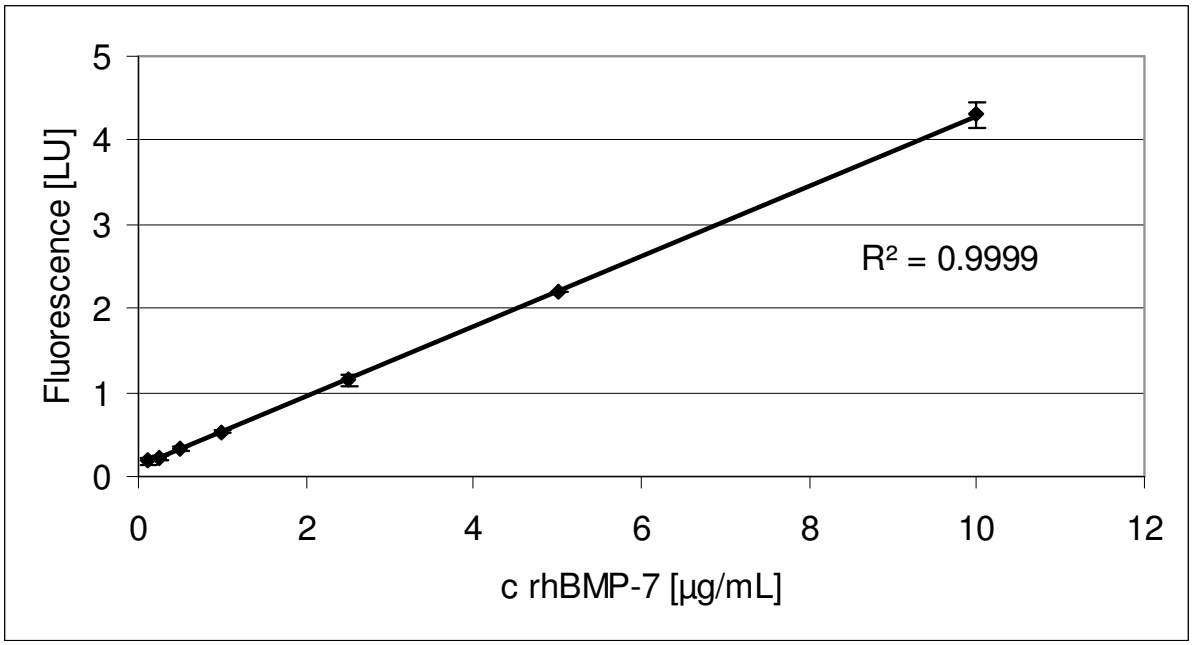

Figure 4-3: Calibration curve of rhBMP-7 (n=2, glycine buffer pH 4.0, 0.4 % SDS, fluorescence detection signal: λ_{ex} = 230 nm, λ_{em} = 330).

4.3.3 Quantification of rhBMP-7 via Western blot

A calibration curve was prepared diluting rhBMP-7 in glycine buffer pH 4.0 and performing a Western blot analysis (see 4.2.4) with quantities ranging from 1 - 40 ng. Figure 4-4 shows an exemplary image of the quantitative rhBMP-7 Western blot and the respective calibration curve is depicted in Figure 4-5.

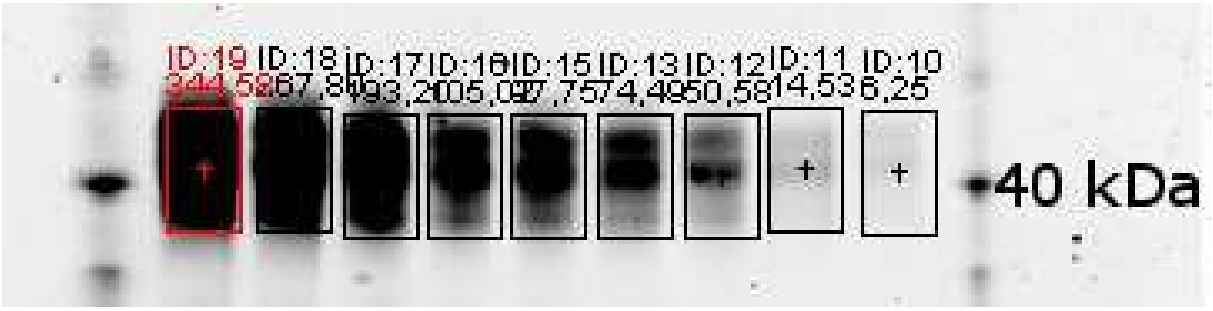

Figure 4-4: rhBMP-7 Western blot with selection boxes for automatic intensity calculation.

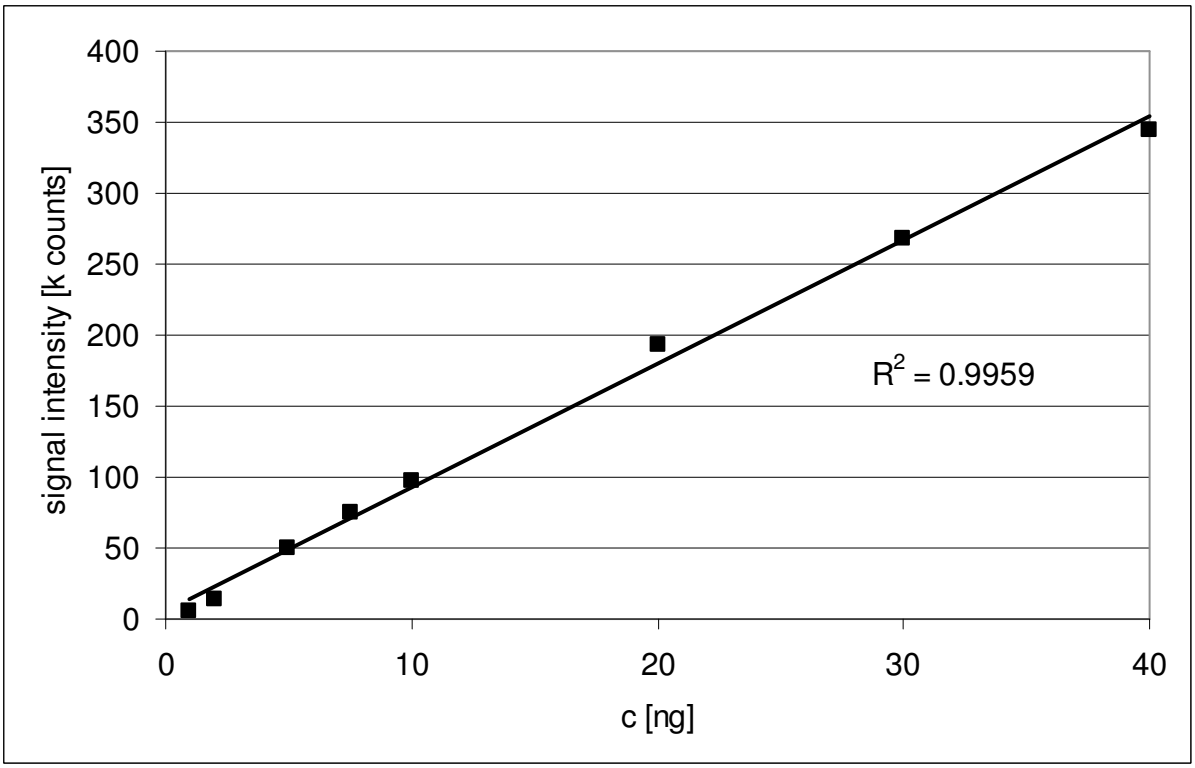

Figure 4-5: Calibration curve of a quantitative rhBMP-7 Western blot analysis.

Numerous Western blot analyses of rhBMP-7 were performed to select the finally ideal conditions regarding signal-to-noise ratio and correlation coefficient (see 4.2.4). The sensitivity was increased by a factor of ~10 compared to SEC (see 4.3.2). Furthermore, the assay was not affected by the presence of collagen compared to SDS-Page (see 4.3.1). Consequently, the developed Western blot analysis was decided to be the method of choice for further analysis and quantification of rhBMP-7. The combination of different growth factors showed beneficial results regarding bone regeneration [Zhang et al., 2009]. Heterodimers of BMP-2/7, BMP-2/6, and BMP-4/7 were found to promote increased bone formation in vivo compared to the effects of the respective homodimers [Aono et al., 1995; Israel et al., 1996]. The combination of BMP-2 and BMP-7 homodimers is superior regarding osteogenic differentiation compared to the isolated effects of the two bone morphogenetic proteins [Buket Basmanav et al., 2008; Laflamme and Rouabhia, 2008]. Among the "ForZebRA"-cooperation the combination of BMP-2 overexpressing hMSCs seeded on rhBMP-7 loaded CCCs was to be evaluated. Therefore, an aseptic manufacturing of the rhBMP-7 loaded scaffold needed to be developed (see 4.2.6) including sterile filtration of the rhBMP-7 solution. As rhBMP-7 has a high tendency of surface adsorption a substantial loss of protein was expected. However, quantitative Western

blot analysis showed that after sterile filtration of the rhBMP-7 solution with a PVDF filter 101.8 ± 4.2 % protein were recovered. The aseptically manufactured rhBMP-7 loaded CCCs were transferred to Ph.D. cand. Ms. Uta Leicht for cell culture testing at the Clinical Center of the University of Munich.

4.3.4 Extraction of rhBMP-7 from collagen/ceramic composites and evaluation of the binding behavior

Aim of the setup was to extract rhBMP-7 from the previously loaded scaffolds and to gain insight into its integrity. As the increase in pH was responsible for high binding to the carrier material (see 4.3.1), HCl solution pH 1 was chosen for extraction to inverse the binding procedure. Arg/His buffer pH 6.5 was additionally chosen, as this buffer has previously been described as a promising extraction buffer for rhBMP-2 from CCCs [Geiger, 2001]. High arginine concentrations (0.5 M) were shown to even completely suppress adsorption of BMP-2 [Duggirala et al., 1996]. Figure 4-6 exemplarily shows a Western blot analysis for rhBMP-7 recovery. The extracted rhBMP-7 fractions (lanes 5-12) showed no signs of degradation or aggregation compared to the native rhBMP-7, used for calibration (lanes 2-4).

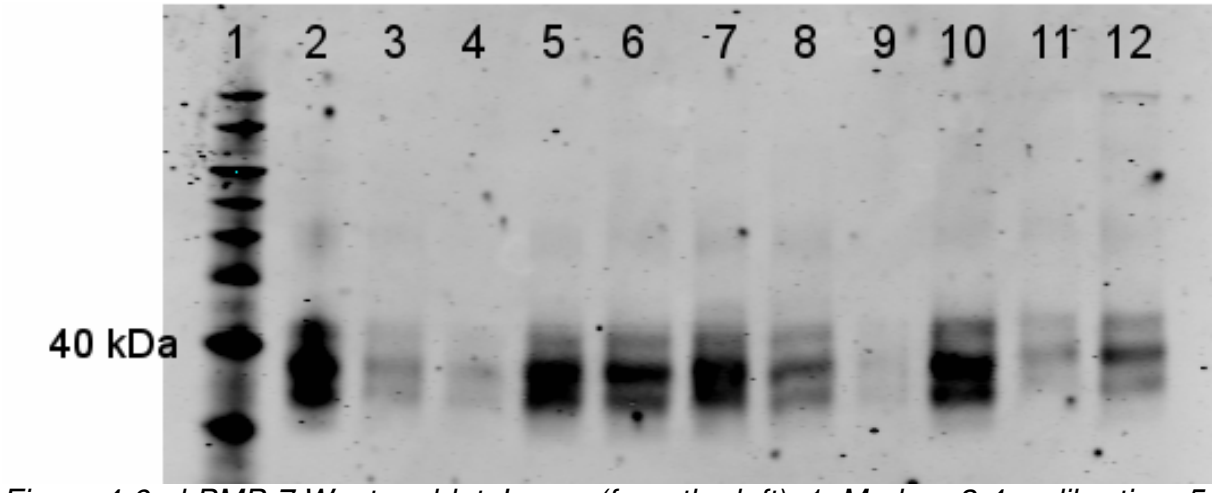

Figure 4-6: rhBMP-7 Western blot; Lanes (from the left): 1: Marker; 2-4: calibration; 5: Blank HCl; 6: Blank Arg/His; 7: Collagen HCl; 8: Collagen Arg/His; 9: BCP HCl; 10: BCP Arg/His; 11: CCC HCl; 12: CCC Arg/His.

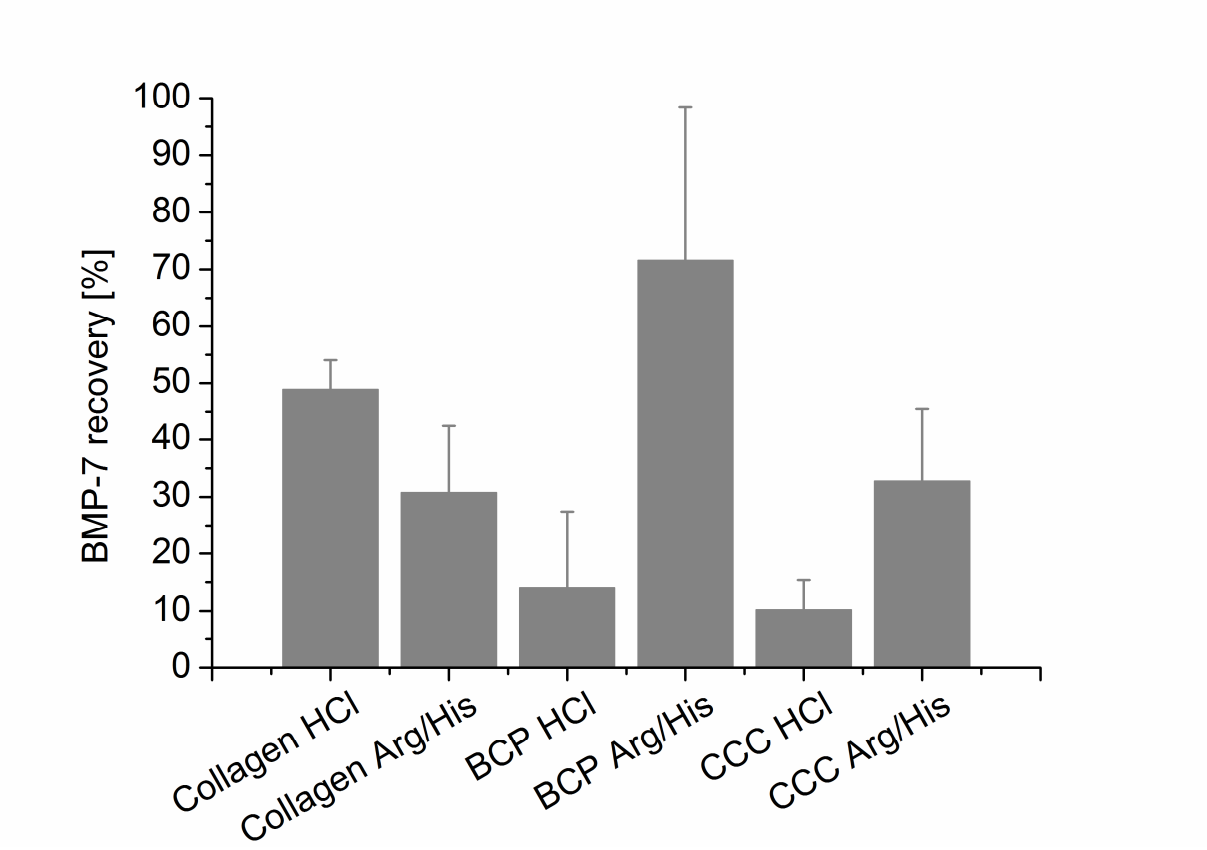

Figure 4-7: rhBMP-7 recovery determined by quantitative Western blot analysis

Figure 4-7 shows the recovery of rhBMP-7 from collagen, BCP, and the CCC. The recovery from collagen showed lower recovery for Arg/His with 30.7 ± 11.6 % compared to 48.9 ± 5.2 % for HCl ($p < 0.05$). In contrast, Arg/His was much more effective extracting 71.6 ± 26.8 % compared to HCl extracting 14.0 ± 13.4 % of rhBMP-7 from BCP granules ($p < 0.05$). The lowest rhBMP-7 fractions were recovered from CCCs, 32.7 ± 12.7 % with Arg/His and 10.2 ± 5.1 % with HCl. The total rhBMP-7 amount extracted from CCCs with both extraction methods was lower compared to BCP and significantly lower compared to collagen ($p < 0.05$). Thus, the CCCs as a combination of collagen and BCP exhibit a synergistic binding capacity for rhBMP-7 and adsorption is the mechanism underlying the high incorporation efficiency [Luginbuehl et al., 2004]. We expect the developed scaffolds to exhibit high retention of rhBMP-7 at the site of application as Geiger proved higher retention of rhBMP-2 by the use of CCCs [2001]. The scaffolds are promising candidates for the upcoming in vitro studies at the Clinical Center of the University of Munich as sustained release of bone morphogenetic proteins is considered to be ideal for bone regeneration [Bessa et al., 2008].

4.4 Conclusion

Goal of the present study was to aseptically manufacture rhBMP-7 loaded collagen/ceramic composites, while minimizing protein alteration. Applying a second buffer with a higher pH to the rhBMP-7 enriched collagen/ceramic composite, causing a shift towards the isoelectric point of rhBMP-7, was proven to be the method of choice to obtain high incorporation efficiency. Detecting rhBMP-7 with the developed SEC method interfered with the excessive presence of collagen. The established, specific immunologic detection via Western blot analysis was shown to be insusceptible to collagen artifacts and ~10 times more sensitive for rhBMP-7 compared to SEC. The quantitative Western blot enabled to investigate the loss upon sterile filtration of rhBMP-7, necessary for aseptic manufacturing. A PVDF filter was proven not to decrease the yield of rhBMP-7 after filtration. Upon the extraction of rhBMP-7 from the collagen/ceramic composites by lowering the pH or applying Arg/His buffer, no signs of degradation were detectable by Western blot. Arg/His buffer pH 6.5 was the most effective tool, extracting 32.7 ± 12.7 % of the previously incorporated rhBMP-7. This overall low recovery highlights the strong retentive potential for rhBMP-7 of the carrier material. The combination of collagen and biphasic calcium phosphate showed a synergy in binding compared to the isolated carrier materials. Therefore, we conclude that the rhBMP-7 loaded collagen/ceramic composites developed in this study are promising candidates for further in vitro and in vivo studies, which will be conducted at the Clinical Center of the University of Munich.

4.5 Acknowledgments

We thank the Bavarian Research Foundation for financial support. The above work is part of the “ForZebRA”-project. We further thank Medtronic Sofamor Danek GmbH (Deggendorf, Germany) for the donation of biphasic calcium phosphate granules.

4.6 References

Aono A., Hazama M., Notoya K., Taketomi S., Yamasaki H., Tsukuda R., Sasaki S., Fujisawa Y., Potent ectopic bone-inducing activity of bone morphogenetic protein-4/7 heterodimer, Biochemical and Biophysical Research Communications, 210 (1995) 670-677.

Bessa P. C., Casal M., Reis R. L., Bone morphogenetic proteins in tissue engineering: the road from laboratory to clinic, part II (BMP delivery), Journal of Tissue Engineering and Regenerative Medicine, 2 (2008) 81-96.

Bostrom M. P. G., Lane J. M., Berberian W. S., Missri A. A. E., Tomin E., Weiland A., Doty S. B., Glaser D., Rosen V. M., Immunolocalization and expression of bone morphogenetic proteins 2 and 4 in fracture healing, Journal of Orthopaedic Research, 13 (1995) 357-367.

Buket Basmanav F., Kose G. T., Hasirci V., Sequential growth factor delivery from complexed microspheres for bone tissue engineering, Biomaterials, 29 (2008) 4195-4204.

Cook S. D., Wolfe M. W., Salkeld S. L., Rueger D. C., Effect of recombinant human osteogenic protein-1 on healing of segmental defects in non-human primates, Journal of Bone and Joint Surgery. American Volume, 77 (1995) 734-750.

Duggirala S. S., Mehta R. C., Deluca P. P., Interaction of recombinant human bone morphogenetic protein-2 with poly (d,l Lactide-co-glycolide) microspheres, Pharmaceutical Development and Technology, 1 (1996) 11-19.

Friedlaender G. E., Perry C. R., Cole J. D., Cook S. D., Cierny G., Muschler G. F., Zych G. A., Calhoun J. H., Laforte A. J., Yin S., Osteogenic protein-1 (bone morphogenetic protein-7) in the treatment of tibial nonunions, Journal of Bone & Joint Surgery, American Volume, 83 (2001) S151-S158.

Friess W., Uludag H., Foskett S., Biron R., Sargeant C., Characterization of absorbable collagen sponges as rhBMP-2 carriers, International Journal of Pharmaceutics, 187 (1999) 91-99.

Fuguet E., Ràfols C., Rosés M., Bosch E., Critical micelle concentration of surfactants in aqueous buffered and unbuffered systems, Analytica Chimica Acta, 548 (2005) 95-100.

Gao T., Lindholm T. S., Marttinen A., Urist M. R., Composites of bone morphogenetic protein (BMP) and type IV collagen, coral-derived coral hydroxyapatite, and tricalcium phosphate ceramics, International Orthopaedics, 20 (1996) 321-325.

Geiger M., Porous collagen/ceramic composite carriers for bone regeneration using recombinant human bone morphogenetic protein-2 (rhBMP-2), Dissertation, (2001), Friedrich-Alexander-University, Erlangen.

Geiger M., Li R. H., Friess W., Collagen sponges for bone regeneration with rhBMP-2, Advanced Drug Delivery Reviews, 55 (2003) 1613-1629.

Giannoudis P. V., Einhorn T. A., Marsh D., Fracture healing: The diamond concept, Injury, 38 (2007) S3-S6.

Griffith D. L., Keck P. C., Sampath T. K., Rueger D. C., Carlson W. D., Three-dimensional structure of recombinant human osteogenic protein 1: structural paradigm for the transforming growth factor beta superfamily, Proceedings of the National Academy of Sciences of the United States of America, 93 (1996) 878-883.

Hofbauer L. C., Heufelder A. E., Updating the metalloprotease nomenclature: bone morphogenetic protein 1 identified as procollagen C proteinase, European Journal of Endocrinology, 135 (1996) 35-36.

Israel D. I., Nove J., Kerns K. M., Kaufman R. J., Rosen V., Cox K. A., Wozney J. M., Heterodimeric bone morphogenetic proteins show enhanced activity in vitro and in vivo, Growth Factors, 13 (1996) 291-300.

Jeon O., Song S. J., Yang H. S., Bhang S.-H., Kang S.-W., Sung M. A., Lee J. H., Kim B.-S., Long-term delivery enhances in vivo osteogenic efficacy of bone morphogenetic protein-2 compared to short-term delivery, Biochemical and Biophysical Research Communications, 369 (2008) 774-780.

Laflamme C., Rouabhia M., Effect of BMP-2 and BMP-7 homodimers and a mixture of BMP-2/BMP-7 homodimers on osteoblast adhesion and growth following culture on a collagen scaffold, Biomedical Materials, 3 (2008) 015008.

Luca L., Capelle M. A. H., Machaidze G., Arvinte T., Jordan O., Gurny R., Physical instability, aggregation and conformational changes of recombinant human bone morphogenetic protein-2 (rhBMP-2), International Journal of Pharmaceutics, 391 (2010) 48-54.

Luginbuehl V., Meinel L., Merkle H. P., Gander B., Localized delivery of growth factors for bone repair, European Journal of Pharmaceutics and Biopharmaceutics, 58 (2004) 197-208.

Meyer, M., Baltzer, H., Schwikal, K., Collagen fibres by thermoplastic and wet spinning, Materials Science and Engineering: C, 30 (2010) 1266-1271.

PromoCell GmbH, Instruction manual rhBMP-7, Heidelberg, Germany, Access: November 24, 2011, http://www.promokine.info/fileadmin/PDFs/All_PDFs/C-67319.pdf

Seeherman H., Li R., Wozney J., A review of preclinical program development for evaluating injectable carriers for osteogenic factors, Journal of Bone & Joint Surgery, American Volume, 85 (2003) 96-108.

Shen B., Wei A., Whittaker S., Williams L. A., Tao H., Ma D. D. F., Diwan A. D., The role of BMP-7 in chondrogenic and osteogenic differentiation of human bone marrow multipotent mesenchymal stromal cells in vitro, Journal of Cellular Biochemistry, 109 (2010) 406-416.

Stryker GmbH & Co. KG, Osigraft, Zusammenfassung der Merkmale des Arzneimittels, Duisburg, Germany, Access: December 9, 2011, Last updated: June 6, 2008, http://www.stryker.de/de_pdf_hinweise-osigraft.pdf

Urist M. R., Bone: formation by autoinduction, Science, 150 (1965) 893-899.

Vaccaro A. R., Whang P. G., Patel T., Phillips F. M., Anderson D. G., Albert T. J., Hilibrand A. S., Brower R. S., Kurd M. F., Appannagari A., Patel M., Fischgrund J. S., The safety and efficacy of OP-1 (rhBMP-7) as a replacement for iliac crest autograft for posterolateral lumbar arthrodesis: minimum 4-year follow-up of a pilot study, The Spine Journal, 8 (2008) 457-465.

Warnke P. H., Springer I. N. G., Wiltfang J., Acil Y., Eufinger H., Wehmöller M., Russo P. A. J., Bolte H., Sherry E., Behrens E., Terheyden H., Growth and transplantation of a custom vascularised bone graft in a man, The Lancet, 364 (2004) 766-770.

Zhang Y., Shi B., Li C., Wang Y., Chen Y., Zhang W., Luo T., Cheng X., The synergetic bone-forming effects of combinations of growth factors expressed by adenovirus vectors on chitosan/collagen scaffolds, Journal of Controlled Release, 136 (2009) 172-178.

Zimmermann G., Müller U., Löffler C., Wentzensen A., Moghaddam A., Therapieerfolg bei atrophen Tibiaschaftpseudarthrosen, Der Unfallchirurg, 110 (2007) 931-938.

5 Oxygen Generating Collagen/Ceramic Composites

Abstract

Aim of the present study was to develop a formulation providing sustained oxygen-release in order to achieve elevated oxygen levels in a collagen/ceramic composite scaffold for several days. This can help to maintain cell viability in larger tissue engineering constructs, where oxygen diffusion limits cell survival. The oxygen was provided by granulated materials based on calcium peroxide. A bigger particle size enabled to reduce the initial burst, but did not provide sustained oxygen release. Neither CaO_2 formulations containing hard fat nor poly(lactic-*co*-glycolic acid) rendered the desired release profile. Granulation with ethyl cellulose (EC) led to reduced initial burst and to significantly elevated oxygen levels throughout the investigation time period of 72 h. This lead candidate was incorporated into collagen/ceramic composite scaffolds and similar oxygen release behavior was found. Catalase added to the release medium or embedded into the freeze-dried ready-to-use oxygen generating collagen/ceramic composites allowed to keep hydrogen peroxide levels at a minimum without influencing the oxygen release.

5.1 Introduction

In the field of tissue engineering it has been shown that adequate filling materials facilitate tissue regeneration [Groeneveld et al., 1999]. Scaffolds intended for bone regeneration are usually either cultivated with cells in vitro [Ge et al., 2009b] or implanted without prior cell seeding [Ge et al., 2009a]. An ex vivo cell seeding followed by implantation can lead to increased hypoxia inside the scaffolds due to inadequate perfusion [Liu et al., 2009]. However, homogeneous oxygen distribution is of crucial importance for the quality of the engineered tissue [Volkmer et al., 2008]. In mammalians, cells are supplied with the essential oxygen by diffusion from surrounding blood vessels. A distance from the blood vessels exceeding 100 – 200 µm can be enough that adequate oxygen supply is no longer ensured [Carmeliet and Jain, 2000]. Several approaches have been evaluated to overcome this problem in larger implants, like improved scaffold porosity, incorporation of angiogenic signals (e.g. VEGF) directly or via genetically engineered cells, seeding of endothelial cells, prevascularization prior to seeding, or increased oxygen capacity of the used cell culture medium [Karande et al., 2004; Nomi et al., 2002]. Another approach is the use of oxygen generating biomaterials [Oh et al., 2009]. Oxygen generating biomaterials were shown to extend cell viability under hypoxic conditions and to prevent the necrosis of unvascularized tissue in vivo for several days [Harrison et al., 2007]. The material of interest used in the present study is a collagen/ceramic composite (CCC). Numerous collagen and ceramic based materials have been used for tissue engineering and cells have been successfully cultivated on mineralized collagen [Cunniffe and O'Brien, 2011; Gelinsky et al., 2008; Shepherd and Best, 2011]. Goal of our study was to develop a sustained release-formulation for the in-situ oxygen generation and its incorporation into CCCs to bridge the timeframe between implantation and neovascularization of the constructs.

5.2 Materials and Methods

All water used was highly purified and deionized using a USF ELGA PURELAB Plus UV/UF water purifier (Ransbach-Baumbach, Germany). Hard fat qualities Witepsol® E75, E85, and W45 were from CONDEA (Witten, Germany). Poly(lactic-*co*-glycolic acid) PLGA 50:50 Resomer® RG 503 (RG 503) or RG 502H (RG 502H) were from Boehringer Ingelheim (Ingelheim, Germany). Calcium peroxide (CaO_2) and catalase from bovine liver were from Sigma-Aldrich (St. Louis, MO, USA). Ethyl cellulose NF (EC) was from Dow Chemical Company (Midland, MI, USA). Disodiumhydrogen-phosphate-dihydrate, potassiumdihydrogenphosphate of analytical grade and colorimetric peroxide test strips were from Merck KGaA (Darmstadt, Germany). Sodium azide was from ACROS ORGANICS (Thermo Fisher Scientific, Morris Plains, NJ, USA). Biphasic calcium phosphate granules (BCP, 60 % Hydroxyapatite, 40 % ß-Tricalcium-Phosphate, 0.8 – 1.6 mm) were provided from Medtronic Sofamor Danek (Deggendorf, Germany). All other chemicals were purchased from Sigma-Aldrich and of analytical grade. Porcine-skin derived collagen-suspension was prepared according to Meyer et al. [2010] and freeze-dried (Christ Epsilon 2-6D®, Osterode am Harz, Germany) to obtain insoluble porcine collagen type I raw material.

5.2.1 Preparation of CaO_2 granules by compacting and grinding

CaO_2 was compacted using a hydraulic compactor (Maassen, Reutlingen, Germany) with a pressure of 1 t. The pellet was grinded by means of mortar and pestle. The particle size fraction of interest (90 - 355 µm) was obtained by sieving.

5.2.2 Preparation of CaO_2/lipid composite granules by compacting and grinding

Lipids of interest (see Table 5-1) were melted at 50 °C and CaO_2 was homogeneously dispersed. After cooling to 22 °C the material was grinded using mortar and pestle. Sieving rendered the desired particle size fraction of 90 – 355 µm.

Table 5-1: Formulations of CaO_2/lipid composite granules based on 100 g.

Formulation	E75 20%	E75 30%	E85 30%	E85 50%	W45 20%	W45 30%
CaO_2	80 g	70 g	70 g	50 g	80 g	70 g
Lipid component	20 g	30 g	30 g	50 g	20 g	30 g

5.2.3 Preparation of CaO_2/PLGA composite granules by dissolving and grating

RG 503 and RG 502H were dissolved in acetone and CaO_2 was homogeneously dispersed (22 g of CaO_2 per 78 g of PLGA). After acetone evaporation the material was grinded using a grater and sieved to obtain the 90 – 355 µm particle size fraction.

5.2.4 Preparation of CaO_2/ethylcellulose composite granules by dissolving and grating

Ethyl cellulose (EC) was dissolved in ethanol at a concentration of 8 %. CaO_2 with and without the addition of catalase was granulated by a step-wise addition of small portions of approx. 2 g ethanolic EC-solution (compositions see Table 5-2). The ethanol was evaporated and the material was grinded using a grater and sieved to obtain the 90 – 355 µm particle fraction.

Table 5-2: Formulations of CaO_2/ethyl cellullose composite granules based on 100 g.

Formulation	30 %	30 % EC + Catalase	45 %	60 %
CaO_2	70 g	69.51 g	55 g	40 g
Ethyl cellulose	30 g	29.79 g	45 g	60 g
Catalase	-	0.70 g	-	-

5.2.5 Manufacturing of oxygen generating collagen/ceramic composites

CCCs were prepared by dispersing the collagen raw material in water (pH adjusted to 3.7 with concentrated acetic acid) at a concentration of 4 % (w/w). After swelling for 4 h, the dispersions were homogenized with an ESGE® immersion blender (Unold, Germany). BCP granules (50 % (m/m) related to collagen dispersion) were homogeneously admixed to the collagen dispersion. Samples were prepared without further additives (CCC blank), with the addition of granulated CaO_2 (see 5.2.1), CaO_2/EC granules (see 5.2.4) with and without embedded catalase (formulations see Table 5-3).

Table 5-3: Formulations of oxygen generating CCCs; calculation based on dry mass of 1 CCC.

Formulation	CCC blank	CCC CaO_2	CCC EC/CaO_2	CCC EC/CaO_2 Catalase
Collagen	11.11 mg	11.04 mg	11.01 mg	11.00 mg
BCP	138.89 mg	137.96 mg	137.57 mg	137.56 mg
CaO_2	-	1 mg	1 mg	1 mg
Ethyl cellulose	-	-	0.43 mg	0.43 mg
Catalase	-	-	-	10 µg

Dispersion-aliquots were distributed into custom-made poly(methyl methacrylate) wells (diameter 9 mm, height 5 mm) and freeze dried according to the following protocol (Table 5-4):

Table 5-4: Freeze-drying protocol of CCCs.

Process phase	Time [hh:mm]	Temperature [°C]	Vacuum [mbar]
Loading	00:00	-40	---
Freezing	02:00	-40	---
Primary drying	00:01	-15	1.03
Primary drying	00:29	-15	1.03
Primary drying	23:00	-15	1.03
Secondary drying	00:01	20	0.1
Secondary drying	00:29	20	0.1
Secondary drying	14:00	20	0.1

5.2.6 Evaluation of oxygen release

Samples of interest (n=3) were placed in 100 mL DURAN® laboratory glass bottles containing 80 mL 250 mM phosphate buffer pH 7.4 (1 L contained 5.24 g potassium-dihydrogenphosphate, 37.6 g disodiumhydrogenphosphate-dihydrate, and 0.2 g sodium azide). A hole was cut into the screw cap to hold the oxygen sensors (Needle-Type Housing Fiber-Optic Oxygen Microsensor, PreSens Precision Sensing, Regensburg, Germany). The sensors were placed in a central position inside the buffer (for oxygen generating granules) or directly inside the oxygen generating CCCs. The glass bottles were placed on a magnetic stirrer (300 RPM for oxygen generating granules, no magnetic stir bar for oxygen generating CCCs) in a chamber heated to 37 °C. Calibration of the sensors was performed with nitrogen (0 % oxygen) and pure 250 mM phosphate buffer pH 7.4 (100 % oxygen saturation). Due to software conversion, the release buffer being 100 % saturated with ambient oxygen is displayed as 20.9 % relative oxygen saturation. Oxygen generating CCCs were analyzed individually containing 1 mg CaO_2 each, whereas CaO_2 granules were tested at quantities reflecting 100 mg CaO_2 each. The peroxide content was measured with colorimetric peroxide test strips after 72 h.

5.3 Results and Discussion

5.3.1 CaO_2 – influence of particle size on oxygen generation

In presence of water, 1 mol of CaO_2 generates 1 mol of hydrogen peroxide, which decomposes into ½ mol of O_2 (Equation 5-1). The blanks depicted in Figure 5-1 show around 20.9 % relative oxygen saturation reflecting the characteristic oxygen content of the atmosphere. CaO_2 containing samples resulted in a substantial increase in the oxygen content with a maximum reached after approx. 15 min and baseline levels in the open system allowing exchange with the atmosphere were reached after approx. 12 - 24 h. The highest oxygen concentration was measured for the CaO_2 powder (median size: 15 µm) after 0.25 h with 43.6 ± 0.8 %, whereas CaO_2 with a particle size of 90 - 355 µm reached only 38.7 ± 1.3 % after 0.60 h ($p < 0.01$). CaO_2 is poorly water soluble and consequently a slower hydrolysis with a reduced surface area and larger particle size corresponds with our observations [Bauer et al., 2006]. A high initial release can explain higher oxygen concentrations throughout the whole measurement time for the CaO_2 powder (median size: 15 µm). A difference < 1 % to the blanks was reached after 27 h for the CaO_2 powder (median size: 15 µm) and after 12 h for the 90 - 355 µm CaO_2. Overall, the influence of the particle size on oxygen release behavior was lower as expected. Thus, the approach to generate a sustained release of oxygen by the use of CaO_2 with a larger particle size was limited, as particles > 355 µm were regarded as inappropriate for the desired application. Hydrolysis of CaO_2 resulted in the formation of calcium phosphate due to the presence of phosphate ions in the used buffer.

$$CaO_2 + 2H_2O \longrightarrow H_2O_2 + Ca(OH)_2$$

$$2H_2O_2 \longrightarrow 2H_2O + O_2$$

Equation 5-1: Reaction of oxygen generation from CaO_2.

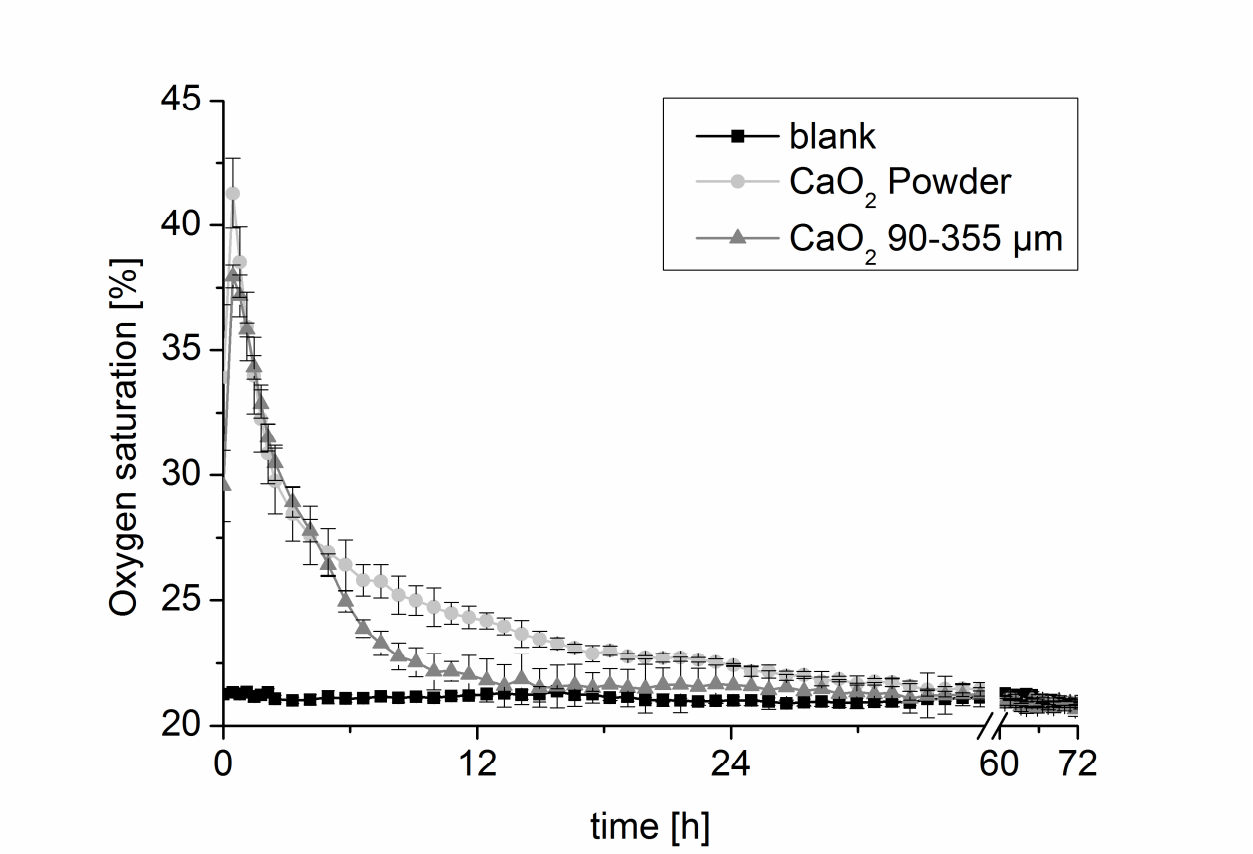

Figure 5-1: Oxygen saturation of phosphate buffer in presence of CaO_2 powder (median size: 15 µm) or compacted CaO_2 with 90 - 355 µm particle size.

5.3.2 Oxygen release from CaO_2 containing composite granules

5.3.2.1 Oxygen release from CaO_2/lipid composite granules

Lipids can be used to obtain implantable sustained release systems for pharmaceutical drugs [Wang, 1989]. Inflammatory response after implantation is not higher compared to commonly used PLGA based implants [Reithmeier et al., 2001]. To obtain a sustained release of oxygen, granules of CaO_2 and different hard fat qualities (see Table 5-5) as lipid components were prepared and the release behavior was evaluated. Hard fat is commonly used as suppository base and releases the active pharmaceutical ingredient (API) upon melting [Gjellan and Graffner, 1994]. A lower melting point of the suppository base leads to faster disintegration and thus release [Hammouda et al., 1993]. The hydroxyl value, representing the availability of free hydroxyl groups, also influences the release of the API. Poorly water soluble APIs were shown to be released slower from bases with

higher hydroxyl values [Webster et al., 1998], whereas suppository bases with a high hydroxyl value provide faster release of hydrophilic APIs [Akala et al., 1991]. Therefore we expected the fastest release of the hydrophilic CaO_2 for the composition with the highest hydroxyl value and the lowest melting point Witepsol® W45. Figure 5-2 shows the release profiles of the tested CaO_2/lipid composite granules in comparison to CaO_2 powder (median size: 15 µm) (see 5.3.1).

Table 5-5: Overview of the used hard fat components, adapted from [Sasol GmbH, 2007].

Hard Fat	Ascending melting point [°C]	Hydroxyl value [mg KOH/g]
Witepsol® E75	38	<15
Witepsol® E85	42 - 44	5 - 15
Witepsol® W45	33.5 - 35.5	40 - 50

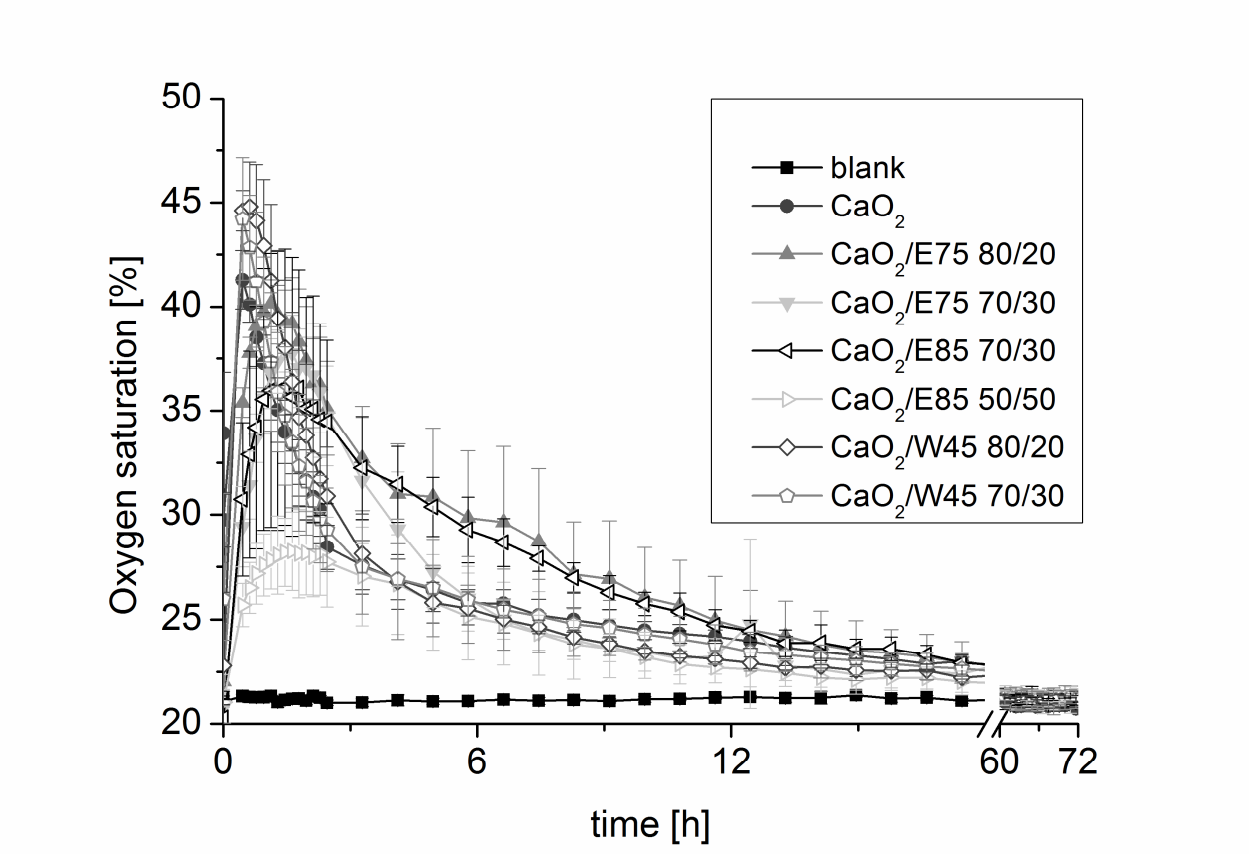

Figure 5-2: Oxygen saturation of phosphate buffer in presence of CaO_2 powder (median size: 15 µm) or CaO_2/lipid composite granules (90 - 355 µm).

Generally the observed differences between the compositions containing different Witepsol® types were lower as expected. Although E75 80/20 and E85 70/30 appear to generate slightly higher oxygen concentrations after approx. 6 h, these differences were not statistically significant (see Table 5-6).

Table 5-6: Statistical analysis (t-test) of oxygen release after 6 h, 24 h, and highest oxygen release (c_{max}), displayed as (6h/24h/c_{max}). P-values > 0.05 are displayed as "not significant" (ns), others are rounded to the second decimal place.

	c_{max}	E75 8/2	E75 7/3	E85 7/3	E85 5/5	W45 8/2	W45 7/3
CaO_2	43.6	ns/ns/0.02	ns/ns/0.01	ns/ns/ns	ns/ns/<0.01	ns/0.01/ns	ns/ns/ns
E75 8/2	40.2		ns/ns/ns	ns/ns/ns	ns/ns/<0.01	ns/ns/0.01	ns/ns/ns
E75 7/3	38.1			ns/ns/ns	ns/ns/<0.01	ns/ns/<0.01	ns/ns/ns
E85 7/3	37.5				ns/ns/ns	ns/ns/ns	ns/ns/ns
E85 5/5	28.4					ns/ns/<0.01	ns/ns/<0.01
W45 8/2	45.1						ns/ns/ns
W45 7/3	44.8						

The 50/50 composition of CaO_2 with Witepsol® E85 showed the overall lowest burst release being significantly lower compared to the CaO_2 powder (median size: 15 µm) and all other formulations, except E85 70/30 (see Table 5-6). It led to a reduction ($p < 0.005$) of the maximum oxygen concentration (c_{max}) to 28.4 ± 1.7 % after 1.5 h compared to 43.6 ± 0.8% after 0.25 h for CaO_2 powder (median size: 15 µm). None of the tested formulations provided longer significantly elevated oxygen concentrations compared to CaO_2 powder (median size: 15 µm). W45 80/20 provided a significantly decreased oxygen concentration after 24 h (see Table 5-6).

5.3.2.2 Oxygen release from CaO_2/PLGA composite granules

PLGA based drug delivery systems are well established in marketed products providing sustained release of APIs, such as leuprorelin (Lupron Depot®, Enantone®, Trenantone®, Eligard®), goserelin (Zoladex®), triptorelin (Decapeptyl®), somatotropin (Nutropin Depot®), buserelin (Profact®), bromocriptine (Parlodel LP®), risperidon (Risperdal consta®), naltrexone (Vivitrol®), or minocyclin (Arestin®) [Álvarez et al.,

2011; Sah and Lee, 2006; Schwach et al., 2003; Wischke and Schwendeman, 2008]. The mechanisms underlying drug release from PLGA based systems are drug diffusion, polymer degradation and erosion. Water influx leads to hydrolysis of the polymer and thereby degradation to oligomers and monomers leading to erosion of the matrix. For PLGA, typically bulk erosion occurs due to water influx being faster than hydrolysis [Göpferich, 1997; Langer and Peppas, 1983]. As an alternative to lipid matrix materials, we used PLGA to obtain sustained oxygen release from CaO_2/PLGA composite granules. Harrison et al. generated PLGA films containing sodium percarbonate, exhibiting release of oxygen over 24 h. Their films enabled to prevent necrosis of unvascularized tissue for several days using a skin flap model in mice [2007]. Figure 5-3 shows the oxygen saturation levels of the buffer for the two investigated CaO_2/PLGA composite granules compared to blank and CaO_2 powder (median size: 15 µm).

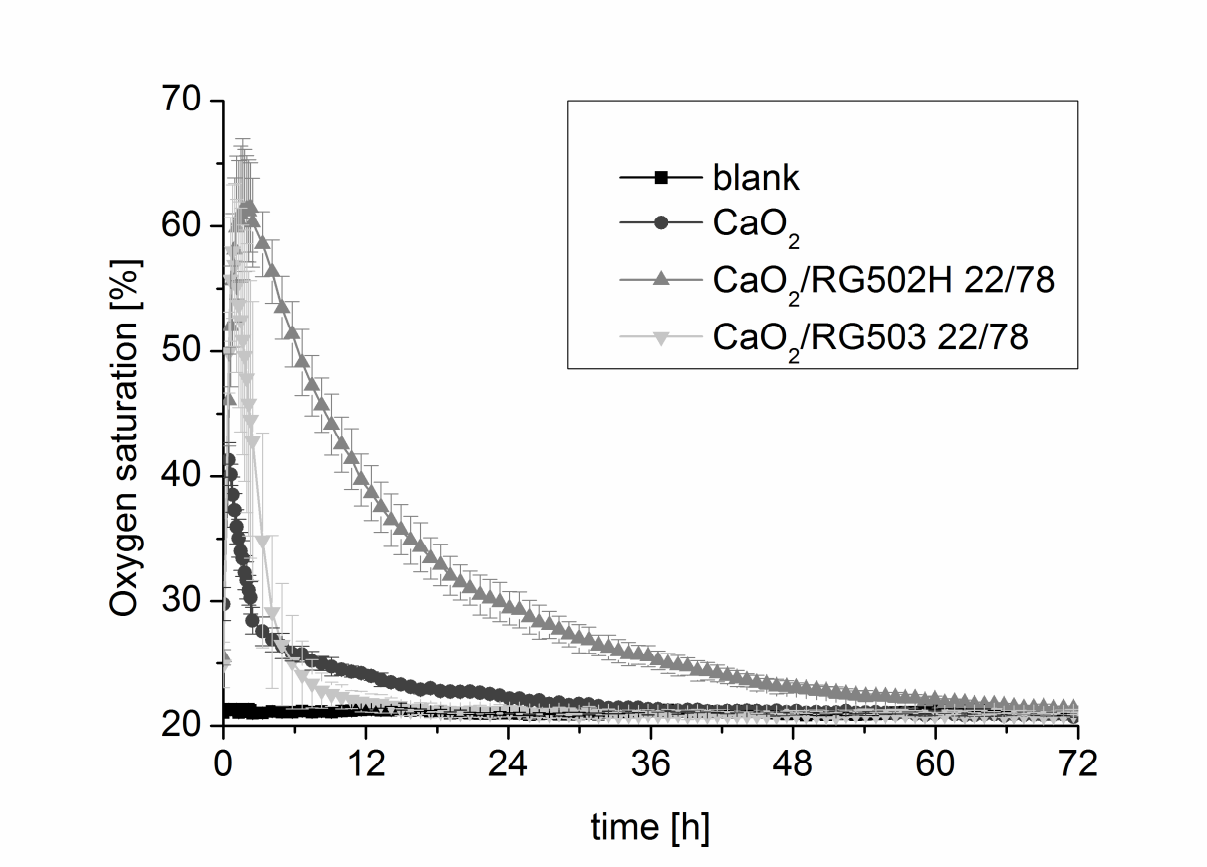

Figure 5-3: Oxygen saturation of phosphate buffer in presence of CaO_2 powder (median size: 15 µm) or CaO_2/PLGA composite granules (90 - 355 µm).

The different CaO_2/PLGA composite granules provided significantly higher c_{max} values compared to CaO_2 powder (43.6 ± 0.8 %) ($p < 0.05$) but did not significantly

differ in c_{max} among each other (61.6 ± 4.8 % (RG 502H) vs. 55.0 ± 7.7 % (RG 503)). The CaO_2/RG 503 composite granules provided a high initial burst release of oxygen followed by a drop below the oxygen level created by CaO_2 powder (median size: 15 µm). In contrast, the CaO_2/RG 502H formulation appeared to exhibit a sustained high oxygen saturation level. It even provided oxygen levels elevated by 1 % after 59 h and by 0.4 ± 0.1 % after 72 h ($p < 0.05$) compared to blanks. We expect this to result from the lower molecular weight and the free carboxylic end-groups of the RG 502H. It has been shown that a reduced molecular mass [Park, 1994] and non-esterified carboxylic end-groups [Göpferich, 1997] increase the degradation rate of PLGA polymers. Faster degradation is accompanied by acidic degradation products of PLGA leading to a decreased pH value inside the matrix [Mäder et al., 1996]. With regards to Equation 5-1, a pH decrease leads to faster hydrolysis rates of CaO_2. We conclude that the RG 502H based formulation improves the solubility of the embedded CaO_2. Nevertheless, a high initial burst release can go hand in hand with elevated hydrogen peroxide concentrations which are known to be unfavorable regarding cell survival [Lee et al., 2006]. Due to the high initial burst release of oxygen for the tested PLGA based systems those formulations were regarded as unfavorable for the desired application.

5.3.2.3 Oxygen release from CaO_2/ethyl cellulose composite granules

As an alternative to lipid and PLGA based CaO_2 systems, granules of CaO_2 in combination with different amounts of ethyl cellulose were prepared and the release behavior was evaluated. Figure 5-4 shows the release profiles of the tested CaO_2/EC composite granules in comparison to the CaO_2 powder (median size: 15 µm).

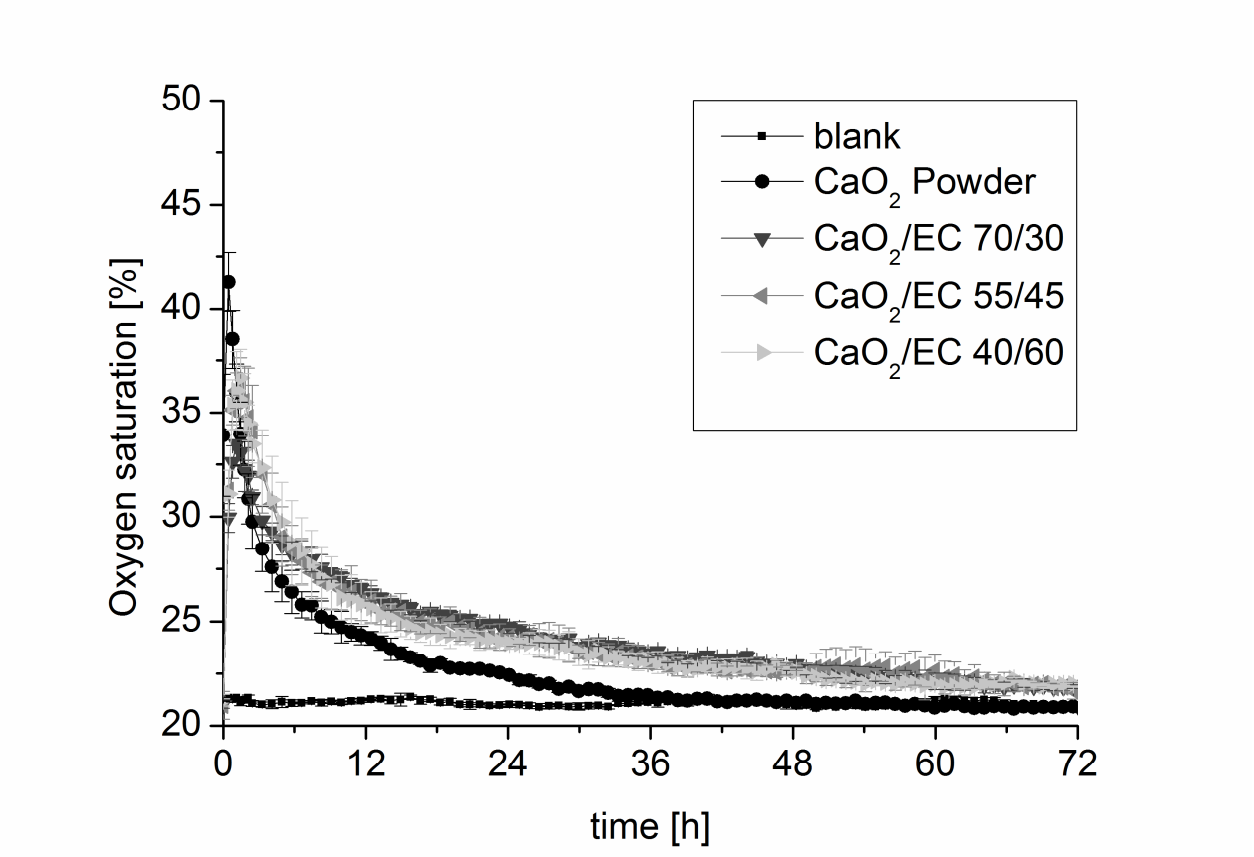

Figure 5-4: Oxygen saturation of phosphate buffer in presence of CaO_2 powder or CaO_2/EC composite granules (90 - 355 µm).

The combination of CaO_2 with different amounts of ethyl cellulose led to a significant ($p < 0.05$) reduction of initial burst release to 35.7 ± 2.1 % and t_{max} was delayed to 1.3 ± 0.1 h compared to CaO_2 powder (0.25 h, 43.6 ± 0.8 %) and CaO_2 with a particle size of 90 - 355 µm (0.6 h, 38.7 ± 1,3 %) (see 5.3.1). No significant difference in t_{max}, c_{max}, or in oxygen concentration was found among the formulations with different ethyl cellulose content throughout the whole investigation period. After 72 h the CaO_2/EC systems generated a 1.0 ± 0.1 % higher oxygen level compared to the formulations without ethyl cellulose ($p < 0.005$) and 0.5 ± 0.1 % higher oxygen saturation compared to CaO_2/RG 502H 22/78 ($p < 0.05$) (see 5.3.2.2). EC is frequently used to engineer oral sustained release formulations for hydrophilic drug substances either by direct compression or granulation. The release is mainly controlled by diffusion and partially by erosion of the matrix [Katikaneni et al., 1995; Reddy et al., 2003]. Rotstein et al. further found that EC-layers can function as a diffusive barrier for hydrogen peroxide [1992]. Therefore, we consider the EC formulation well suited for the desired purpose to design a sustained oxygen release

system from CaO_2. The CaO_2/EC 70/30 formulation delivered a reduced burst and a substantially extended timeframe of elevated oxygen levels, while it contained the lowest EC concentration tested and was therefore chosen to be incorporated into the CCCs.

5.3.3 Oxygen release from oxygen generating collagen/ceramic composites and the effect of catalase

Consequently, the oxygen concentration inside CCCs was evaluated in order to show whether the processing of the CaO_2 into the composites affects the oxygen generation. The samples contained 1 mg of CaO_2 each, either as pure CaO_2 or as ethyl cellulose containing granules with a particle size of 90 - 355 µm. Catalase was either added to the buffer or directly embedded into the CaO_2/EC 70/30 formulation (see 5.2.5). Catalase is used due to its ability to catalyze the decomposition of cytotoxic hydrogen peroxide into oxygen and water [Abdi et al., 2011; Oh et al., 2009], what also raises the question whether it on the other hand side can affect the equilibrium of oxygen generation. Figure 5-5 shows the oxygen release from CCCs with embedded CaO_2 granules (90 - 355 µm) with and without the addition of catalase. The oxygen release from CCCs containing CaO_2/EC formulations with and without embedded catalase and catalase in the release buffer is depicted in Figure 5-6. The oxygen release profiles were not affected by the presence of catalase in any form. Each mg of CaO_2 (equivalent to 0.014 mmol) generates 0.014 mmol of hydrogen peroxide (see Equation 5-1). Cytotoxicity of H_2O_2 starts at 0.3 mmol/L [Lee et al., 2006]. Assuming that CaO_2 would completely and instantly generate H_2O_2 without further decomposition into H_2O and O_2 a volume of 46.7 mL would be sufficient to keep the concentration of H_2O_2 below the cytotoxic 0.3 mmol/L level (equivalent to 10.2 mg/L H_2O_2). Also Harrison et al. showed that although even 3.57 mmol (equivalent to 121.4 mg) of hydrogen peroxide were generated intermediately in close vicinity to an area of 10 x 20 mm, oxygen generating constructs prevented necrosis in vivo [2007]. Therefore, it can be assumed that the H_2O_2 concentration generated in vivo by our constructs will be uncritical. In our studies the hydrogen peroxide content determined with colorimetric test strips after 72 h of release was 2 mg/L (0.1 mmol/L) for the samples without catalase, whereas in the catalase containing samples hydrogen peroxide content was below 0.5 mg/L

(0.025 mmol/L). The amount of catalase added or incorporated should theoretically be able to decompose the generated H_2O_2 to H_2O and O_2 within 14 min at pH 7 and 25 °C [Sigma-Aldrich, 2011]. Therefore, it is remarkable that H_2O_2 is still detectable even after 72 h. Whether catalase was added to the release buffer or directly incorporated into the CaO_2/EC granules did not affect the hydrogen peroxide contents.

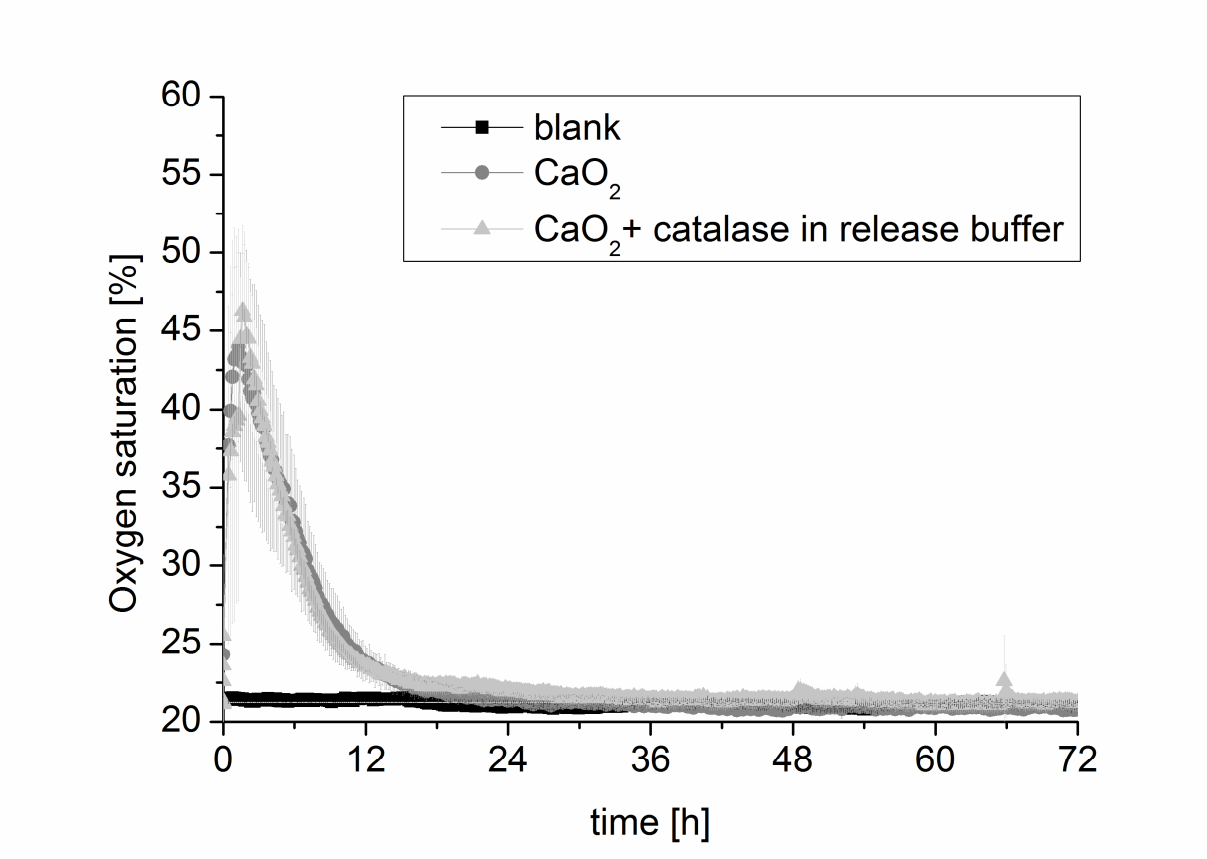

Figure 5-5: Oxygen saturation measured inside CCCs with CaO_2 (90 - 355 µm) with or without the addition of catalase to the release medium (phosphate buffer).

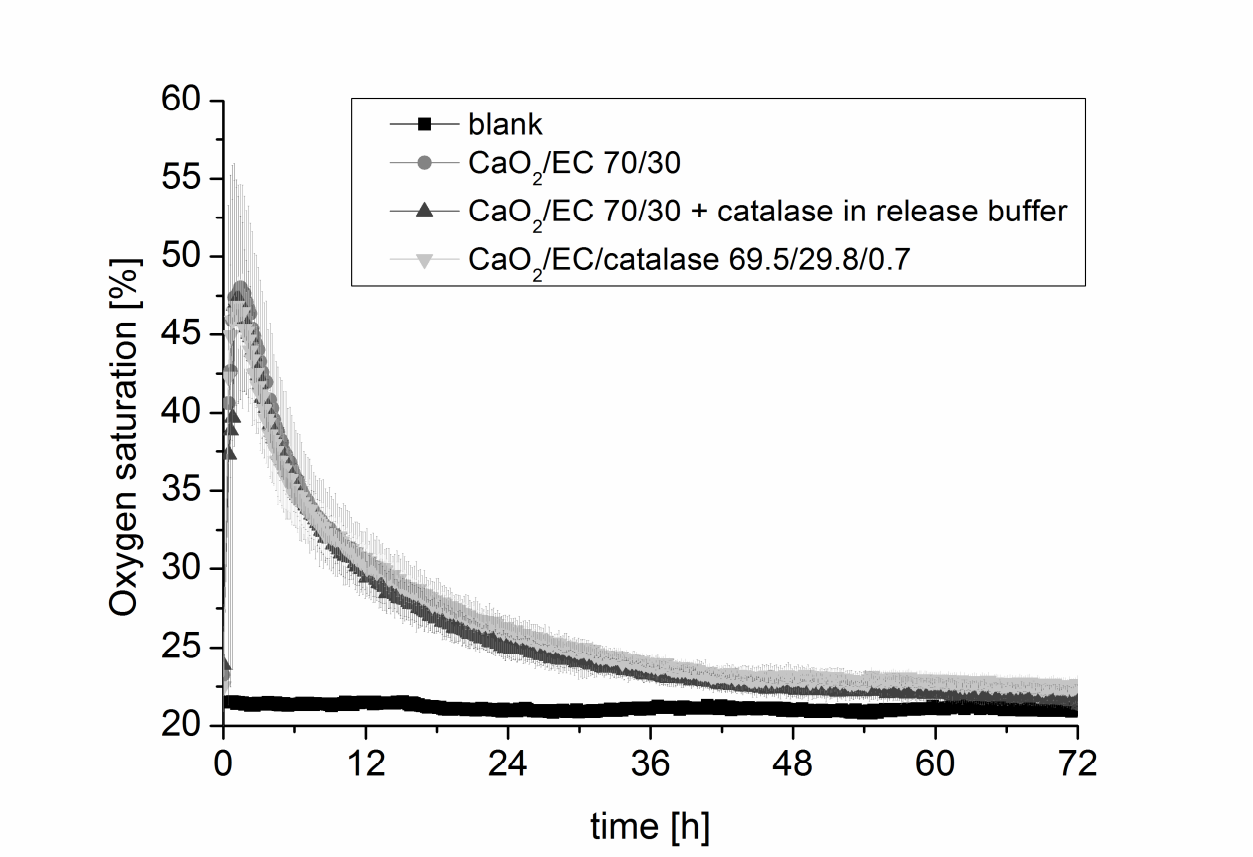

Figure 5-6: Oxygen saturation measured inside the CCCs containing CaO_2 in form of CaO_2/EC formulations with or without the addition of catalase to the release buffer and catalase incorporated into the CCCs.

5.3.4 Oxygen release from CaO_2/ethyl cellulose composite granules containing collagen/ceramic composites

Figure 5-7 exemplarily shows a comparison of the oxygen generation profiles of collagen ceramic composites with either CaO_2 or CaO_2/EC 70/30 incorporated. No significant influence of the processing into the final composites on the initial burst release of oxygen was detected. Comparing all tested CaO_2 containing CCCs with all CaO_2/EC containing CCCs, oxygen saturation of the CaO_2 containing samples was not significantly higher compared to blanks after 36 h, whereas the oxygen concentration for the samples containing CaO_2/EC formulations was 0.9 ± 0.6 % higher compared to the system with CaO_2 (90 - 355 µm) embedded without EC ($p < 0.005$) even after 72 h of release. The developed formulation combining CaO_2 with ethyl cellulose is therefore a successful tool for the manufacturing of CCCs providing elevated oxygen levels over three days. The further incorporation of

catalase enabled to significantly reduce the concentration of hydrogen peroxide, measured after 72 h from 1.5 ± 0.5 mg/L to 0.375 ± 0.29 mg/L ($p < 0.05$) and therewith far below the concentration of 10.2 mg/L considered to be cytotoxic [Lee et al., 2006]. It is again remarkable that H_2O_2 is still detectable after 72 h. As one cannot exclude that higher H_2O_2 concentrations occur during the release period, following in vitro studies should find ideal quantities of CaO_2 and catalase for the desired application site. We consider the developed scaffolds to be a promising biomaterial for larger defect sites, where adequate oxygen supply is a critical factor for the quality of the engineered tissue [Volkmer et al., 2008].

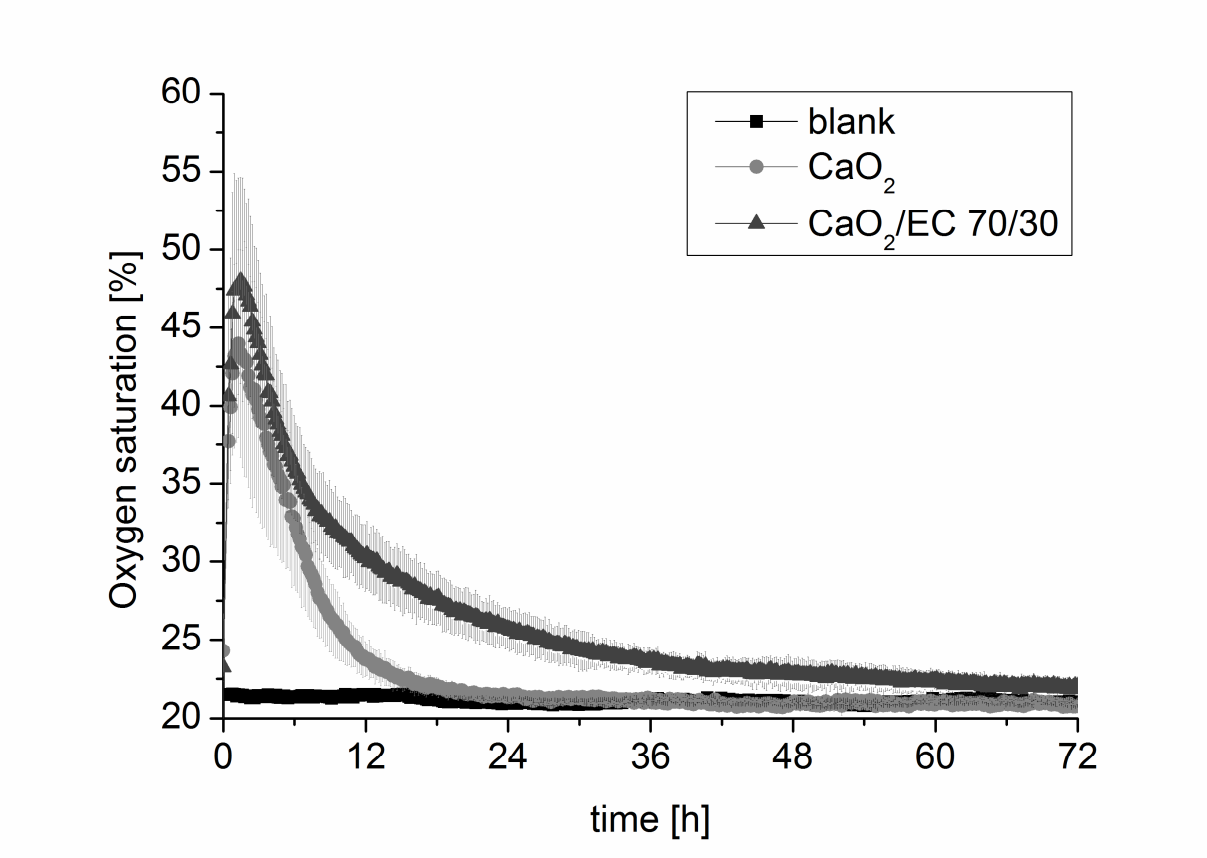

Figure 5-7: Oxygen saturation measured inside the CCCs enriched with either CaO_2 granules (90 - 355 µm) or CaO_2/ethyl cellulose 70/30 granules (90 - 355 µm).

5.4 Conclusion

In the present study we developed a calcium peroxide formulation for sustained oxygen generation in a collagen/ceramic composite. The oxygen generation from calcium peroxide was affected by the particle size as smaller particles resulted in faster oxygen generation. As dissolution of the particles is limited, the effect is in accordance with the Noyes-Whitney equation. The release testing of composite granules with calcium peroxide and different hard fat qualities demonstrated no significant difference to pure calcium peroxide, except for the formulation containing 50 % hard fat, where the initial burst was reduced. The combination of calcium peroxide with different PLGA qualities showed that the more hydrophilic RG 502H even acts as a solubility enhancer creating high oxygen levels. The granulation of calcium peroxide with ethanolic ethyl cellulose solution rendered composite granules generating elevated oxygen levels by 1 ± 0.1 % compared to compressed CaO_2 without EC after 72 h of release ($p < 0.005$), while the initial burst was reduced. The incorporation of this lead candidate into collagen/ceramic composites followed by release testing showed comparable results increasing the oxygen levels by 0.9 ± 0.6 % after 72 h of release ($p < 0.005$). Additionally incorporated catalase significantly reduced the content of cytotoxic hydrogen peroxide ($p < 0.05$) without having an influence on oxygen generation. Therefore, the developed formulation for the sustained release of oxygen and its combination with catalase, to ensure low hydrogen peroxide concentrations, appears to be promising for further in vitro and in vivo studies. It allows the manufacturing of larger tissue engineering constructs, where a lack of oxygen inside the scaffolds limits cell survival.

5.5 Acknowledgments

We thank the Bavarian Research Foundation for financial support. The above work is part of the “ForZebRA”-project. Medtronic Sofamor Danek GmbH (Deggendorf, Germany) is acknowledged for the donation of biphasic calcium phosphate granules.

5.6 References

Abdi S. I. H., Ng S. M., Lim J. O., An enzyme-modulated oxygen-producing micro-system for regenerative therapeutics, International Journal of Pharmaceutics, 409 (2011) 203-205.

Akala E. O., Adedoyin A., Ogunbona F. A., Suppository formulation of amodiaquine - In vitro release characteristics, Drug Development and Industrial Pharmacy, 17 (1991) 303-307.

Álvarez A. L., Espinar F. O., Méndez J. B., The application of microencapsulation techniques in the treatment of endodontic and periodontal diseases, Pharmaceutics, 3 (2011) 538-571.

Bauer K. H., Frömming K.-H., Führer C., Lehrbuch der Pharmazeutischen Technologie: Mit einer Einführung in die Biopharmazie, Wissenschaftliche Verlagsgesellschaft mbH, Stuttgart, (2006)

Carmeliet P., Jain R. K., Angiogenesis in cancer and other diseases, Nature, 407 (2000) 249-257.

Cunniffe G., O'Brien F., Collagen scaffolds for orthopedic regenerative medicine, JOM Journal of the Minerals, Metals and Materials Society, 63 (2011) 66-73.

Ge Z., Tian X., Heng B. C., Fan V., Yeo J. F., Cao T., Histological evaluation of osteogenesis of 3D-printed poly-lactic-co-glycolic acid (PLGA) scaffolds in a rabbit model, Biomedical Materials, 4 (2009a) 21001.

Ge Z., Wang L., Heng B. C., Tian X., Lu K., Fan V. T. W., Yeo J. F., Cao T., Tan E., Proliferation and differentiation of human osteoblasts within 3D printed poly-lactic-co-glycolic acid scaffolds, Journal of Biomaterials Applications, 23 (2009b) 533-547.

Gelinsky M., Welzel P. B., Simon P., Bernhardt A., König U., Porous three-dimensional scaffolds made of mineralised collagen: Preparation and properties of a biomimetic nanocomposite material for tissue engineering of bone, Chemical Engineering Journal, 137 (2008) 84-96.

Gjellan K., Graffner C., Comparative dissolution studies of rectal formulations using the basket, the paddle and the flow-through methods: II. Ibuprofen in suppositories of both hydrophilic and lipophilic types, International Journal of Pharmaceutics, 112 (1994) 233-240.

Göpferich A., Polymer bulk erosion, Macromolecules, 30 (1997) 2598-2604.

Groeneveld E. H. J., van den Bergh J. P. A., Holzmann P., ten Bruggenkate C. M., Tuinzing D. B., Burger E. H., Mineralization processes in demineralized bone matrix grafts in human maxillary sinus floor elevations, Journal of Biomedical Materials Research, 48 (1999) 393-402.

Hammouda Y. E., Kasim N. A., Nada A. H., Formulation and in vitro evaluation of verapamil HCl suppositories, International Journal of Pharmaceutics, 89 (1993) 111-118.

Harrison B. S., Eberli D., Lee S. J., Atala A., Yoo J. J., Oxygen producing biomaterials for tissue regeneration, Biomaterials, 28 (2007) 4628-4634.

Karande T. S., Ong J. L., Agrawal C. M., Diffusion in musculoskeletal tissue engineering scaffolds: design issues related to porosity, permeability, architecture, and nutrient mixing, Annals of Biomedical Engineering, 32 (2004) 1728-1743.

Katikaneni P. R., Upadrashta S. M., Neau S. H., Mitra A. K., Ethylcellulose matrix controlled release tablets of a water-soluble drug, International Journal of Pharmaceutics, 123 (1995) 119-125.

Langer R., Peppas N., Chemical and physical structure of polymers as carriers for controlled release of bioactive agents: a review, Journal of Macromolecular Science, Part C: Polymer Reviews, 23 (1983) 61-126.

Lee D., Lim B. S., Lee Y. K., Yang H. C., Effects of hydrogen peroxide (H_2O_2) on alkaline phosphatase activity and matrix mineralization of odontoblast and osteoblast cell lines, Cell Biology and Toxicology, 22 (2006) 39-46.

Liu J., Barradas A., Fernandes H., Janssen F., Papenburg B., Stamatialis D., Martens A., van Blitterswijk C., de Boer J., In vitro and in vivo bioluminescent imaging of hypoxia in tissue-engineered grafts, Tissue Engineering Part C: Methods, 16 (2009) 479-485.

Mäder K., Gallez B., Liu K. J., Swartz H. M., Non-invasive in vivo characterization of release processes in biodegradable polymers by low-frequency electron paramagnetic resonance spectroscopy, Biomaterials, 17 (1996) 457-461.

Meyer, M., Baltzer, H., Schwikal, K., Collagen fibres by thermoplastic and wet spinning, Materials Science and Engineering: C, 30 (2010) 1266-1271.

Nomi M., Atala A., Coppi P. D., Soker S., Principals of neovascularization for tissue engineering, Molecular Aspects of Medicine, 23 (2002) 463-483.

Oh S. H., Ward C. L., Atala A., Yoo J. J., Harrison B. S., Oxygen generating scaffolds for enhancing engineered tissue survival, Biomaterials, 30 (2009) 757-762.

Park T. G., Degradation of poly(d,l-lactic acid) microspheres: effect of molecular weight, Journal of Controlled Release, 30 (1994) 161-173.

Reddy K., Mutalik S., Reddy S., Once-daily sustained-release matrix tablets of nicorandil: Formulation and in vitro evaluation, AAPS PharmSciTech, 4 (2003) 480-488.

Reithmeier H., Herrmann J., Göpferich A., Lipid microparticles as a parenteral controlled release device for peptides, Journal of Controlled Release, 73 (2001) 339-350.

Rotstein I., Lewinstein I., Zuwabi O., Stabholz A., Friedman M., Effect of cervical coating of ethyl cellulose polymer and metacrylic acid copolymer on the radicular penetration of hydrogen peroxide during bleaching, Dental Traumatology, 8 (1992) 202-205.

Sah H., Lee B.-J., Development of new microencapsulation techniques useful for the preparation of PLGA microspheres, Macromolecular Rapid Communications, 27 (2006) 1845-1851.

Sasol GmbH, Product information WITEPSOL® and MASSA ESTARINUM®, Witten, Germany, Access: October 11, 2011, Last updated: June 6, 2007, http://www.warnergraham.com/images/WitepsolProdInfo.pdf

Schwach G., Oudry N., Delhomme S., Lück M., Lindner H., Gurny R., Biodegradable microparticles for sustained release of a new GnRH antagonist – part I: screening commercial PLGA and formulation technologies, European Journal of Pharmaceutics and Biopharmaceutics, 56 (2003) 327-336.

Shepherd J., Best S., Calcium phosphate scaffolds for bone repair, JOM Journal of the Minerals, Metals and Materials Society, 63 (2011) 83-92.

Sigma-Aldrich, Safety data sheet calcium peroxide, Access: January 29, 2012, Last updated: July 23, 2010, http://www.sigmaaldrich.com/catalog/DisplayMSDSContent.do

Sigma-Aldrich, Product information catalase assay kit, Access: November 14, 2011, http://www.sigmaaldrich.com/etc/medialib/docs/Sigma/Bulletin/cat100bul.Par.0001.File.tmp/cat100bul.pdf

Volkmer E., Drosse I., Otto S., Stangelmayer A., Stengele M., Kallukalam B. C., Mutschler W., Schieker M., Hypoxia in static and dynamic 3D culture systems for tissue engineering of bone, Tissue Engineering. Part A, 14 (2008) 1331-1340.

Wang P. Y., Lipids as excipient in sustained release insulin implants, International Journal of Pharmaceutics, 54 (1989) 223-230.

Webster J. A., Dowse R., Walker R. B., In vitro release of amoxycillin from lipophilic suppositories, Drug Development and Industrial Pharmacy, 24 (1998) 395-399.

Wischke C., Schwendeman S. P., Principles of encapsulating hydrophobic drugs in PLA/PLGA microparticles, International Journal of Pharmaceutics, 364 (2008) 298-327.

6 Final summary

The focus of this thesis was on the development of improved biomaterials for regenerative medicine. At first, an in-situ hardening system based on PLGA was developed. The formulations further contained a water miscible organic solvent, an inorganic component (α-TCP), and a pore forming agent (NaCMC). After injection into an aqueous surrounding, the occurring solvent exchange process led to the precipitation of PLGA and to the formation of a solid scaffold, exhibiting high porosity while maintaining good mechanical resistance to uniaxial compression. To combine the osteoconductive scaffold with an osteogenic working principle, the formulations were tested for cell compatibility in order to find a formulation enabling to directly incorporate cells. Therefore, the formulation recipes were optimized regarding their initial content of aqueous medium without influencing the properties of the resulting scaffold while the organic solvents were tested for cell compatibility. The most promising formulations were subsequently enriched with SCP-1 cells. During the solvent exchange process after administration into cell culture medium, cells were not able to attach to the scaffold matrix and were therefore washed out. Cultivating the cells on α-TCP before preparing the in-situ hardening formulation enabled their successful incorporation into the scaffold after solvent exchange. However, cell viability could not be maintained. Nevertheless, a putty-like system exhibiting high porosity and good mechanical stability was successfully developed.

In a different approach insoluble porcine collagen type I was treated with *Streptomyces mobaraensis* derived transglutaminase (mTG). Neither increased denaturation temperature nor reduced enzymatic degradation rates were observed, but an increased tensile strength was obtained. A Western blot analysis showed, although numerous washing steps to remove mTG were performed, that substantial mTG amounts remained non-covalently associated with the collagen material. To quantify the mTG amount in the washing fluids as well as in the modified collagen materials, an ELISA was developed. The analyses demonstrated that approximately 40 % of the initially applied mTG were still associated with the collagen material. A further reduction of mTG-residuals was achieved by a treatment with guanidinium chloride. Dialysis at pH 2 and pH 12 enabled a complete removal of mTG, but

comprised the drawback of amide bond hydrolysis and thereby decreased tensile strength.

Subsequently, the aseptic manufacturing of rhBMP-7 loaded collagen/ceramic composites was addressed. While other analytical methods comprise the drawback of poor specificity, Western blot analysis was our method of choice to detect and quantify rhBMP-7. After sterile filtration through a PVDF-filter, rhBMP-7 was completely recovered. Loading experiments showed that a pH shift towards the isoelectric point resulted in high incorporation efficiency, while the combination of collagen and biphasic calcium phosphate granules exhibited synergistic binding properties for rhBMP-7. Amongst the different extraction strategies the use of Arg/His buffer pH 6.5 was most effective recovering 32.7 ± 12.7 % of the previously loaded rhBMP-7. No signs of degradation were detected for the extracted rhBMP-7.

Finally, several excipients were tested for their potential to allow the manufacturing of a formulation providing sustained oxygen release from calcium peroxide. The use of different hard fat types only led to a reduced initial burst for a formulation containing 50 % hard fat. Combining calcium peroxide with PLGA resulted in even higher oxygen release compared to isolated calcium peroxide. Granules made of calcium peroxide and ethyl cellulose allowed to generate formulations providing sustained oxygen release and to reduce the initial burst. The calcium peroxide/ethyl cellulose granules were subsequently incorporated into collagen/ceramic composites and release testing showed oxygen levels which were significantly increased by 0.9 ± 0.6 % after 72 h of incubation ($p < 0.005$). The additional incorporation of catalase reduced the amount of cytotoxic hydrogen peroxide. We consider the developed oxygen generating collagen/ceramic composites to be a promising biomaterial for larger tissue engineering constructs, where oxygen availability is a limiting factor.

Thus, these developments of advanced biomaterials for bone tissue engineering might overall contribute to regenerative medicine to meet the requirements of an aging society.

List of Abbreviations

API	active pharmaceutical ingredient
Arg	arginine
AUC	area under the curve
BCP	biphasic calcium phosphate
BMP	bone morphogenetic protein
BSA	bovine serum albumine
CAD	computer aided design
CaO_2	calcium peroxide
CCC	collagen/ceramic composite
c_{max}	maximum concentration
DMSO	dimethyl sulfoxide
EC	ethyl cellulose
ECM	extracellular matrix
EDC	1-ethyl-3-(3-dimethyl-aminopropyl)carbodiimide
ELISA	enzyme-linked immunosorbent assay
ESC	embryonal stem cell
FDA	fluoresceindiacetate
FDA	U. S. Food and Drug Administration
Glu	glutamine
Gly	glycine
gTG	guinea pig liver transglutaminase
H_2O	water
H_2O_2	hydrogen peroxide
H_2SO_4	sulfuric acid
HA	hydoxyapatite
HCl	hydrochloric acid
His	histidine
HMDC	hexamethylene diisocyanate
IEP	isoelectric point
IgG	immunoglobulin G
iPSC	induced pluripotent stem cell
IsHS	in-situ hardening system

LD_{50}	lethal dose (50 %)
MSC	mesenchymal stem cell
mTG	microbial transglutaminase
N	normal
NaCMC	sodium carboxymethyl-cellulose
NaOH	sodium hydroxide
NMP	1-methyl-2-pyrollidone
O_2	oxygen
PBS	phosphate buffered saline
PBST	phosphate buffered saline containing 0.1 % polysorbate 20
PCL	polycaprolactone
PEG	polyethylene glycol
PGA	polyglycolide
PI	propidium iodide
PLA	polylactide
PLGA	poly(lactic-*co*-glycolic acid)
PVDF	polyvinylidene fluoride
rhBMP	recombinant human bone morphogenetic protein
rpm	rounds per minute
RT	room temperature
SDS	sodium dodecylsulfate
SDS-Page	sodium dodecylsulfate polyacrylamide gel electrophoresis
SEC	size exclusion chromatography
TCP	tri-calcium-phosphate
TGF	transforming growth factor
T_m	melting temperature
t_{max}	time to maximum concentration at
TRIS	tris(hydroxyethyl)-aminomethane
VEGF	vascular endothelial growth factor

Publications and Presentations associated with this work

Journal articles (published)

Schloegl W., Klein A., Fürst R., Leicht U., Volkmer E., Schieker M., Jus S., Guebitz G. M., Stachel I., Meyer M., Wiggenhorn M., Friess W., Residual transglutaminase in collagen – Effects, detection, quantification, and removal, European Journal of Pharmaceutics and Biopharmaceutics, 80 (2012) 282-288.

Journal articles (submitted)

Schloegl W., Marschall V., Witting M. Y., Volkmer E., Drosse I., Leicht U., Schieker M., Wiggenhorn M., Schaubhut F., Zahler S., Friess W., Porosity and mechanically optimized PLGA based in-situ hardening systems (submitted to European Journal of Pharmaceutics and Biopharmaceutics)

Oral presentations

Schloegl W., Marschall V., Volkmer E., Drosse I., Schieker M., Wiggenhorn M., Friess W., Transglutaminase enhanced collagen/ceramic composites as scaffolds for orthopedic indications, 7th World Meeting on Pharmaceutics, Biopharmaceutics and Pharmaceutical Technology, March 09, 2010, Valetta, Malta

Poster presentations

Schloegl W., Stachel I., Meyer M., Guebitz G. M., Jus S., Friess W., Transglutaminase – an enzymatic crosslinking method for collagen, 7th World Meeting on Pharmaceutics, Biopharmaceutics and Pharmaceutical Technology, March 10, 2010, Valetta, Malta

Schloegl W., Klein A., Leicht U., Volkmer E., Schieker M., Jus S., Guebitz G. M., Stachel I., Meyer M., Wiggenhorn M., Friess W., Transglutaminase crosslinking of Collagen – interactions, detection and effects, Jahrestagung Deutsche Gesellschaft für Biomaterialien, November 18, 2010, Heilbad Heiligenstadt, Germany

Additional Publications and Presentations

Journal articles

Jus S., Stachel I., Schloegl W., Pretzler M., Friess W., Meyer M., Birner-Gruenberger R., Guebitz G. M., Cross-linking of collagen with laccases and tyrosinases, Materials Science and Engineering C, 31 (2011) 1068-1077.

Poster presentations

Leicht U., Volkmer E., Wiese H., Matthias P., Schloegl W., Friess W., Schieker M., Effects of different chain extenders on the properties of poloxamer-based hydrogels as cell carriers for tissue engineering, Bone Tech, October 7-10, 2010, Hannover, Germany